# EFFECTS OF MECHANICAL AND MINERALOGICAL PROPERTIES ON CERCHAR ABRASIVITY INDEX AND SPECIFIC ENERGY OF SOME THAI ROCKS

NARAWIT  KATHANCHAROEN

A Thesis Submitted in Partial Fulfillment of the Requirements for the
Degree of Doctor of Philosophy in Civil, Transportation
and Geo-resources Engineering
Suranaree University of Technology
Academic Year 2023

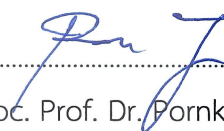# ผลกระทบเชิงกลและแร่วิทยาต่อดัชนีความสึกกร่อนและพลังงานจำเพาะเซอคาร์ของหินไทยบางชนิด
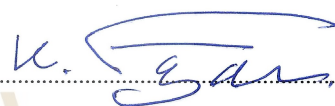
นายนราวิชญ์ ค้าทันเจริญ

วิทยานิพนธ์นี้เป็นส่วนหนึ่งของการศึกษาตามหลักสูตรปริญญาวิศวกรรมศาสตรดุษฎีบัณฑิต
สาขาวิชาวิศวกรรมโยธา ขนส่ง และทรัพยากรธรณี
มหาวิทยาลัยเทคโนโลยีสุรนารี
ปีการศึกษา 2566

# EFFECTS OF MECHANICAL AND MINERALOGICAL PROPERTIES ON CERCHAR ABRASIVITY INDEX AND SPECIFIC ENERGY OF SOME THAI ROCKS

Suranaree University of Technology has approved this thesis submitted in partial fulfillment of the requirements for the Degree of Doctor of Philosophy.
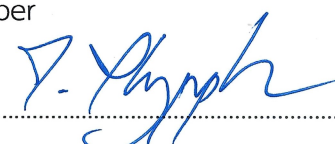
Thesis Examining Committee

.......................................................
(Assoc. Prof. Dr. Pornkasem Jongpradist)
Chairperson

.......................................................
(Emeritus Prof. Dr. Kittitep Fuenkajorn)
Member (Thesis Advisor)

.......................................................
(Asst. Prof. Dr. Prachya Tepnarong)
Member

.......................................................
(Asst. Prof. Dr. Decho Phueakphum)
Member

.......................................................
(Dr. Thanittha Thongprapha)
Member

.......................................................
(Assoc. Prof. Dr. Yupaporn Ruksakulpiwat)
Acting Vice Rector for Academic Affairs
and Quality Assurance

.......................................................
(Assoc. Prof. Dr. Pornsiri Jongkol)
Dean of Institute of Engineering

นราวิชญ์ ค้าทันเจริญ : ผลกระทบเชิงกลและแร่วิทยาต่อดัชนีความสึกกร่อนและพลังงาน
จำเพาะเซอคาร์ของหินไทยบางชนิด (EFFECTS OF MECHANICAL AND MINERALOGICAL
PROPERTIES ON CERCHAR ABRASIVITY INDEX AND SPECIFIC ENERGY OF SOME
THAI ROCKS) อาจารย์ที่ปรึกษา : ศาสตราจารย์ (เกียรติคุณ) ดร.กิตติเทพ เฟื่องขจร, 144 หน้า.

คำสำคัญ: ความทนทานต่อการขัดสี/กำลังรับแรงของหิน/มุมเสียดทาน/ความแข็งของหิน/ความแข็ง
ตามสเกลของโมห์ส

การศึกษานี้มีวัตถุประสงค์เพื่อหาความสัมพันธ์ระหว่างดัชนีการสึกกร่อนของเซอคาร์กับ
สมบัติทางกลและทางแร่วิทยาของหินจำนวน 21 ชนิดที่พบในอุตสาหกรรมเหมืองแร่และการก่อสร้าง
ในประเทศไทย โดยเป็นตัวแทนของหินที่มีความแข็งระดับอ่อนถึงปานกลาง ซึ่งดัชนีความสึกกร่อน
ของเซอคาร์ของหินเหล่านี้ไม่ค่อยได้รับการตรวจสอบจากที่ใดมาก่อน ผลการศึกษาระบุว่าดัชนีความ
สึกกร่อนของเซอคาร์และกำลังรับแรงของหินมีความสัมพันธ์ในระดับพอใช้ ดัชนีความสึกกร่อนของ
เซอคาร์มีค่าเพิ่มขึ้นเชิงเส้นตรงตามการเพิ่มขึ้นของมุมแรงเสียดทานภายใน อย่างไรก็ตาม ดัชนีความ
สึกกร่อนของเซอคาร์ไม่มีความสัมพันธ์กับความเค้นยึดติด การศึกษาแร่ประกอบหินที่ได้จากการ
วิเคราะห์การเลี้ยวเบนของรังสีเอ็กซ์ถูกนำมาใช้ร่วมกับความแข็งของหินตามสเกลของโมห์ส เพื่อ
กำหนดความแข็งเชิงปริมาตร ของตัวอย่างหิน พบว่าความแข็งเชิงปริมาตรสามารถสร้างความสัมพันธ์
กับการสึกกร่อนของหินได้ดีกว่าปริมาณควอตซ์สมมูลที่ใช้กันอย่างแพร่หลาย โดยพารามิเตอร์ทั้งสองมี
ความสัมพันธ์กับดัชนีความสึกกร่อนของเซอคาร์ที่ดีกว่าเมื่อวิเคราะห์หินตะกอนเนื้อเม็ดและหินเนื้อ
ผลึกแยกจากกัน ปริมาตรร่องรอยขูดมีค่าลดลงอย่างทวีคูณเมื่อความทนทานต่อการขัดสีของหิน
เพิ่มขึ้น พลังงานจำเพาะของเซอคาร์ มีค่าเพิ่มขึ้นตามการเพิ่มขึ้นของดัชนีความสึกกร่อนของเซอคาร์
ซึ่งบ่งชี้ว่าหินที่มีค่าความสึกกร่อนสูงต้องการพลังงานที่สูงขึ้นสำหรับการตัดและทำให้เกิดปริมาตร
ร่องรอยขูดน้อยกว่าหินที่มีความทนทานต่อการขัดสีต่ำ ผลการวิจัยสามารถใช้คาดคะเนการสึกหรอ
ของเครื่องมือการขุดในหินที่มีความแข็งระดับอ่อนถึงปานกลาง โดยใช้ความสัมพันธ์ระหว่างผลการ
ทดสอบดัชนีความสึกกร่อนของเซอคาร์กับความแข็งเชิงปริมาตรของหิน

สาขาวิชา เทคโนโลยีธรณี          ลายมือชื่อนักศึกษา ...........................................
ปีการศึกษา 2566                  ลายมือชื่ออาจารย์ที่ปรึกษา ...........................................

NARAWIT KATHANCHAROEN: EFFECTS OF MECHANICAL AND MINERALOGICAL PROPERTIES ON CERCHAR ABRASIVITY INDEX AND SPECIFIC ENERGY OF SOME THAI ROCKS. THESIS ADVISOR: EMERITUS PROF. DR. KITTITEP FUENKAJORN, Ph.D., P.E., 144 PP.

Keyword: Abrasiveness/ Rock strength/ Friction angle/ Rock hardness/ Mohs scale hardness

The objective of this study is to determine the correlations between CERCHAR abrasivity index (CAI) and mechanical and mineralogical properties of twenty-one rock types encountered in mining and construction industry in Thailand. These rocks represent soft to medium strong rocks on which their CAI properties have rarely been investigated elsewhere. Results indicate that fair correlation is obtained between CAI and rock strength. CAI's increase linearly with internal friction angle, they however show no correlation with the cohesion. The study of minerals composing each rock type obtained from XRD analysis are used with their corresponding Mohs scale hardness to determine volumetric hardness ($H_V$) of the specimens. $H_V$'s can correlate with rock abrasivity better than the widely used equivalent quartz contents. Both parameters give better correlations with CAI when clastic and crystalline rocks are analyzed separately. Scratching groove volume reduces exponentially with increasing rock abrasiveness. CERCHAR specific energy (CSE) increases with CAI's, suggesting that rocks with high abrasivity require higher energy to cut, and yield lower excavated volume than those with lower abrasivity. The research findings can be used to predict the wear of excavation tools in soft to medium strong rocks using the correlations between CAI test results and $H_V$ values.

School of Geotechnology                   Student's Signature ........................

Academic Year 2023                        Advisor's Signature ........................

# ACKNOWLEDGEMENTS

I would like to express thanks to Emeritus Prof. Dr. Kittitep Fuenkajorn, thesis advisor, who gave a critical review. I appreciate his encouragement, suggestions, and comments during the research period. I would like to express thanks to Assoc. Prof. Dr. Pornkasem Jongpradist, Asst. Prof. Dr. Prachya Tepnarong, Asst. Prof. Dr. Decho Phueakphum and Dr. Thanittha Thongprapha for their valuable suggestions and comments on my research works as thesis committee members. Grateful thanks are given to all staffs of Geomechanics Research Unit, Institute of Engineering who supported my work.

Finally, I most gratefully acknowledge my parents for all their support and encouragement throughout the period of this study.

Narawit  Kathancharoen

# TABLE OF CONTENTS

# TABLE OF CONTENTS (Continued)

# TABLE OF CONTENTS (Continued)

# TABLE OF CONTENTS (Continued)

**Page**

# LIST OF TABLES

# LIST OF FIGURES

# LIST OF FIGURES (Continued)

# LIST OF FIGURES (Continued)

# SYMBOLS AND ABBREVIATIONS

| | | |
|---|---|---|
| CAI | = | CERCHAR abrasivity index |
| $\sigma_c$ | = | Uniaxial compressive strength |
| $\sigma_t$ | = | Brazilian tensile strength |
| $I_S$ | = | Point load strength |
| E | = | Young's modulus |
| $\nu$ | = | Poisson's ratio |
| EQC | = | Equivalent quartz content |
| A | = | Mineral amount |
| R | = | Rosiwal mineral abrasiveness |
| SE | = | Specific energy |
| SSE | = | Scratching specific energy |
| CSE | = | CERCHAR specific energy |
| W | = | Work done |
| V | = | Material removed volume or mean groove volume |
| d | = | Diameter of wear flat area of stylus tip |
| $d_{sc}$ | = | Wear flat of stylus tip for saw cut surface specimen |
| N | = | Normal load |
| F | = | Horizontal force or ploughing force |
| $d_n$ | = | Vertical displacement |
| $d_s$ | = | Scratching distance |
| d | = | Wear flat width of stylus tip. |
| T | = | Torque |
| P | = | Screw pitch |
| c | = | Cohesion |
| $\phi$ | = | Friction angle |

# SYMBOLS AND ABBREVIATIONS (Continued)

S.G.     =     Specific gravity

n        =     Porosity

$V_V$    =     Pore volume of specimen

%V       =     Percentage of mineral content by volume

$V_{total}$ =  Specimen volume

%W       =     Weight percentage of mineral contents

$W_{sat}$ =    Weight of soaked specimen

$W_{dry}$ =    Weight of surface-dried specimen

$\rho_{water}$ =  Density of water

$\rho_{rock}$ =   Density of rock specimen

$H_M$    =     Mohs hardness
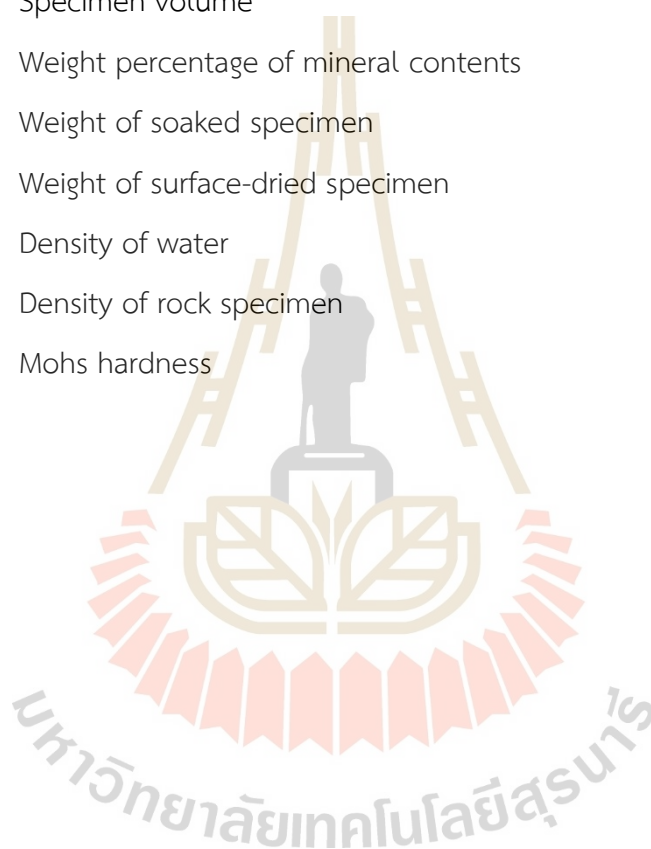
# CHAPTER I

# INTRODUCTION

## 1.1 Background and Rationale

The abrasiveness of rocks is an important factor for wear of TBM tunnelling and rock drilling. These operations are used in a wide range of applications, including civil industry, mining operations, and groundwater. Different rock types and geologic conditions are the factors for the appropriate drilling head selection for saving the cost of drill head wear. Many researchers have studied and developed several methods for assessing the abrasiveness of rock. One of them is CERCHAR abrasivity index (CAI) test, which is commonly used to estimate rock abrasiveness because it is simple and quick. Although many studies have been conducted, the results of these studies remain uncertain to determine the properties that most accurately affect the rock abrasiveness.

## 1.2 Research Objective

The objective of this study is to investigate parameters affecting results of CAI test on six rock groups collecting from several regions of Thailand, including clastic, plutonic, carbonate, sulfate, silicate, and volcanic rock groups, and to determine the correlation between CAI and physical (density and porosity), mechanical (uniaxial and triaxial strength, elastic modulus, Poisson's ratio, cohesion and friction angle), and mineral properties (quartz percentage) of the rock specimens.

## 1.3 Scope and Limitations

The scope and limitations of the research include as follows.

1) All specimens used are obtained from several regions of Thailand including

• Clastic group: Phu Kradueng, Phu Phan, Sao Khua and Phra Wihan sandstones

• Plutonic group: Diorite and Granite

• Carbonate group: Limestone, Marble and Travertine

• Sulfate group: Anhydrite and Gypsum

• Silicate group: Pyrophyllite and Dickite

• Volcanic group: Andesite, Basalt, Volcanic tuff and Rhyolite

2) The uniaxial and triaxial compression tests use confining pressures ranging from 0 to 15 MPa.

3) The CERCHAR test is performed on saw cut surfaces.

4) Mineral compositions are analyzed by using X-ray diffractometer.

5) Ploughing forces and grooves of CAI specimens are measured.

6) The research findings are published in international journals.

## 1.4 Research Methodology

The research methodology shown in Figure 1.1 comprises 8 steps: including literature review, samples collection and preparation, CERCHAR testing, uniaxial compressive test, triaxial compressive test, X-ray diffraction analysis, mathematical relations, discussions and conclusions, and thesis writing.

```
┌─────────────────────────────┐
│      Literature Review       │
└─────────────────────────────┘
              │
              ▼
┌─────────────────────────────┐
│ Samples Collection and Preparation │
└─────────────────────────────┘
              │
              ▼
┌─────────────────────────────┐
│        CERCHAR testing       │
│   • Ploughing Force Measurement │
│   • Ploughing Groove Depth   │
│     Measurement              │
└─────────────────────────────┘
              │
              ▼
┌─────────────────────────────┐
│ Uniaxial and Triaxial Compression Tests │
└─────────────────────────────┘
              │
              ▼
┌─────────────────────────────┐
│   X-ray Diffraction analysis │
└─────────────────────────────┘
              │
              ▼
┌─────────────────────────────┐
│ Development of Mathematical Relations │
└─────────────────────────────┘
              │
              ▼
┌─────────────────────────────┐
│   Discussions and Conclusions │
└─────────────────────────────┘
              │
              ▼
┌─────────────────────────────┐
│        Thesis Writing        │
└─────────────────────────────┘
```
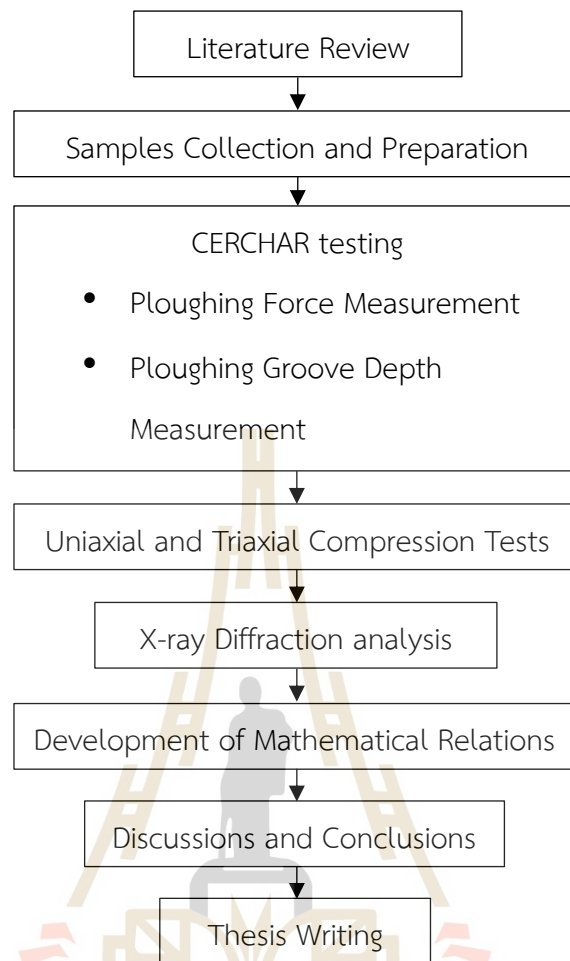
Figure I.1 Research methodology.

### 1.4.1  Literature Reviews

Literature review is carried out to study research about rock abrasiveness, abrasive testing, CERCHAR testing, and factors affecting CAI. The sources of information are from journals, technical reports, and conference papers. A summary of the literature review is given in chapter 2.

### 1.4.2  Samples Collection and Preparation

Rock samples used in this study have been obtained from many regions in Thailand. The sample preparation is carried out in the laboratory at the Suranaree University of Technology. The specimens are prepared to obtain cylindrical shape with

diameter of 54 and the length-to-diameter of 1, 2 and 2.5 for CERCHAR, triaxial and uniaxial compression testing.

### 1.4.3 CERCHAR testing

CERCHAR testing is performed on saw-cut surface with West apparatus to determine CAI that indicates the ability of wear abrasive of rocks. The methods and procedures of the testing are performed in accordance with ASTM standard practice. In addition to the testing standard, the groove depth, vertical displacement, and crank rotation torque during the scratching are measured.

### 1.4.4 Uniaxial and Triaxial compression test

Uniaxial and triaxial compression tests are performed on cylindrical core samples, which are prepared according to ASTM D7012-14 standard practice. The axial and lateral deformations of specimen are measured. The load at failure and modes of failure are recorded. They are used to calculate the strength and deformation modulus of the specimen. Mohr's circles are constructed to determine the cohesion and friction angle for each rock type.

### 1.4.5 X-ray Diffraction analysis

The X-ray diffraction analysis is performed on finely ground rock powder after uniaxial and triaxial compression tests. The results of the analysis are used to determine the percentage of each mineral in the rock which is one of the factors affecting CAI.

### 1.4.6 Mathematical Relations

The mathematical equations describe the relationship between CAI and the physical and mechanical properties and mineral compositions of rock are developed. The other parameters calculated from the additional measurements from the CERCHAR test such as the scratching forces, the volume of scratching grooves on the rock surface and scratching energy are analyzed.

### 1.4.7 Discussions and Conclusions

Discussions are made to explain the results and the meaning of the CAI relations. Explanations and conclusions of the issues of the relations are offered.

### 1.4.8 Thesis Writing

All research activities, methods, and results are documented and complied in the thesis.

## 1.5 Thesis Contents

Chapter 1 describes the background of problems and significance of the study. The research objectives, methodology, scope and limitations are identified. Chapter 2 summarizes the results of the literature review. Chapter 3 describes the sample preparations. Chapter 4 describes the laboratory testing. Chapter 5 presents the results of CERCHAR testing. Chapter 6 describes the testing results analysis. Chapter 7 describes discussion and conclusion of the research results and provides recommendations for future research studies.
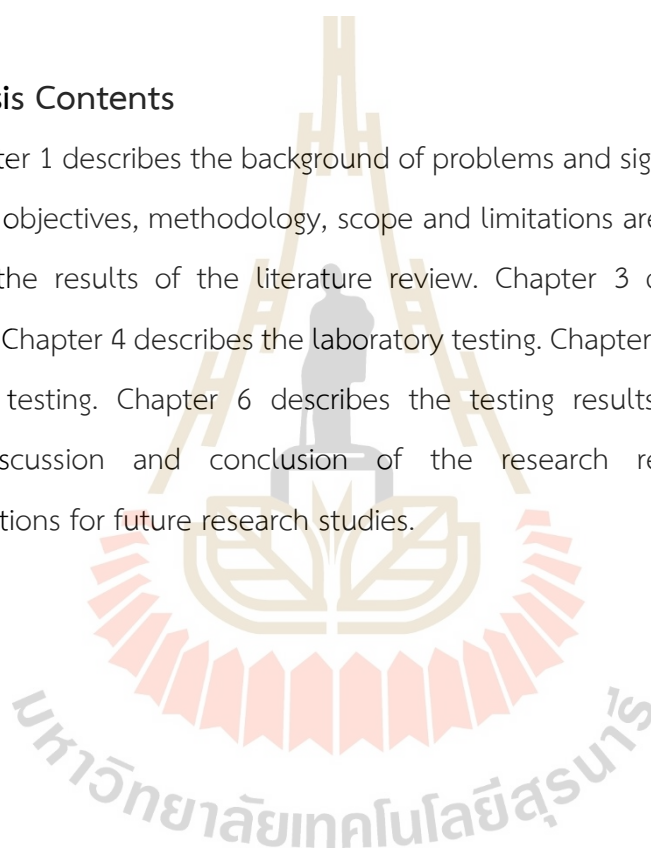
# CHAPTER II

# LITERATURE REVIEW

This chapter presents results of literature review carried out to improve an understanding of rock abrasiveness, CERCHAR abrasivity index (CAI) testing, factors affecting CAI, and CERCHAR scratching energy.

## 2.1    Rock abrasiveness

Rock abrasiveness is the primary factor in determining the equipment life and directly affects operation cost due to the wear of equipment. It is well known in the mining industry where the assessment of rock abrasiveness has been invented.

Many researchers use different methods for determining rock abrasiveness. Janc, Jovicic, and Vukelić (2020) present the overview of existing laboratory tests to assessing the rocks and soils abrasiveness. The general test methods include CERCHAR abrasivity test and LCPC abrasivity test (Laboratoire des Ponts et Chaussées), the standardized tests from France, and the group of tests for tunnelling that not standardized NTNU (Norwegian University of Science and Technology) and RIAT (rolling indentation abrasion test) abrasivity tests. Some methods are included in compilation by Nilsen, Dahl, Holzhauser, and Raleih (2006). They have compiled the widely used methods for determining abrasiveness. Several abrasion tests have been proposed by other researchers, but they are not as simply controlled as the CERCHAR test (Atkinson, Cassapi, and Singh, 1986).

There is an assessment of the abrasion using mineralogical compositions (Thuro and Käsling, 2009) of the rock by analyzing a thin section and the determination of a parameter. Equivalent quartz content (EQC) is the most commonly used parameter (Moradizadeh, Cheshomi, Ghafoori, and TrighAzali, 2016). The multiplication with the uniaxial compressive strength defines the Rock Abrasivity Index (RAI) (Plinninger, 2010).

The RAI is the parameter that can be related with other rock abrasive parameters (Majeed and Abu Bakar, 2016) and tool rock interaction such as drill bit lifetime (Prieto, 2012).

## 2.2    CERCHAR testing

The CERCHAR abrasiveness test has been widely used in the French coal mining industry. It is used in the British coal mining industry to assess the abrasiveness of rocks for machine in the tunnelling industry (West, 1989).

In 2010, American Society for Testing and Materials (ASTM) has standardized the CERCHAR testing (ASTM D7625-10, 2010) and later withdrawn in 2019. Alber et al. (2014) proposed to International Society for Rock Mechanics (ISRM) suggested method for determining the rock abrasivity by the CERCHAR testing, which is similar to the ASTM standard, but they have modified some procedure of measurement and correction.

There are two configurations of testing apparatus: the original design as developed at the CERCHAR Centre, and a modified design as given by West (1989). The designs of the two apparatus are similar, there are some differences that are described by Plinninger, Käsling, Thuro, and Spaun (2003). Another type of CERCHAR test (Figure 2.1) was manufactured at the Colorado School of Mines (CSM) in the mid-80s (Rostami, Ozdemir, Bruland, and Dahl, 2005). Hamzaban, Memarian, and Rostami (2014) have created a new CERCHAR device for determining frictional forces and depth of pin penetration into the rock surface during the test. The measured parameters are used to develop an analytical model for calculation of the size of the wear flat and pin tip penetration into the rock during the test. This test has been improved to be more accurate by Sotoudeh, Memarian, Hamzaban, and Rostami (2014).
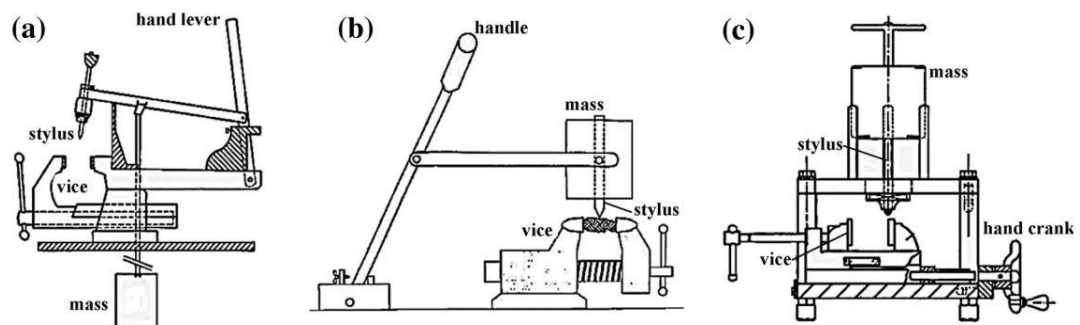
Figure II.1    CERCHAR testing devices, CERCHAR Centre (a), CSM (b), West (c) (Rostami et al. 2005)

The method of CERCHAR test using a steel stylus having a 90 degrees conical tip, which is pinned perpendicular on the rock surface under a constant force of 70 N. The length of stylus scratching to the rock surface must be exactly 10 mm. The wear flat width of stylus tip is measured in units of 0.1 mm. The CAI calculation from the wear width stylus is different according to the standard and suggested method. The test is repeated five times with five individual re-sharpened pins for each specimen to achieve an average CAI value. The use of stylus hardened to fifty-five HRC is advised. A microscope for examined the wear flat stylus should have a minimum magnification of 25 times for ISRM (Alber et al., 2014) and 30 times for ASTM (ASTM D7625-10, 2010)

## 2.3    Factors affecting CERCHAR abrasiveness index

The CAI value has a direct relation to abrasion, which affects the wear life of cutting tools. The CAI value is well known as a crucial factor for the cutting process. Therefore, the factors affecting CAI value are important. Numerous factors have been investigated by researchers, including test parameters (such as pin tip measurement, stylus hardness, surface conditions, and scratching length), rock physical and mechanical properties, and mineral compositions.

### 2.3.1 Test parameters

Plinninger et al. (2003) and Gharahbagh, Rostami, Ghasemi, and Tonon (2011) have compiled a number of testing parameters influencing the CERCHAR abrasivity test and the CAI value, such as testing equipment, measuring apparatus and procedure, testing needles shape and material properties, stylus hardness, surface conditions, testing length, evaluation of test results, and number of tests. These parameters were described by several researchers as presented below.

#### 2.3.1.1 Pin tip measurement

The direction of the CAI measurement is a crucial factor affecting the CAI, including top and side views. Majeed and Abu Bakar (2016) found a significant increase of 17 and 19 % in the correlation between top and side view measurements for saw cut and rough surfaces, respectively. Gharahbagh et al. (2011) observe minimal variation in test results when measuring the diameter of the wear flat from a side view compared to a top view. Conversely, Aydın (2019) find that wear flat measurement can be conducted from either a top view or a side view, as his results show no difference between the two views with an empirical equation of top view CAI equal to 1.0097 times side view CAI with an coefficient of determination ($R^2$) value of 0.99.

#### 2.3.1.2 Surface conditions

In previous research, Plinninger et al. (2003) show that inhomogeneous rock types often lacked suitable rock surfaces from hammer-breaking rock samples. To address this problem, they establish a positive linear relationship between CAI values obtained from rough and smooth surfaces, with CAI values on rough surfaces being approximately 0.5 higher than those on smooth surfaces. In 2010, Käsling and Thuro observed a slightly lower CAI value on smooth surfaces compared to that on rough surfaces, with a ratio of approximately 0.878. Aydın (2019) indicates a positive linear relationship between CAI on rough and smooth surfaces, with an $R^2$ of 0.96. The study shows that the CAI values on rough surfaces increased as the CAI values on smooth surfaces increased. The CAI values on rough surfaces are found to be about

12% higher than those on smooth surfaces, which is consistent with previous research conducted by Aydın, Yaralı, and Duru (2016) and Yaralı and Duru (2016), who find values of 15% and 18% higher than those on smooth surfaces, respectively. These studies recommend the use of saw-cut or smooth surfaces for CAI measurements, as the variation in measurement is generally lower than that of the rough surface (Aydın, 2019).

### 2.3.1.3  Scratching length

Al-Ameen and Waller (1994) conduct research on the development of wear fiat diameter on the stylus, specifically observing the first 3 mm scratching on hard rocks, include igneous and metamorphic rocks and some sedimentary rocks, has a greater impact on wear flat diameter or CAI compared to the whole length, whereas in soft rocks, such as sedimentary rocks, the stylus tip remains indented into the rock for the entire sliding distance, not only the first 3 mm. This is confirmed by Plinninger et al. (2003), that 70% of pin wear occurs within the first millimeter of the testing length, about 85% of the CAI is achieved after 2 mm, and only 15% of the change in CAI occurs within the last 8mm. based on their results, as shown in Figure 2.2, lengthening the scratch distance is considered useless. To achieve a noticeable greater wear flat on the testing stylus, they suggest the testing length would need to be extended to between 50 and 100 mm. Balani, Chakeri, Barzegari, and Ozcelik (2017) demonstrate through PFC3D Modeling that wear in the first 2 mm is high and the last 8 mm residual, the amount of wear does not change significantly. Jacobs and Hagan (2009) report that scratching below 40 mm did not result in significant CAI changes but scratched reaching 50 mm resulted in CAI doubling compared to 10 mm scratches. Zhang, Konietzky, Song and Huang (2020) also find that about 60% of the CAI value is reached after the first 1 mm, and about 80% of the CAI is achieved after the first 3 mm. Their finding confirmed previous studies that lengthening the testing distance is unnecessary due to their result shown that the CAI value has only a 20% increment after a 15-mm testing distance compared to the standard distance of 10 mm.
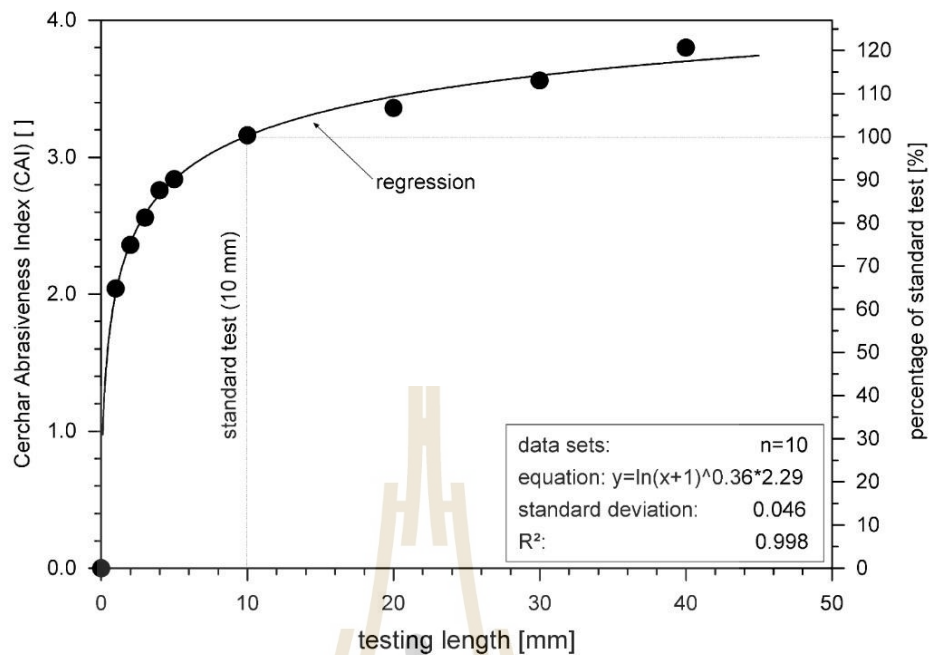
Figure II.2 Relationship between CAI and testing length (Plinninger et al., 2003).

### 2.3.1.4  Scratching rate

Balani et al. (2017) conduct a study on numerical modelling using various test speeds (3.33, 10, and 20 mm/s) on saw-cut surface sandstone samples. They find that the amount of wear does not change when the test speed changed, there is no relationship between test speed and abrasion test results in laboratory experiments. Hamzaban, Karami, and Rostami (2019) noted that an increase in pin speed affected tip wear. At the initial stage, the pin tip wear slightly decreased with an increase in pin speed, but after a certain speed, the CAI increased. Additionally, increasing the pin speed results in a decreased difference between harder and softer pins. Kotsombat, Thongprapha, and Fuenkajorn (2020) discover that low scratching rates result in a deeper groove on rock surfaces with a lower scratching force and lower CAI value on the stylus pins. They imply on the results that the rock surfaces behave as softer material under low scratching rate. Furthermore, the CAI obtained under low scratching rates is lower than those under high rates. In contrast, Zhang, Konietzky,

Song and Huang (2020) found no clear trend observed between CAI and testing velocities. They observed that CAI values are lowest when 10 mm scratching is completed within 20 seconds.

### 2.3.2 Rock physical properties

There have been several researchers who have studied physical properties such as porosity, moisture content, roughness, and orientation of rocks. One of these properties is rock porosity, which plays a significant role in the CERCHAR abrasivity index. The negative relationship between rock porosity and CAI is observed, where the CAI value increases as the rock porosity decreases (Lee, Jeong, and Jeon, 2012; Ozdogan, Deliormanli, and Yenice, 2018; Rostami, Hamidi, and Nejati, 2020; Sirdesai, Aravind, and Panchal, 2021; Yasar and Yilmaz, 2016). Sirdesai et al. (2021) have identified a high coefficient of determination ($R^2$ = 0.91) for the linear correlation between CAI value and rock porosity while studying only one type of rock (granite). Rostami et al. (2020) have also observed a high $R^2$ of 0.73 of this correlation. However, the rock samples in their study were varied, and the exponential correlation was found to be more suitable. Some researchers have found no correlation between CAI value and rock porosity, with an $R^2$ less than 0.1 (Lee et al., 2012; Ozdogan et al., 2018) as shown in Figure 2.3. Additionally, there was a poor relationship observed, with an $R^2$ of 0.26.

### 2.3.3 Rock mechanical properties

Rock strength is one of the important factors affecting CAI values. Several mechanical properties, including rock strength, rock deformation (Young's modulus and Poisson's ratio), and rock hardness, are considered by many researchers in this context.

**Fitted Line Plot**
CAI = 1.715 - 0.1665 Porosity (%)

| S | 1.33990 |
| R-Sq | 5.5% |
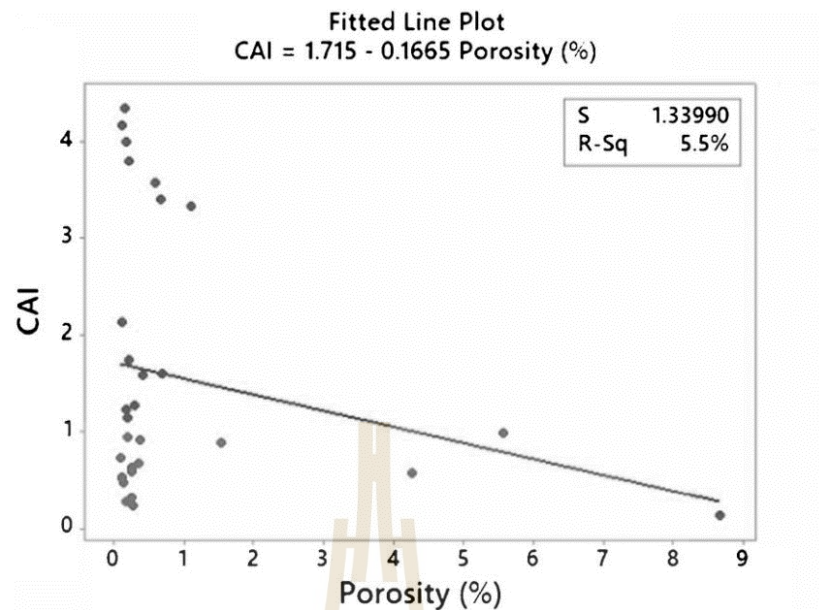
Figure II.3 Relationship between CAI and rock porosity (Ozdogan et al., 2018).

### 2.3.3.1 Strength of rock

Strength parameters consist of uniaxial compressive strength ($\sigma_c$), Brazilian tensile strength ($\sigma_t$), and point load strength ($I_S$) are influence on CAI values proposed by Capik and Yilmaz (2017) and Teymen (2020). This is confirmed by many researchers who study the relationship and found a strong linear relationship (with high value of coefficient of determination values) between CAI values and $\sigma_c$ and $\sigma_t$ (Er and Tuğrul, 2016; Sirdesai et al., 2021)

The mechanical property that are frequently studied is uniaxial compressive strength. Deliormanlı (2012) states that uniaxial compressive strength plays an important role for abrasiveness of the rock as same as the research conclusion of Al-Ameen and Waller (1994) that proposed the abrasiveness is largely influenced by the rock strength ($\sigma_c$). The both are studied and focused on the influence of rock strength on rock abrasiveness. All researchers study the CAI value and $\sigma_c$ relationship are find that CAI value increases with $\sigma_c$ increases. The strong linear relationships between CAI values and $\sigma_c$ is proposed by Deliormanlı (2012), Sirdesai et al. (2021),

Teymen (2020) and Zhang et al. (2021) (Figure 2.4). They present the high value of coefficient of determination ($R^2 > 0.80$) for the CAI values and $\sigma_c$ relationship. On the contrary, Lee et al. (2012), Ozdogan et al. (2018), and Zhang, Konietzky, and Frühwirt (2020) show poor linear relationships between CAI values and $\sigma_c$ with $R^2$ lower than 0.20. The positive linear relation between CAI value and $\sigma_c$ is found by several researchers such as He, Li, Li, Wang, and Guo (2016). and Ko, Kim, Son, and Jeon (2016). Only two researchers found the nonlinear correlation including Al-Ameen and Waller (1994) who use polynomial relation in term of 1 millimeter sliding distance of CAI vesus the rock strength, as shown in Figure 2.5. They give the reason because the initial wear flat diameter on the stylus tip cannot be attributed to the abrasive mineral content due to the small sliding distance and Rostami et al. (2020) who propose power relationship. Some results show the $\sigma_c$ interception that mean at CAI value is equal to zero, $\sigma_c$ is more than zero (Altindag, Sengun, Sarac, Mutluturk, and Guney, 2009; Deliormanlı, 2012; and Yasar and Yilmaz, 2016), but the most of researches are CAI interception (CAI value is more than zero when $\sigma_c$ is equal to zero) that are shown by most researchers such as Hamzaban, Memarian, and Rostami (2018), Ozdogan et al. (2018) and Ündül and Er (2017). Only the ressearches of Rostami et al. (2020) and Wengang, Liang, Zixu, and Yanmei (2021) show the zero interception (CAI is equal to zero when $\sigma_c$ is equal to zero).

### 2.3.3.2 Rock deformation

No researchers study only Young's modulus relations with CAI value, but some researchers still conduct this relations and find the moderately strong relationship between CAI values and Young's modulus (E) with $R^2$ about 0.65 (Hamzaban et al., 2018; Teymen, 2020). But He et al. (2016), Lee et al. (2012) and Zhang, Konietzky, and Frühwirt, (2020) have found the poor relationships between CAI values and E with $R^2$ less than 0.30. The very strong linear relations ($R^2 = 0.98$) are found by Sirdesai et al. (2021) due to they tested only one type of rock (granite). There is also another relationship between CAI value versus a product of Young's modulus and equivalent quartz content are presented by Plinninger et al. (2003) and Balani et

al. (2017). They find the fair linear relationship with $R^2$ of 0.56 and 0.68. For Poisson's ratio (v), research of Lee et al. (2012) is only one investigated. Their results show no relation between CAI values and v.
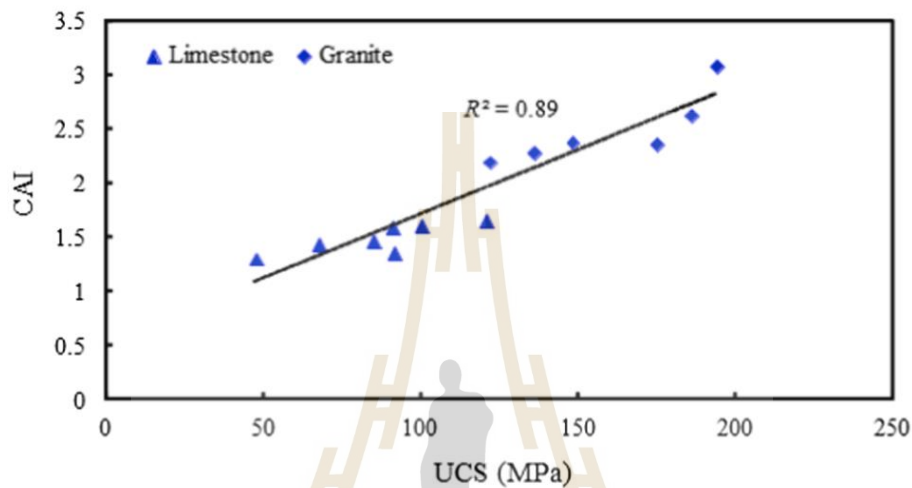


Figure II.4   Relationships between the CAI and UCS of limestone and granite rock (Zhang et al., 2021).
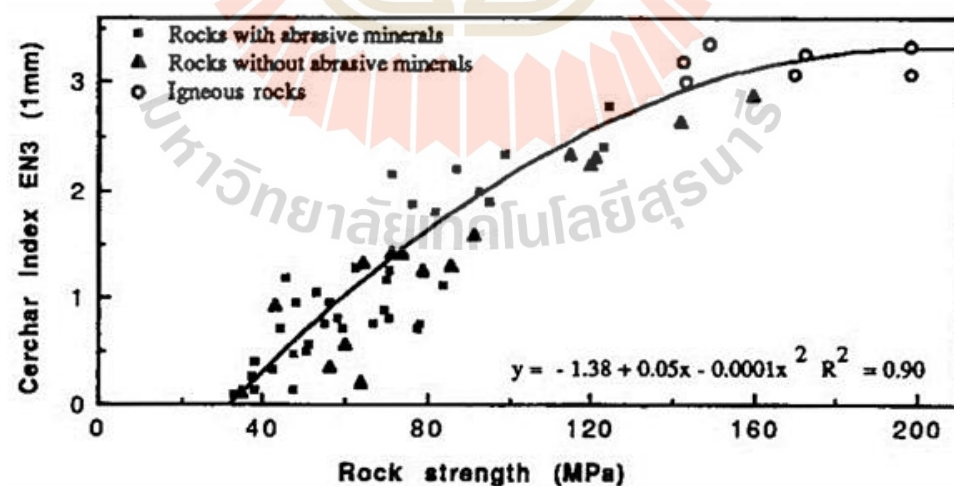


Figure II.5   CERCHAR index (1 mm) versus measured rock strength (Al-Ameen and Waller, 1994).

### 2.3.3.3 Hardness of rock

There are several methods for determining rock hardness. Each method has its own variables, such as Shore hardness, Schmidt hardness, Vickers hardness, and others. Some researchers found strong linear relationships between CAI values and their Shore hardness with $R^2$ more than 0.74 (Er and Tuğrul, 2016; Lee et al., 2012; Ozdogan et al., 2018).

### 2.3.4 Mineral compositions

Mineral compositions are important properties that many researchers consider (Li et al., 2021; Suana and Peters, 1982; Ündül and Er, 2017; Yaralı, Yaşar, Bacak, and Ranjith, 2008). Many mineral properties are used to correlate with CAI value such as quartz or abrasive mineral content, grain size and shape of abrasive mineral, mineral hardness, and equivalent quartz content (EQC). Some researchers conduct the other parameters relation with combined two or more parameters related to the mineral parameters, such as rock abrasivity index (RAI), which is calculated by multiplying a rock's UCS and EQC, as presented by Cheshomi and Moradizadeh (2021), Plinninger (2010), and Prieto (2012).

### 2.3.4.1 Grain size and shape

Yaralı et al. (2008) and Er and Tuğrul (2016) propose that quartz grain size plays a significant role in determining the CAI value. They find a linear relationship between CAI and average grain size with high correlation coefficient of 0.955 and 0.689 respectively with increasing of quartz grain size, CAI increases. Yaralı et al. (2008) present that sandstones with average quartz grain size more than 0.5 mm are classified as very abrasive, whereas those with a grain size less than 0.5 mm are classified as abrasive. In the case of siltstones, if the average quartz grain size is smaller than 0.1 mm and the cement type is either silica or ferrous silica, then they are classified as abrasive rocks. However, if the cement type is either clay or carbonate, the rocks may be moderately abrasive strong (positive correlation) linear relationship between the CAI and quartz content and quartz size. Suana and Peters (1982) study

the relation between CAI and rock mineralogy and petrography and explained that the grain size has no influence on the CAI as long as the grain size ranges between 50 microns and 1000 microns. If grain sizes are larger than 1 mm it is necessary to perform more number of tests than the standard specified to get a better mean value. But their result finds no grain size dependency of the CAI deviation between 5 and 10 tests in the analysed range is observed (Lassnig, Latal, and Klima, 2008). Beste, Lundvall, and Jacobson (2004) found that the quartz grains size greater than 1 mm caused the highest tip wear rate due to scratch through the rough edges along the grain boundaries. He et al. (2016) investigate the size and shape coefficient of rock obtained from the area and perimeter of the mineral grain. The size and shape coefficients show positive and negative correlations with CAI value with $R^2$ of 0.50 to 0.41 respectively. Ündül and Er (2017) study the effects of micro-texture on abrasiveness of volcanic rocks. They state that increasing of dimensions of opacified minerals causes a decreasing in CAI values, which is similar effect of plagioclase feldspar on CAI. They report that reduction of CAI related to alteration and previously formed micro-cracks in the mineral grain results in the formation of clay and albite of altered plagioclase in their results.

### 2.3.4.2 Abrasive mineral content

The abrasivity value affected by mineral is not dependent on only quartz but also a mineral with higher hardness, whether it be Mohs hardness scale or others, than material scratched. Many researchers study correlation between CAI value and abrasive mineral content, especially quartz contents. Their research mostly finds a moderately strong correlation with $R^2$ about 0.50 (Er and Tuğrul, 2016; West, 1986; Yaralı et al., 2008) and some correlations are strong correlations found by (Torrijo, Garzón-Roca, Company, and Cobos, 2019; Zhang et al., 2021) with $R^2$ about 0.80. All the moderately strong to strong correlation always have the same positive trend, which CAI value increases with quartz content increases. In part of specimen of these correlations, mostly shows close to or same types of rocks, such as sandstone, mudstone, and siltstone, or only granite rock. Conversely, some studies have found no correlation or poor correlation between CAI value and quartz content, with $R^2$ range

from 0.1 to 0.2, which found by Ko et al. (2016) and Lee et al. (2012). These studies typically include specimens of a greater variety of rock types, including igneous, sedimentary, and metamorphic rocks, which is noticed that differ from the moderately strong to strong correlation that has no more than three types of rocks. For the other mineral types, Bharti, Deb, and Das (2017) present that their rocks are classified as very abrasive because of high silica content. As same as a research of Li et al. (2021), their testing data on sandstone with feldspar clearly has greater abrasivity than granite although sandstone hardness is lower than granite hardness.

### 2.3.4.3  Mineral hardness

In addition to analyzing rock hardness, some groups of researchers have also investigated the relationship between mineral hardness and rock abrasivity. For example, West (1989) studies a correlation between abrasive of rock and Mohs scale of minerals within a range of 2 to 7 on the Mohs scale, finding a positive correlation with $R^2$ of 0.98, as shown in Figure 2.6. Liu, Schieber, Mastalerz, and Teng, (2020) conduct a similar study on the correlation between Leeb hardness value and several mineral content, showing the hardness increased as quartz content increased with an $R^2$ of 0.59. This research supports mineral hardness and mineral content topic. That is the more abrasive mineral content, the more hardness increases. After these researches, Zhang et al. (2021) study a relationships between CAI and weighted hardness, which was calculated by summing the percentage content of each mineral component in a rock multiplied by its Mohs hardness. They find a positive relationship between CAI and weighted hardness, with a high $R^2$ of 0.88, indicating that as the weighted hardness of a rock increases, CAI value increases.
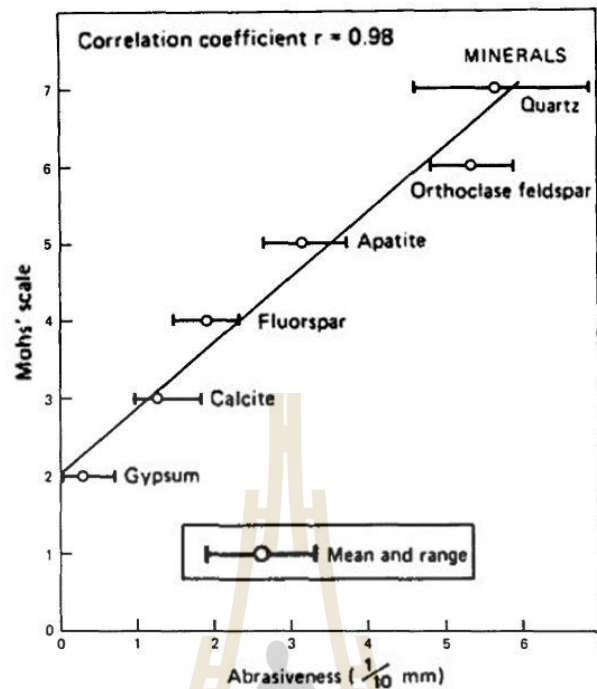
Figure II.6 Mohs hardness grade vs. abrasiveness test value (West, 1986).

### 2.3.4.4 Equivalent quartz content

Equivalent quartz content (EQC) meaning the entire mineral content referring to the abrasivity or hardness of quartz, which determined by using summation of percentage of mineral amount (A) multiplied by its Rosiwal mineral abrasiveness (R). The EQC equation is shown in Equation 2.1 that proposed by Thuro (1997), where n is number of minerals.

$$EQC = \sum_{i=1}^{n} A_i \times R_i \quad (2.1)$$

The relationship between CAI and EQC shows a positive relationship that CAI value increases with EQC increases based on almost all researchers who have studied this topic. Some researchers have found the strong

relationship by using a few types or same type or group of rock specimens, such as limestone and granite rock for Zhang et al. (2021) research ($R^2$ = 0.94) and sandstone, metamorphic, and plutonic group for Moradizadeh et al. (2016) research with $R^2$ is between 0.77 to 0.94, as shown in Figure 2.7. Although using a few types of specimen, it does not confirm that the relationship will show a strong relationship as seen as a results of Yaralı et al. (2008). They use the same group of specimens, including sandstone siltstone and mudstone and found a fair relationship with $R^2$ of 0.58. Fair to moderately strong relationship also found by many researchers (Capik and Yilmaz, 2017; Latal, Bach, and Thuro, 2020; Rostami, Ghasemi, Alavi Gharahbagh, Dogruoz, and Dahl, 2014) with $R^2$ between 0.44 to 0.66. Relation of these research is type of specimens that use many types of testing specimens including about ten types of specimens.
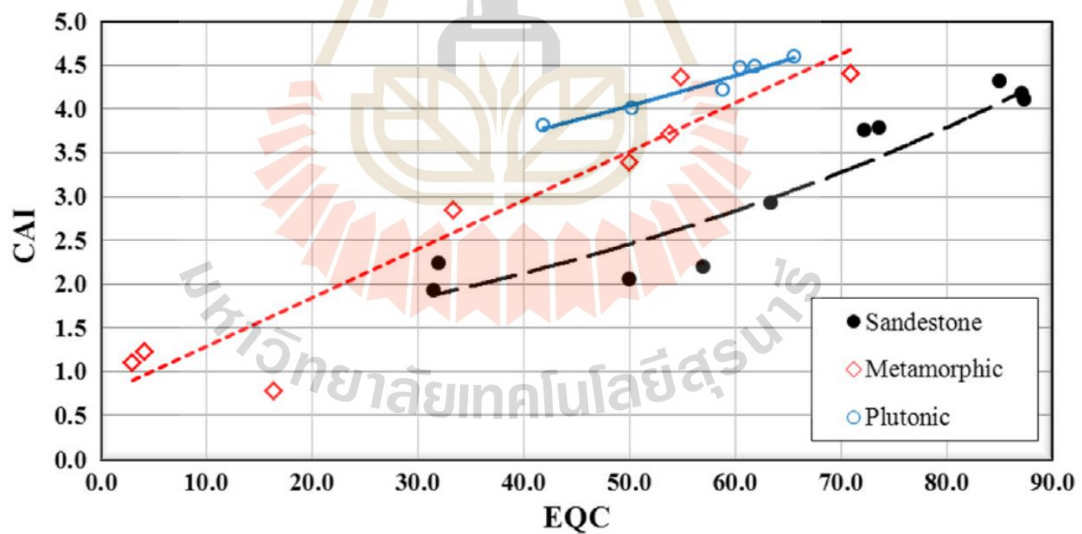


Figure II.7   CERCHAR abrasivity index (CAI) plotted against equivalent quartz content (EQC) for sandstones, metamorphic and plutonic rocks (Moradizadeh et al., 2016).

## 2.4    CERCHAR scratching energy

The energy obtained by a stylus scratching on a rock surface during a CERCHAR test is referred to as specific energy (SE), as defined by Hamzaban et al. in 2018. In 2020, Zhang, Konietzky, and Frühwirt referred to this parameter as scratching specific energy (SSE) or CERCHAR specific energy (CSE). This energy can be calculated by determining the work done (W) during the movement of the pin stylus, obtained by integrating the scratching force applied on the stylus over a scratching distance of 10 mm, and dividing it by the excavated or removed volume (V) of the specimen for the entire length of the scratch.

### 2.4.1    Material removal volume

Several researchers have studied the volume parameters relevant in CERCHAR testing. These parameters include the wear volume of the tested stylus and the groove volume of the material or rock surface after scratching. The wear volume of the tested stylus can be determined using an equation of a cone, where the radius and height of the cone are half of the stylus tip wear width, as shown in Figure 2.8 (a) (Hamzaban et al., 2019; Zhang and Konietzky, 2020). On the other hand, the groove volume is calculated by integrating along the scratching length of a trapezoid area equation (Figure 2.8 (b)) presented by Hamzaban et al. (2019). To determine the volume of the removed material, a scanning electron microscope (SEM) is used to observe the rock surface after scratching (Zhang and Konietzky, 2020). Both volume parameters are used in the calculation of scratch volume to wear ratio (SVWR) (Hamzaban et al., 2019) and CERCHAR abrasion ratio (CAR) (Zhang and Konietzky, 2020; Zhang, Konietzky, Song and Zhang, 2020). In addition, the volume of removed material is used to calculate the CSE (Hamzaban et al., 2018; Zhang, Konietzky and Frühwirt, 2020; Zhang, Konietzky, Song and Zhang, 2020).
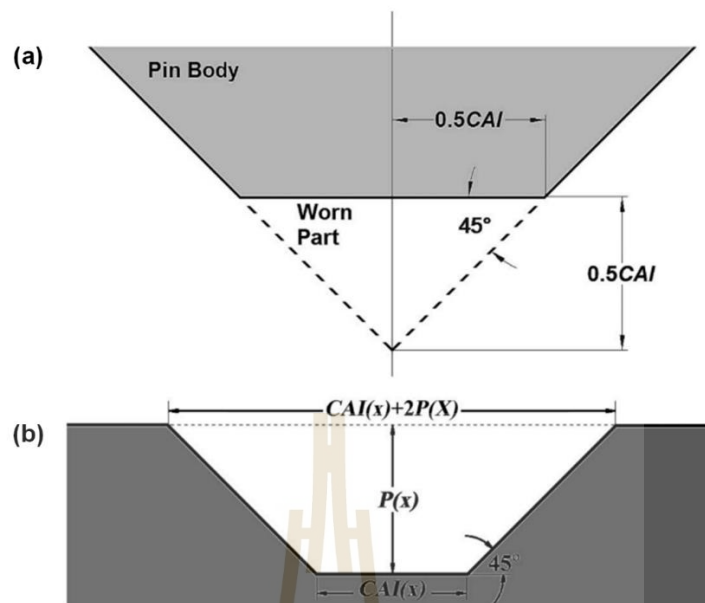
Figure II.8   Geometry of the worn pin tip (a) and the cross section of scratch on the sample surface at a distance of x from the beginning of the motion path (b) (not to scale) (Hamzaban et al., 2019).

### 2.4.2   CERCHAR specific energy

Concept of specific energy in the rock drilling process has been studied since 1965 (Teale, 1965). Specific energy is one of the most important factors for determining the efficiency of cutting or drilling systems stated by Yarali, Duru, and Sakız, (2014). They use the specific energy equation as a function of uniaxial compressive strength that differ from Hamzaban et al. (2018) and Zhang, Konietzky and Frühwirt (2020), that use a work done, which is given by a value of area under the force-displacement curve, divided by a material removal volume in the scratch groove. The other specific energy using a chisel tool has been conducted by Rostami et al. (2020), but the equation is close to specific energy by CERCHAR test.

Relationships between CERCHAR specific energy and other parameters are conducted by two groups of researchers. Hamzaban et al. (2018) found SE increases exponentially as CAI value increases with both stylus hardness of 43 ($R^2$ = 0.649) and

55 ($R^2$ = 0.830) HRC. This confirms the results of Zhang, Konietzky and Frühwirt (2020), who find the exponentially relationship with $R^2$ equal 0.68. The CSE correlations with the rock mechanical properties, including strength, Young's modulus, tensile strength, and P wave velocity, have been compared with the CAI correlation by Zhang, Konietzky and Frühwirt (2020). They find the CSE correlations are better in exponential than the CAI with linear correlations. This is different from the study of Hamzaban et al. (2018), who propose a linear correlation with mechanical properties for rock strength, Young's modulus, and tensile strength.

# CHAPTER III
# SAMPLE PREPARATION

## 3.1    Introduction

This chapter gives a description of rock samples used in this study. The tests are performed on different rock types, obtained within Thailand, to investigate the impacts of various testing parameters. The samples are prepared for the CERCHAR test, and uniaxial compression and triaxial compression tests. The CERCHAR specimen dimensions and all rock units are given.

## 3.2    Rock classification

All rocks in this study are divided into six groups: clastic, plutonic, carbonate, sulfate and chloride, silicate, and volcanic groups. Each rock is taken from various locations in Thailand. Rock data such as period, rock unit, rock code, rock location is given, which are presented in Table 3.1. The rock codes giving in the table follow those given by DMR (2007).

## 3.3    Rock sample preparation

Twenty-one types of rock samples are prepared to obtain core with diameter of 54 mm and length-to-diameter of 1, 2, and 2.5 for the CERCHAR specimens (Figure 3.1), for uniaxial compression test (Figure 3.2), and for triaxial compression test (Figure 3.3). Table 3.2 shows the dimensions and weights of the specimens. They follow ASTM D7625-10 (2010) and D7012-14 (2014) standard practice. The bedding plane orientation is perpendicular to the major axis for sedimentary rocks. Number of specimens for each test complies with its ASTM standard.

Table III.1 Rock units for each group.

| Group | Period* | Rock Unit | Rock Type | Code | Location | Sources |
|---|---|---|---|---|---|---|
| Clastic | K-J | Phu Phan | Sandstone | Kpp | Nakhon Ratchasima | DMR (2010) |
| | K | Sao Khua | Sandstone | Ksk | Nakhon Ratchasima | DMR (2010) |
| | K | Phra Wihan | Sandstone | JKpw | Nakhon Ratchasima | DMR (2010) |
| | J | Phu Kradung | Sandstone | Jpk | Nakhon Ratchasima | DMR (2010) |
| Plutonic | TR | Rayong-Bang Lamung | Granodiorite | Trgr | Chonburi | DMR (2011) |
| | C | Tak Batholith | Granite | Cgr | Tak | Mahawat et al. (1990) |
| | TR | Haad Som Pan | Granite | Kgr | Ranong | DMR (2007) |
| Carbonate | P | Khao Khad | Marble | Pkd | Lopburi | DMR (2007) |
| | P | Khao Khad | Limestone | Pkd | Saraburi | DMR (2007) |
| | P | Khao Khad | Travertine | Pkd | Saraburi | Thambunya et al. (2007) |
| Sulfate and Chloride | P - C | Tak Fa | Gypsum | Tkb | Nakhon Sawan | Utha-aroon and Ratanajaruraks (1996) |
| | P - C | Tak Fa | Anhydrite | Tkb | Nakhon Sawan | |
| | K | Maha Sarakham | Salt | KTms | Nakhon Ratchasima | DMR (2010) |
| Silicate | TR - P | N/A | Pyrophyllite | PTRv | Saraburi | DMR (2007) |
| | TR - P | N/A | Dickite | PTRv | Saraburi | DMR (2007) |
| | TR - P | N/A | Skarn | PTRv | Saraburi | DMR (2007) |
| Volcanic | Q | Khao Kradong | Basalt | Qbs | Buriram | DMR (2010) |
| | Q | Khao Kradong | Vesicular Basalt | Qbs | Nakhon Ratchasima | DMR (2010) |
| | TR - P | Khao Yai | Rhyolite | PTRv | Saraburi | DMR (2007) |
| | TR - P | Khao Yai | Andesite | PTRv | Saraburi | DMR (2007) |
| | TR - P | Khao Yai | Volcanic tuff | PTRv | Saraburi | DMR (2007) |

* Carboniferous (C), Permain (P), Triassic (TR), Jurassic (J), Cretaceous (K), and Quaternary (Q)

Figure III.1   Some specimens used in CERCHAR testing classified in six groups, clastic (a), plutonic (b), carbonate (c), sulfate and chloride (d), silicate (e), volcanic groups (f).

Table III.2 Dimensions and densities of specimens prepared for CERCHAR testing

| Group | Specimen type | Weight (g) | Diameter (mm) | Length (mm) | Density (g/cc) |
|---|---|---|---|---|---|
| Clastic | Phu Phan Sandstone | 293.40 | 54.13 | 53.89 | 2.37 ± 0.03 |
| | Sao Khua Sandstone | 285.70 | 54.17 | 55.11 | 2.25 ± 0.00 |
| | Phra Wihan Sandstone | 281.81 | 54.08 | 54.56 | 2.25 ± 0.01 |
| | Phu Kradung Sandstone | 314.72 | 54.04 | 54.53 | 2.52 ± 0.03 |
| Plutonic | Rayong-Bang Lamung Granodiorite | 343.80 | 54.35 | 57.15 | 2.59 ± 0.02 |
| | Tak Granite | 343.39 | 54.23 | 57.42 | 2.59 ± 0.03 |
| | Haad Som Pan Granite | 342.79 | 54.71 | 56.94 | 2.56 ± 0.03 |
| Carbonate | Khao Khad Marble | 346.15 | 53.74 | 54.94 | 2.78 ± 0.03 |
| | Khao Khad Limestone | 359.75 | 53.52 | 58.44 | 2.74 ± 0.01 |
| | Khao Khad Travertine | 359.28 | 53.78 | 57.55 | 2.75 ± 0.02 |
| Sulfate | Tak Fa Gypsum | 274.65 | 54.07 | 53.46 | 2.24 ± 0.02 |
| | Tak Fa Anhydrite | 367.56 | 54.11 | 55.82 | 2.86 ± 0.05 |
| | Maha Sarakham Salt | 357.63 | 54.21 | 54.62 | 2.11 ± 0.04 |
| Silicate | Pyrophyllite | 345.24 | 53.92 | 57.77 | 2.62 ± 0.04 |
| | Dickite | 310.88 | 53.24 | 53.42 | 2.61 ± 0.01 |
| | Skarn | 312.78 | 53.34 | 54.32 | 2.60 ± 0.02 |
| Volcanic | Khao Kradong Basalt | 372.82 | 54.04 | 57.65 | 2.82 ± 0.00 |
| | Khao Kradong Vesicular Basalt | 319.04 | 54.32 | 56.18 | 2.45 ± 0.04 |
| | Khao Yai Rhyolite | 343.69 | 54.51 | 56.55 | 2.60 ± 0.03 |
| | Khao Yai Andesite | 396.39 | 54.08 | 57.83 | 2.98 ± 0.03 |
| | Khao Yai Tuff | 360.68 | 54.13 | 56.12 | 2.79 ± 0.02 |

Figure III.2   Some specimens used in uniaxial compression test classified in six groups, clastic (a), plutonic (b), carbonate (c), sulfate and chloride (d), silicate (e), volcanic groups (f).
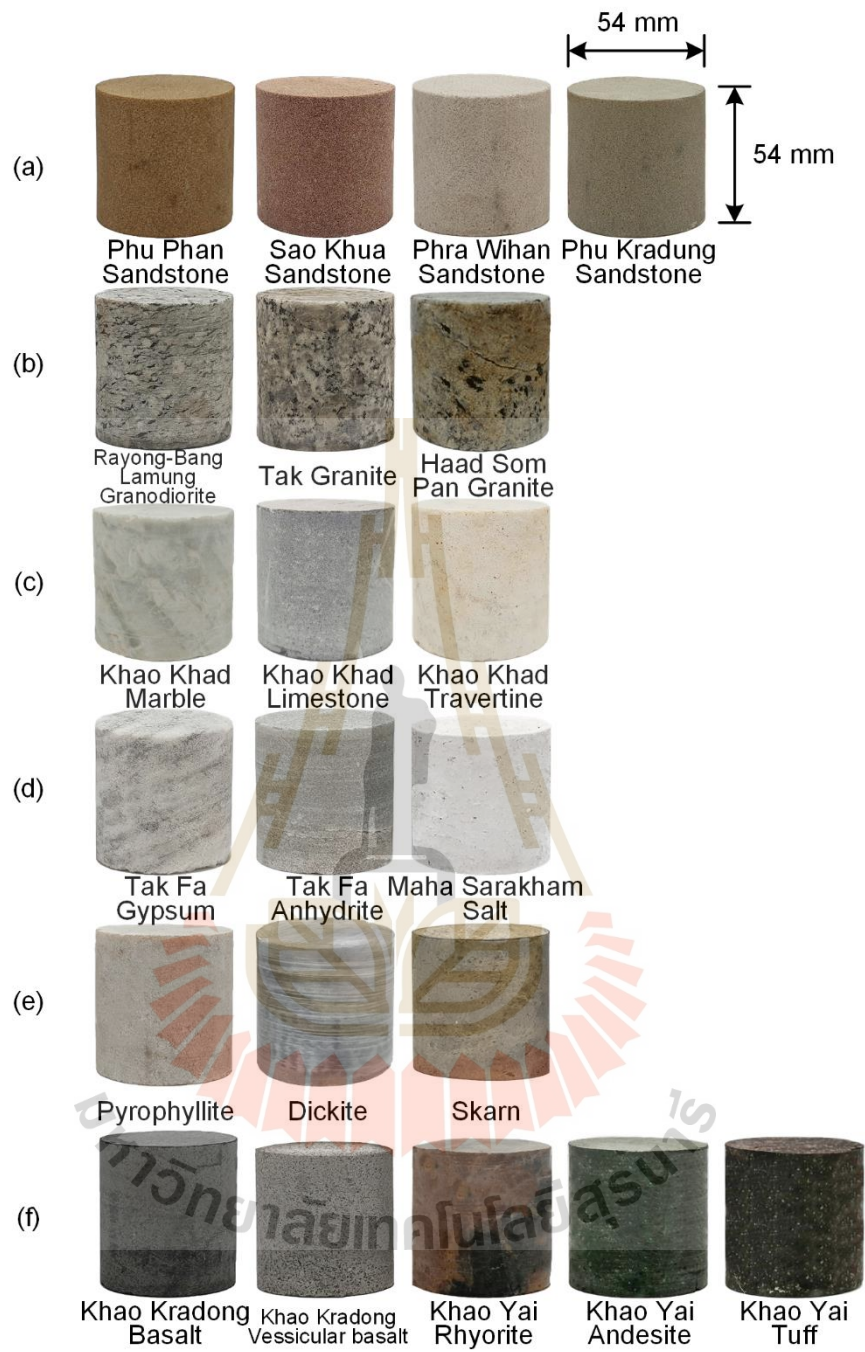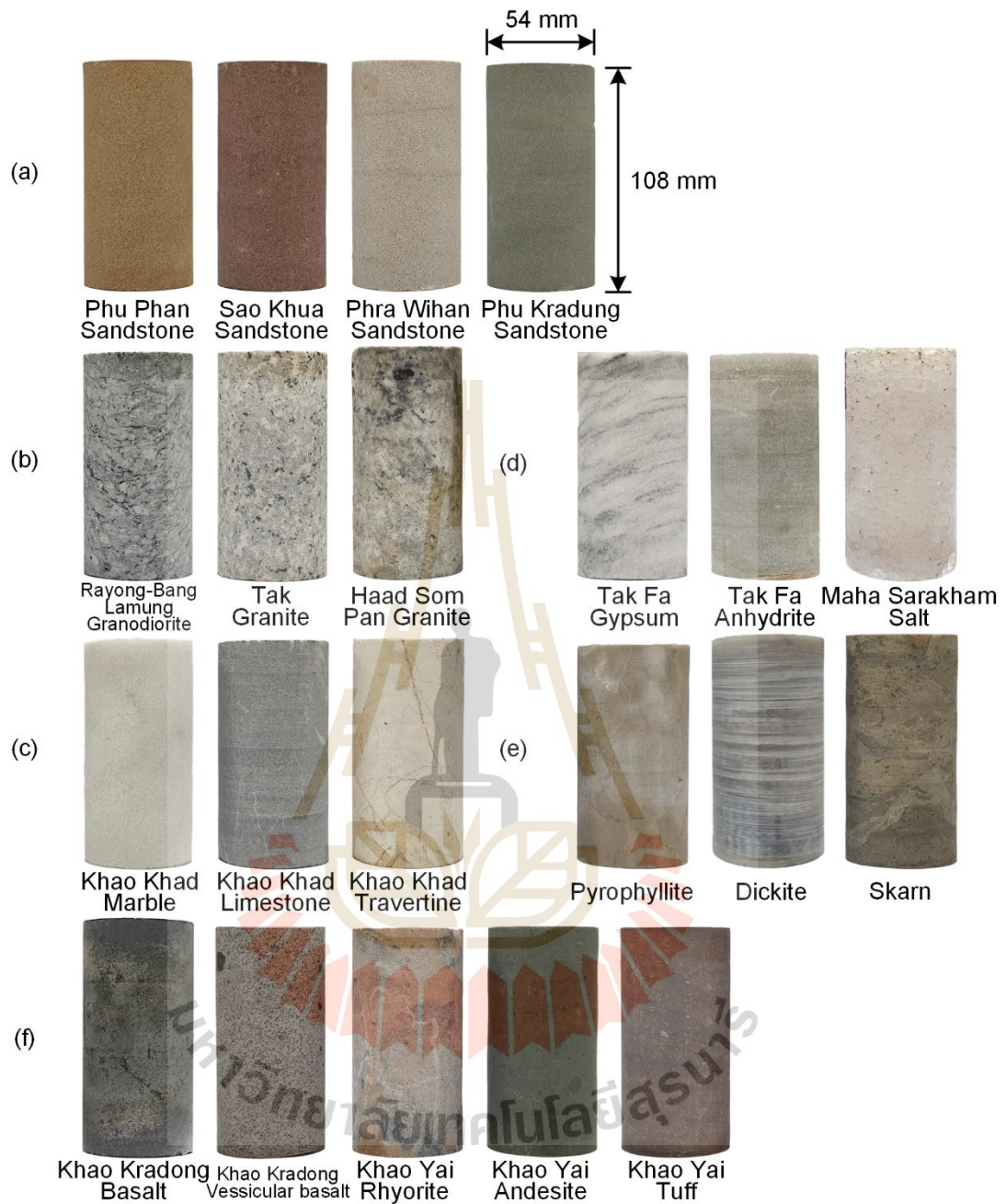
Figure III.3   Some specimens used in triaxial compression test classified in six groups, clastic (a), plutonic (b), carbonate (c), sulfate and chloride (d), silicate (e), volcanic groups (f).

# CHAPTER IV

# TEST APPARATUS AND METHODS

## 4.1 Introduction

Presented in this chapter are the test apparatus and test methods for determining CERCHAR abrasivity index (CAI) and the parameters for calculating CERCHAR specific energy (CSE). These parameters include ploughing force, vertical displacement, and mean groove volume. The test apparatus and methods for determining the physical and mechanical properties, and mineral compositions of the rock specimens are described.

## 4.2 CERCHAR test

The CERCHAR testing is performed on saw-cut surfaces of rock specimens with West apparatus, as shown in Figure 4.1. Figure 4.2 presents the schematic drawing of the CERCHAR device and shows the torque wrench and digital displacement gages that are used to determine the rotation torque to scratch the steel stylus. They are used to calculate ploughing force and determine the vertical displacements of ploughing groove. The steel stylus with Rockwell hardness of 55 (Figure 4.3) is used with 90 degrees conical tip. The test procedure and calculation follow the ISRM Suggested Method for Determining the Abrasivity of Rock by the CERCHAR Abrasivity Test (Alber et al., 2014). The equations for calculating the CAI are shown in Eq (4.1) and Eq (4.2). The schematic drawing of wear flat width of the stylus tip is shown in Figure 4.4. The stylus tip is measured by using a microscope with a minimum magnification of 25 times in accordance with the ISRM suggested method.

Figure IV.1 Device based on West CERCHAR apparatus (West, 1989) with additional torque and vertical displacement measurements.
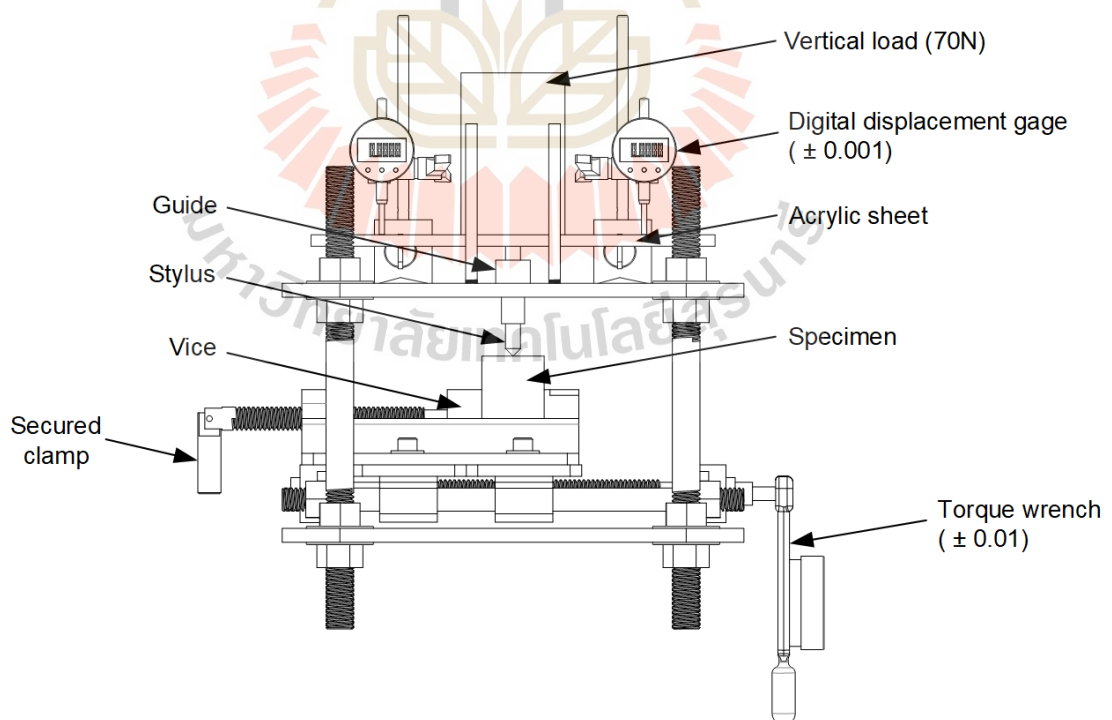


Figure IV.2 Schematic drawing of CERCHAR device used in this study.
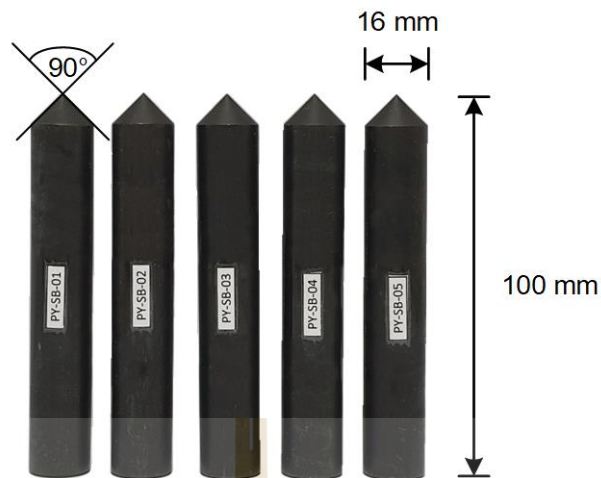
Figure IV.3 Examples of steel stylus-55 HRC for CERCHAR testing

For each rock surface, the scratching is repeated 5 times. Each time with a new stylus on a new scratch location. The wear flat width (d) of the stylus tip (Figure 4.4) is measured by stereomicroscope (Nikon SMZ745T) with magnification of 50 times. The average of d is used to calculate CAI as follows:

$$CAI = d \times 10 \tag{4.1}$$

where CAI is CERCHAR abrasivity index for natural surface, respectively. d is diameter of the wear flat area of the stylus tip with an accuracy of 0.01 mm. If saw cut specimen is tested, the wear flat of stylus tip is calculated from equation, as follows:

$$d = 1.14 \, d_{sc} \tag{4.2}$$

where $d_{sc}$ is the wear flat of stylus tip for the saw cut surface specimen performed in this study.
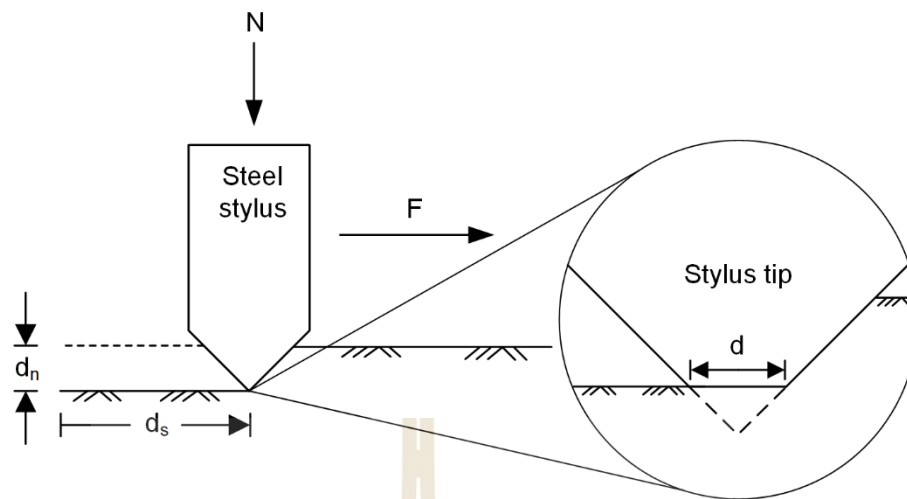
Figure IV.4  Steel stylus test variables, N is normal load (N), F is horizontal force (N), $d_n$ is vertical displacement (mm), $d_s$ is scratching distance (mm), and d is wear flat width of stylus tip.

The variables added beyond the standard suggestions in this study are shown in Figure 4.4. The vertical displacement is measured by using the digital displacement gages with a precision of 0.001 mm to measure groove depth during scratching. The horizontal force applied on the steel stylus can be calculated from torque on the crank using load torque required for driving a ball screw equation from Nidec corporation as shown in Eq. (4.3). The torque for moving the specimen to scratch the steel stylus could be obtained from the torque wrench, the additional torque measuring device from the West apparatus, with an accuracy of 0.01 N·m is shown in Figure 4.5.

$$F = 2\pi T/P \text{ (N)} \tag{4.3}$$

where F is ploughing force (N), T is torque (N·m) and P is screw pitch (0.001 m).
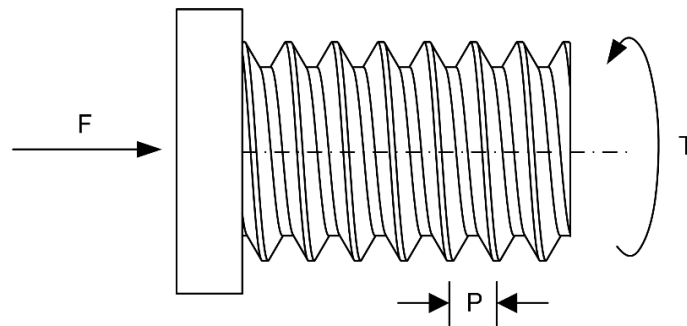
Figure IV.5 Force diagram used to convert torque (T) to horizontal force (F).

## 4.3    Uniaxial compression test

The objective of the uniaxial compression tests is to determine the ultimate strength and deformability of the cylindrical rock specimens. The test procedure follows ASTM D7012-14e1 (2014) standard practice. The axial stress is applied under a constant rate (0.1 MPa/s) until failure. The axial and lateral displacements are measured by 0.01 mm precision dial gages. The increasing of axial and lateral strains is recorded. The post-failure characteristics are observed and recorded. The elastic modulus and Poisson's ratio are determined from the test results. Figure 4.6 shows the uniaxial compression test device used in this study. The results are used to compare with those of CAI testing.
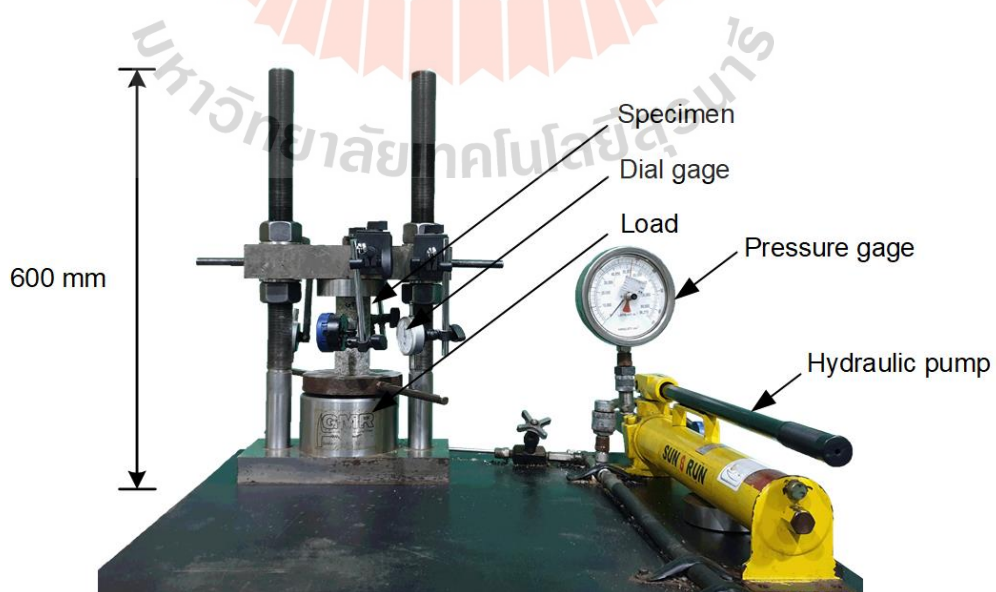


Figure IV.6 Uniaxial compression test device (Model PLT-75 POINT LOAD).

## 4.4    Triaxial compression test

The objective of the triaxial compression tests is to determine the cohesion and friction angle of the specimens based on Coulomb's criterion with different confining pressures. The test method is follows the ASTM D7012-14e1 (2014) standard practice. The constant confining pressures vary from 0.69 to 12 MPa depending on each rock type. While the constant confining pressure is applied, the axial stress is increased with constant rate until failure occurs. Neoprene sheets have been placed at the interfaces between loading platens and rock surfaces. The excess oil that released from the Hoek cell is measured by a high precision pipette to examine the specimen dilation. It can be used to calculate the volumetric strain and the lateral strain of the specimen during loading. The stress at failure and mode of failure are examined. The elastic modulus and Poisson's ratio are determined from the test results. Figure 4.7 shows the triaxial compression test device used in this testing.
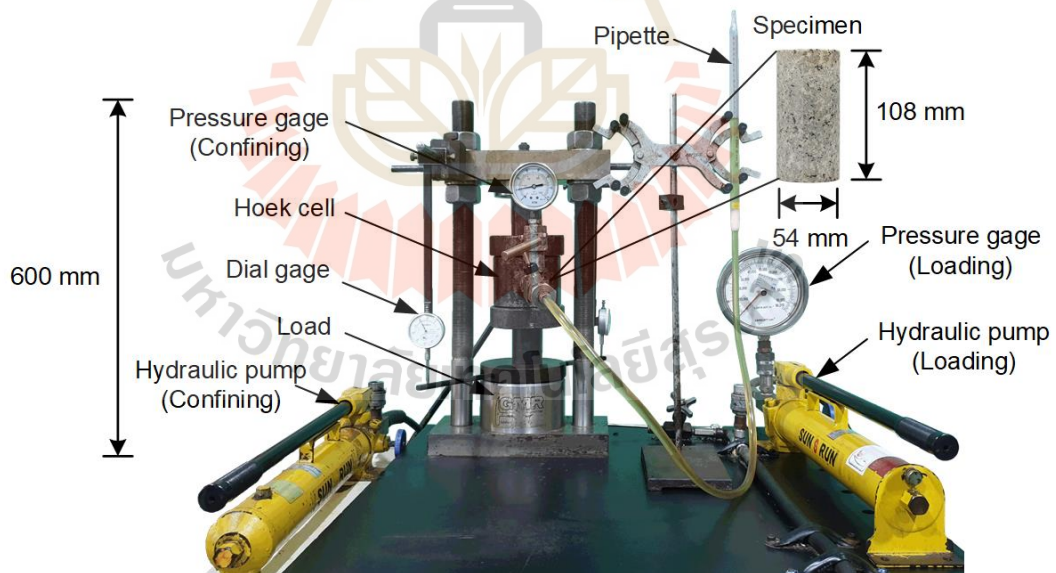


Figure IV.7 Triaxial compression test device (Model PLT-75 POINT LOAD).

## 4.5    X-ray diffraction

After uniaxial and triaxial compression tests are performed. Some specimens are prepared for X-ray diffraction analyze, which is performed using Bruker D8 advance, as shown in Figure 4.8. The test method follows ASTM D5357-19 (2019) standard practice. The specimens are ground to obtain powder with less than 0.25 mm particle size (pass through mesh #60). About 5 to 10 grams are used. DIFFRAC.EVA software is used to determine the weight percent of mineral compositions of the specimens. The mineral compositions will be used to help explain the results of CAI testing.
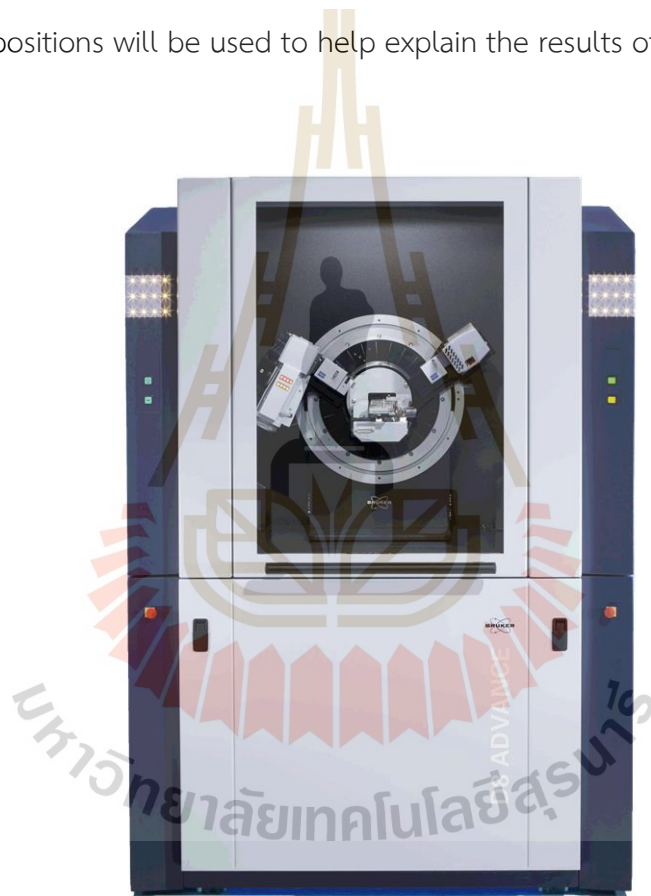


Figure IV.8  X-ray diffraction Bruker, D8 advance (Center for Scientific and Technology
Equipment University of Technology).

# CHAPTER V

# TEST RESULTS

## 5.1    Introduction

Results obtained from the laboratory testing are described in this chapter. They include those of uniaxial and triaxial compression tests, CERCHAR abrasivity index test, and X-ray diffraction analysis. Beyond the suggested method of CERCHAR test, the results of additional measurements from the CERCHAR test include scratching force along the testing length and groove volume on specimen surface after scratching.

## 5.2    Uniaxial and triaxial compression test

The mechanical properties are determined by using the uniaxial and triaxial compression test results following the ASTM D7012-14e-1 (2014). Trends of uniaxial compressive strength of the plutonic and clastic rock groups are higher than the others, besides that the strength of some rocks in the volcanic group such as andesite and basalt are also high. The andesite shows the highest strength (110.1±51.4 MPa) in this study. The sulfate and chloride group gives the lowest strength and elastic properties. The plutonic and silicate groups have high elastic values. Corresponding to the high strength groups, the plutonic and clastic rock groups have low Poisson's ratios except for the sulfate group. The high Poisson's ratio groups are the carbonate and silicate. From the triaxial compression test results, the cohesion and friction angle do not show clear trend with the rock group. The rock with the highest cohesion is Tak granite in the plutonic group and the lowest is Nakhon Sawan gypsum in the sulfate group. Most rocks in plutonic and volcanic groups have high friction angles. The rocks with lowest friction angles are in sulfate group rocks. All results are shown in Tables 5.1 and 5.2, summarizing the uniaxial compressive strengths ($\sigma_c$), Young's modulus (E) and

Poisson's ratio ($\nu$) from stress-strain curves of the uniaxial compression tests, and cohesion (c) and friction angle ($\phi$) from Mohr's circles of the triaxial compression test.

Table V.1 Summary results of uniaxial compression test.

| Rock group | Rock type | Uniaxial compression test | | |
|---|---|---|---|---|
| | | $\sigma_c$ (MPa) | E (GPa) | $\nu$ |
| Clastic | Phu Phan Sandstone | 81.4 ± 11.4 | 11.5± 2.3 | 0.19 ± 0.04 |
| | Sao Khua Sandstone | 53.1 ± 5.5 | 4.8 ± 0.9 | 0.18 ± 0.02 |
| | Phra Wihan Sandstone | 70.4 ± 2.1 | 11.5 ± 1.7 | 0.20 ± 0.02 |
| | Phu Kradung Sandstone | 80.1 ± 18.6 | 5.8 ± 1.2 | 0.12 ± 0.01 |
| Plutonic | Rayong-Bang Lamung Granodiorite | 72.5 ± 12.0 | 20.0 ± 3.2 | 0.20 ± 0.02 |
| | Tak Granite | 84.5 ± 22.1 | 11.6 ± 3.2 | 0.15 ± 0.03 |
| | Haad Som Pan Granite | 37.1 ± 14.0 | 7.3 ± 3.9 | 0.22 ± 0.02 |
| Carbonate | Khao Khad Marble | 36.4 ± 10.5 | 7.6 ± 1.7 | 0.23 ± 0.02 |
| | Khao Khad Limestone | 54.6 ± 13.2 | 14.3 ± 3.0 | 0.33 ± 0.01 |
| | Khao Khad Travertine | 59.6 ± 16.0 | 15.9 ± 2.4 | 0.26 ± 0.02 |
| Sulfate and Chloride | Tak Fa Gypsum | 5.6 ± 0.8 | 5.3 ± 4.0 | 0.20 ± 0.06 |
| | Tak Fa Anhydrite | 32.2 ± 9.5 | 8.7 ± 2.0 | 0.20 ± 0.01 |
| | Maha Sarakham Salt | 22.6 ± 4.4 | 2.1 ± 0.4 | 0.33 ± 0.02 |
| Silicate | Pyrophyllite | 80.8 ± 10.9 | 17.8 ± 3.2 | 0.34 ± 0.03 |
| | Dickite | 32.3 ± 5.5 | 11.2 ± 2.0 | 0.23 ± 0.00 |
| | Skarn | 70.4 ± 18.6 | 14.3 ± 6.6 | 0.20 ± 0.00 |
| Volcanic | Khao Kradong Basalt | 79.2 ± 12.1 | 13.3 ± 1.6 | 0.12 ± 0.02 |
| | Khao Kradong Vesicular Basalt | 63.9 ± 3.9 | 13.2 ± 2.7 | 0.30 ± 0.01 |
| | Khao Yai Rhyolite | 38.5 ± 5.8 | 9.9 ± 1.9 | 0.23 ± 0.02 |
| | Khao Yai Andesite | 110.1 ±51.4 | 13.5 ± 8.7 | 0.32 ± 0.01 |
| | Khao Yai Tuff | 41.1 ± 13.4 | 7.6 ± 2.0 | 0.34 ± 0.01 |

Table V.2 Summary results of triaxial compression test.

| Rock group | Rock type | Triaxial compression test | |
|---|---|---|---|
| | | c (MPa) | φ (Degree) |
| Clastic | Phu Phan Sandstone | 8.6 | 59 |
| | Sao Khua Sandstone | 9.7 | 47 |
| | Phra Wihan Sandstone | 3.6 | 57 |
| | Phu Kradung Sandstone | 14.0 | 51 |
| Plutonic | Rayong-Bang Lamung Granodiorite | 8.6 | 59 |
| | Tak Granite | 15.7 | 56 |
| | Haad Som Pan Granite | 9.9 | 49 |
| Carbonate | Khao Khad Marble | 3.2 | 65 |
| | Khao Khad Limestone | 10.2 | 55 |
| | Khao Khad Travertine | 6.0 | 59 |
| Sulfate and Chloride | Tak Fa Gypsum | 1.6 | 34 |
| | Tak Fa Anhydrite | 7.8 | 26 |
| | Maha Sarakham Salt | 10.6 | 29 |
| Silicate | Pyrophyllite | 15.1 | 50 |
| | Dickite | 5.6 | 45 |
| | Skarn | 10.5 | 50 |
| Volcanic | Khao Kradong Basalt | 12.8 | 55 |
| | Khao Kradong Vesicular Basalt | 9.4 | 54 |
| | Khao Yai Rhyolite | 9.8 | 50 |
| | Khao Yai Andesite | 13.3 | 64 |
| | Khao Yai Tuff | 4.3 | 57 |

## 5.3 CERCHAR abrasivity index results

The steel stylus after 10 mm scratching is measured by using a stereomicroscope with 50 times resolution. Figure 5.1 shows some steel stylus tip image of Phu Phan sandstone in the same direction with their corresponding groove images 5 pins. The averages of wear width (d) obtained from the stylus tip images after scratching are used to calculate the CAI value from Equation (4.1) in Chapter 4. Table 5.2 shows the calculated CAI results and the abrasivity classification based on the classification system of the ISRM suggested method for CERCHAR abrasivity test (Alber et al., 2014). From the overview of each group in the table, almost all the CAI values in each group are related to uniaxial compressive strength more than those of triaxial compression tests. The CAI and $\sigma_c$ of the rocks in the plutonic group are the highest in this study. The volcanic and clastic rock groups have the second and third highest CAI values respectively. This implies that there are other mechanisms governing CAI values beside the $\sigma_c$. The lowest CAI value is from the sulfate group that is agreeable with their $\sigma_c$ which are lower than other groups.
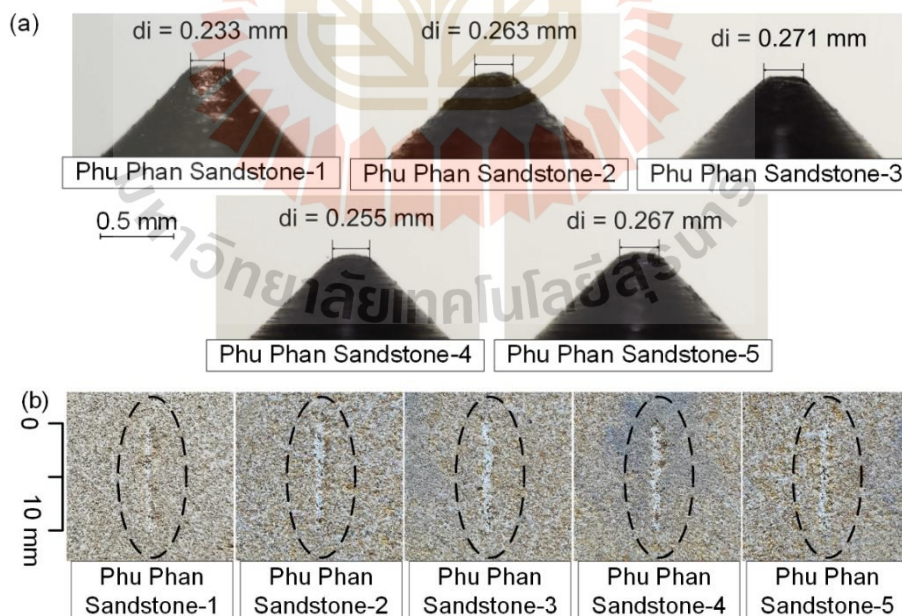


Figure V.1   (a) Some steel stylus tips after CERCHAR testing on Phu Phan sandstone specimens and (b) their corresponding groove images.

Table V.3 Average results of CERCHAR testing.

| Group | Rock type | d (mm) | CAI | ISRM Classification |
|---|---|---|---|---|
| Clastic | Phu Phan Sandstone | 0.265 ± 0.023 | 3.017 ± 0.316 | High |
| | Sao Khua Sandstone | 0.162 ± 0.039 | 1.850 ± 0.462 | Low |
| | Phra Wihan Sandstone | 0.347 ± 0.044 | 3.953 ± 0.722 | High |
| | Phu Kradung Sandstone | 0.151 ± 0.051 | 1.725 ± 0.681 | Low |
| Plutonic | Rayong-Bang Lamung Granodiorite | 0.402 ± 0.046 | 4.583 ± 0.733 | Very high |
| | Tak Granite | 0.428 ± 0.062 | 4.879 ± 0.879 | Very high |
| | Haad Som Pan Granite | 0.422 ± 0.051 | 4.806 ± 0.604 | Very high |
| Carbonate | Khao Khad Marble | 0.174 ± 0.070 | 1.981 ± 0.922 | Low |
| | Khao Khad Limestone | 0.125 ± 0.019 | 1.430 ± 0.280 | Low |
| | Khao Khad Travertine | 0.184 ± 0.024 | 2.094 ± 0.323 | Medium |
| Sulfate and Chloride | Tak Fa Gypsum | 0.031 ± 0.018 | 0.351 ± 0.223 | Extremely low |
| | Tak Fa Anhydrite | 0.095 ± 0.042 | 1.088 ± 0.549 | Low |
| | Maha Sarakham Salt | 0.078 ± 0.025 | 0.892 ± 0.242 | Very low |
| Silicate | Pyrophyllite | 0.294 ± 0.046 | 3.348 ± 0.711 | High |
| | Dickite | 0.138 ± 0.069 | 1.578 ± 0.900 | Low |
| | Skarn | 0.218 ± 0.043 | 2.487 ± 0.526 | Medium |
| Volcanic | Khao Kradong Basalt | 0.307 ± 0.025 | 3.502 ± 0.427 | High |
| | Khao Kradong Vesicular Basalt | 0.311 ± 0.056 | 3.548 ± 0.691 | High |
| | Khao Yai Rhyolite | 0.282 ± 0.083 | 3.219 ± 1.121 | High |
| | Khao Yai Andesite | 0.306 ± 0.041 | 3.493 ± 0.643 | High |
| | Khao Yai Tuff | 0.248 ± 0.096 | 2.827 ± 1.135 | Medium |

## 5.4 Lateral force and vertical displacement

Rotational torque for moving the stylus pin and vertical displacement of the stylus pin during scratching are the additional parameters beyond the suggested method of CERCHAR. The lateral force, which is calculated from torque is related to scratching distance and the vertical displacement. Figures 5.2 through 5.7 show the relations of average lateral force (F) and average vertical displacement ($d_n$) as a function of scratching distance ($d_s$). The best-fitting equation for F-$d_s$ relations of each pin are shown in Equation (5.1). About the first 3 mm of scratching, the force increases rapidly as the scratching distance increases. Beyond 3 mm, the force increases more gradually. The scratching forces of the clastic group tend to be the highest, and the lowest forces are found in the plutonic and silicate groups. In hard rock, the stylus is forced to slide on the rock surface rather than penetrating into it. This is similar to the results obtained by Zhang, Konietzky, Song, and Huang (2020). For that reason, the force of scratching on granite rock is low. For clastic group, vesicular basalt in the volcanic group, and anhydrite in the sulfate group show higher force than the others because of their highs porosity (Table 5.3). The trends of vertical displacement of the clastic group seem to be more consistent or similar. The other groups show more variated results.

$$F = a \cdot (1 - \exp \cdot (- b \cdot d_s)) \qquad (5.1)$$

where a and b are the empirical counts.
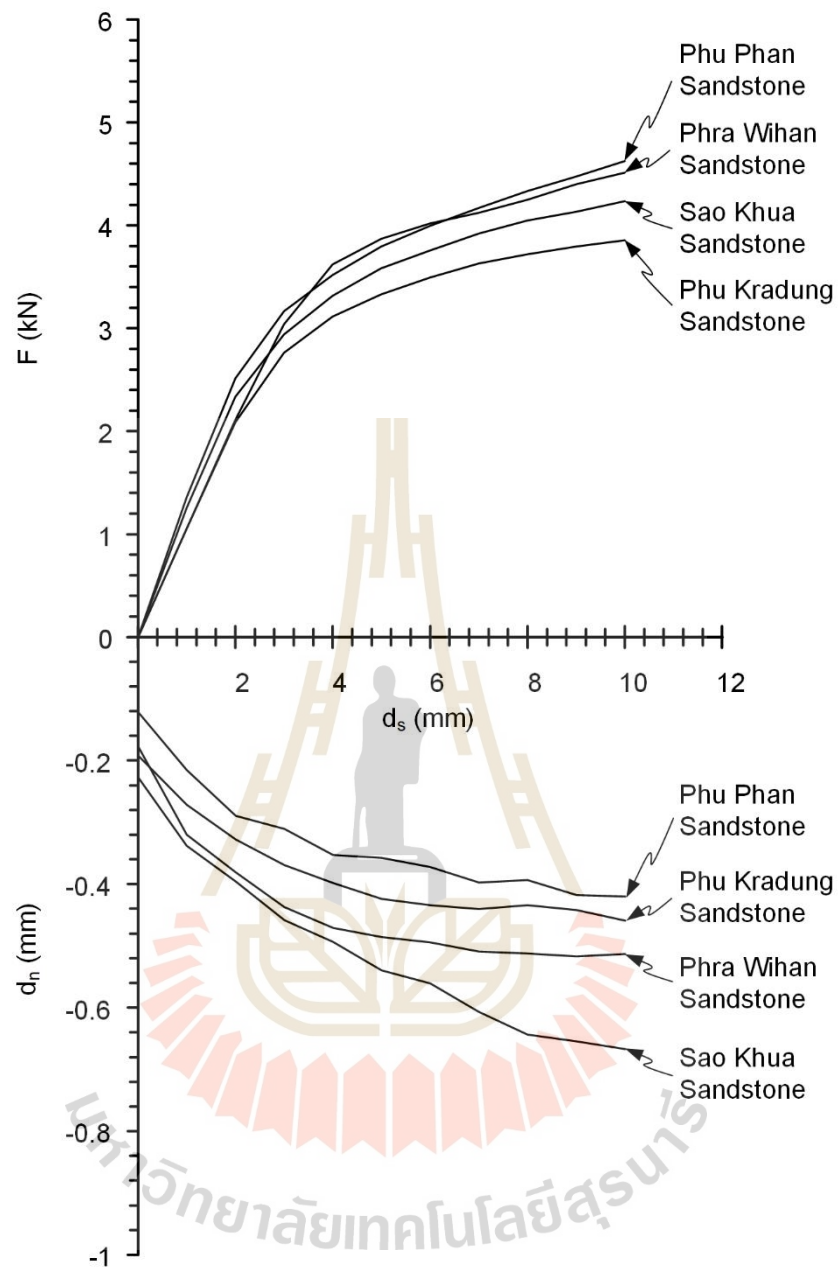
Figure V.2  Scratching forces (F) and vertical displacement ($d_n$) as a function of scratching distance ($d_s$) of clastic rock group.
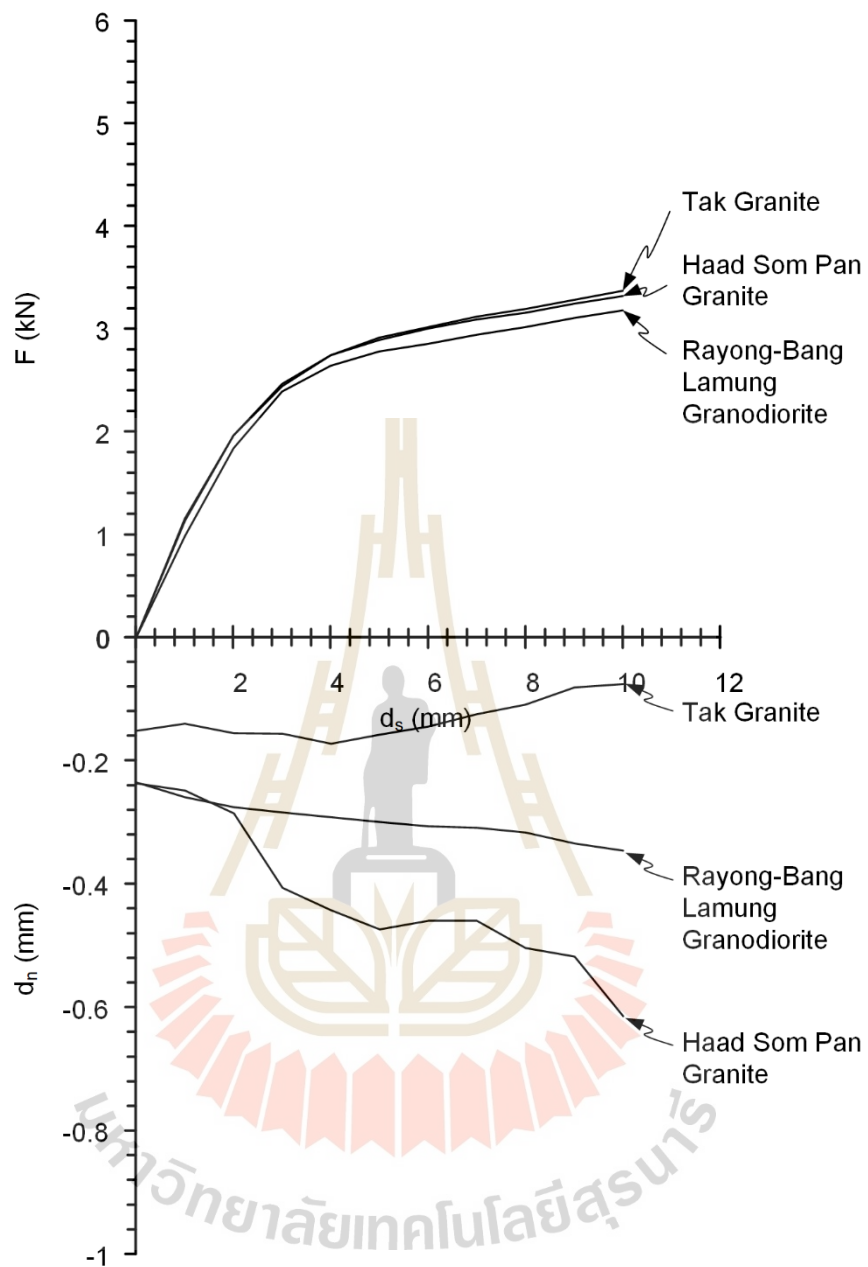
Figure V.3 Scratching forces (F) and vertical displacement ($d_n$) as a function of scratching distance ($d_s$) of plutonic rock group.
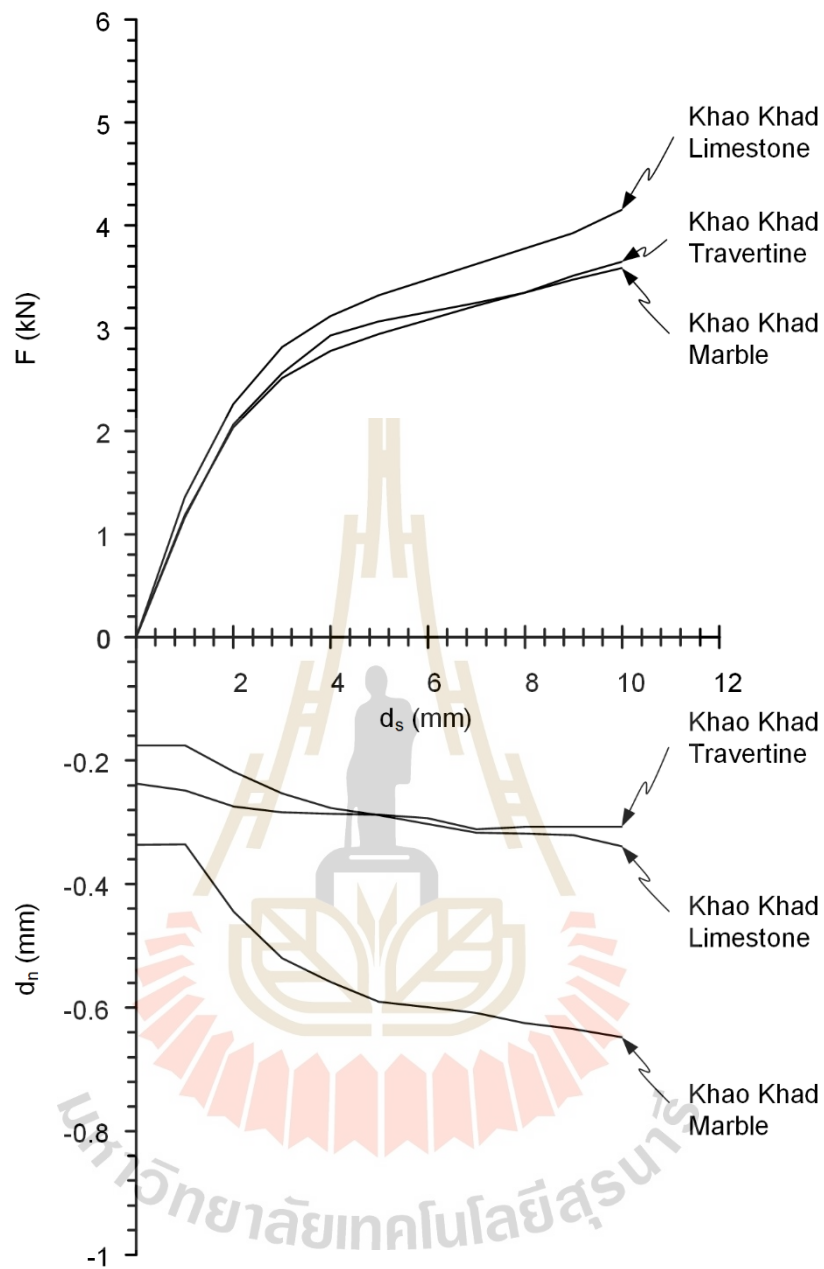
Figure V.4   Scratching forces (F) and vertical displacement ($d_n$) as a function of scratching distance ($d_s$) of carbonate rock group.
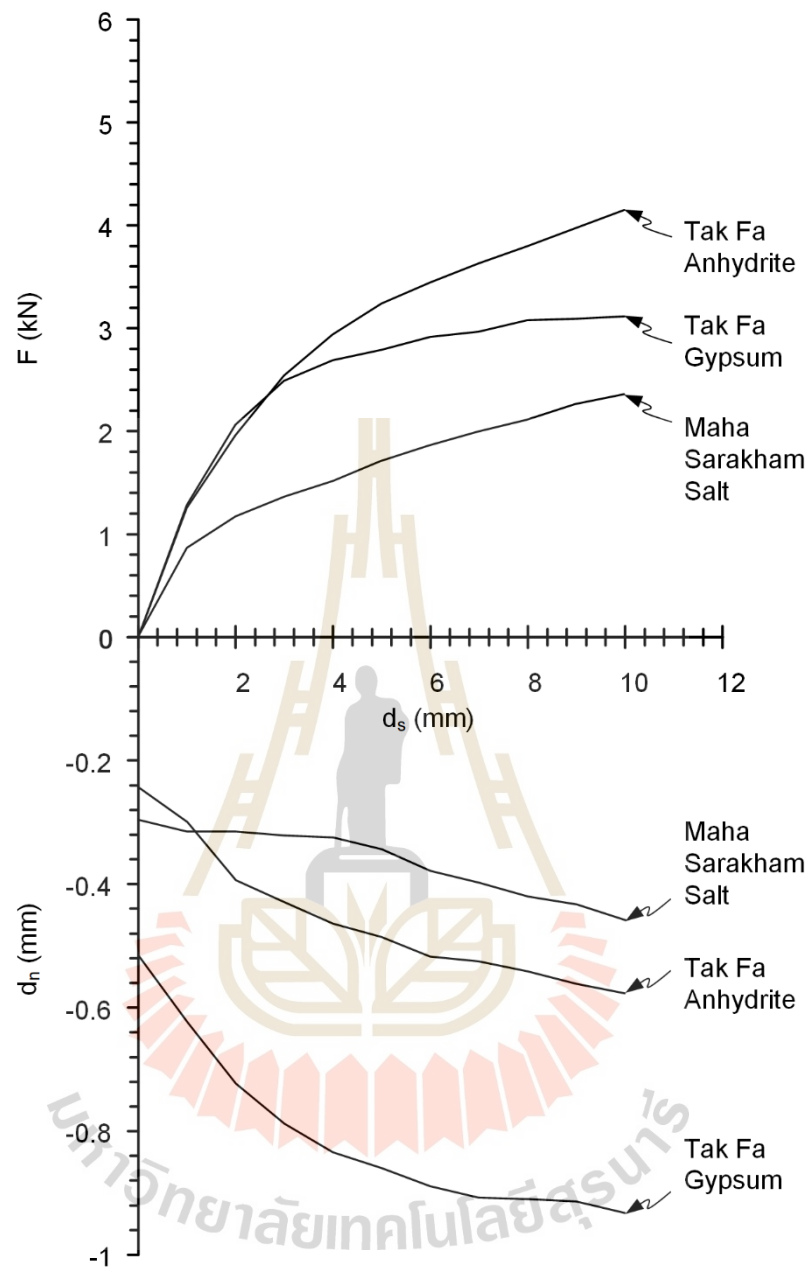
Figure V.5   Scratching forces (F) and vertical displacement ($d_n$) as a function of scratching distance ($d_s$) of sulfate and chloride rock group.
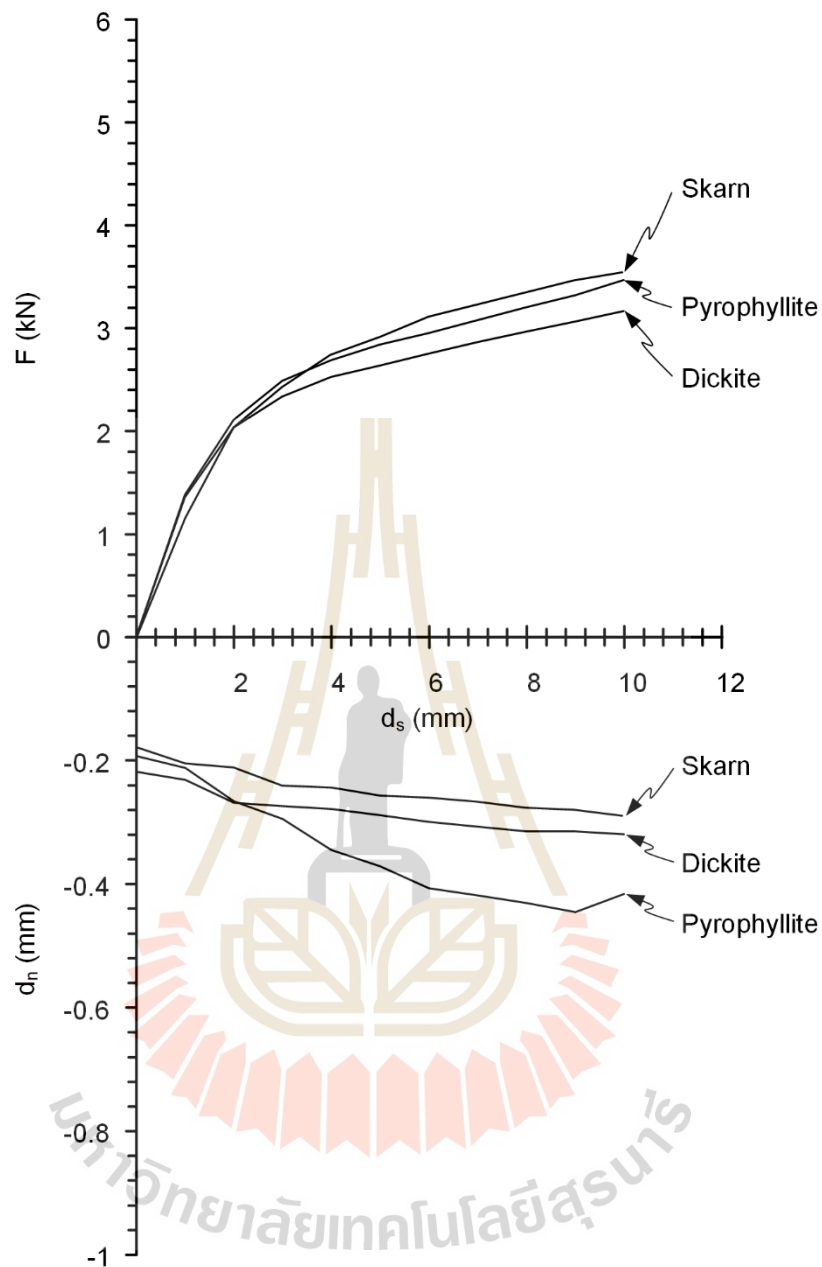
Figure V.6  Scratching forces (F) and vertical displacement ($d_n$) as a function of scratching distance ($d_s$) of silicate rock group.
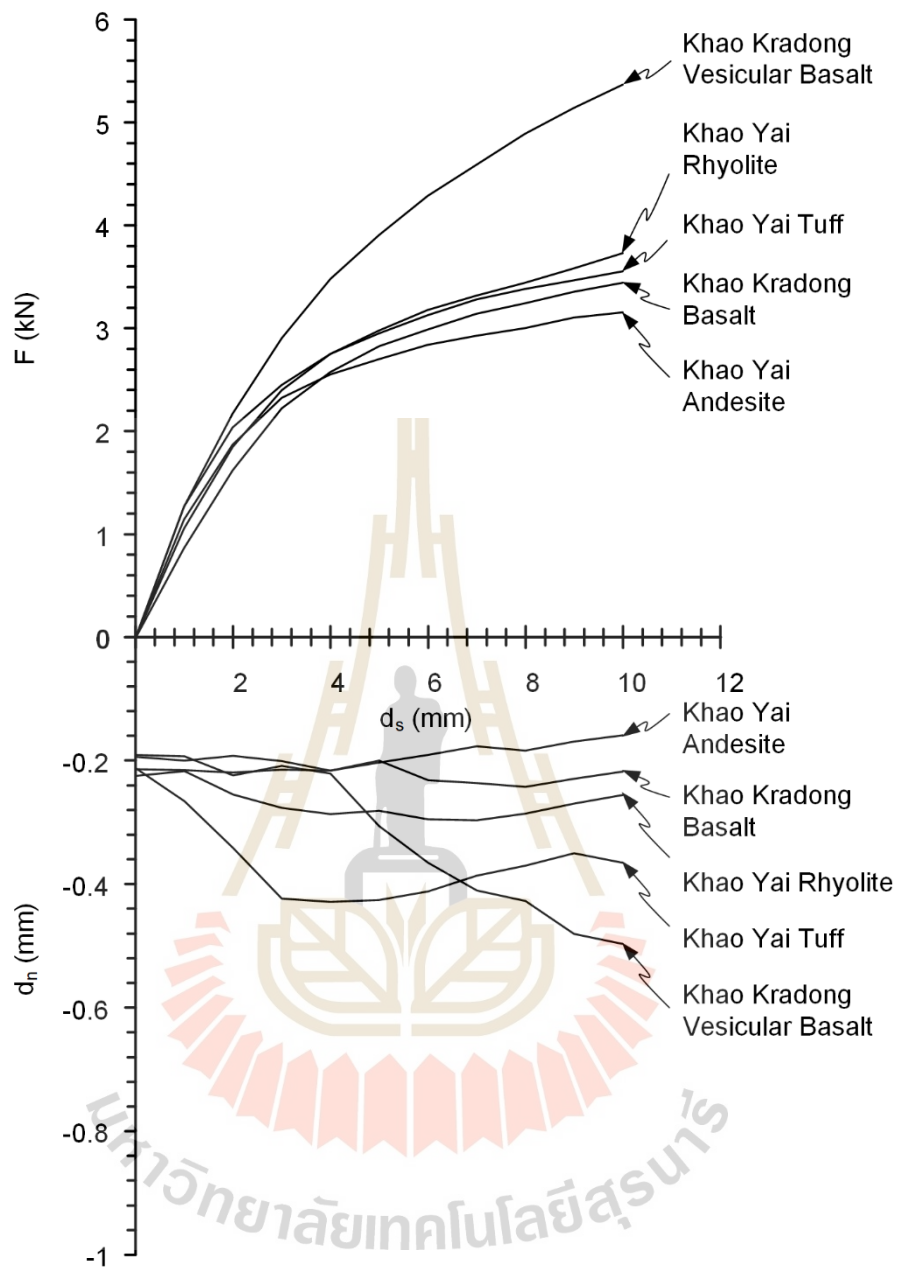
Figure V.7   Scratching forces (F) and vertical displacement ($d_n$) as a function of scratching distance ($d_s$) of volcanic rock group.

The porosity (n) giving in Table 5.3 are calculated from weight of submerged specimens follow ASTM C97 (2018). The equations are shown in Equations (5.1) through (5.3). Some specimens that cannot be submerged because they dissolve in water such as gypsum and salt. Their porosity are calculated follow Equations (5.4) through (5.6) from weight percentage of mineral contents (%W) that calculated from percentage of mineral contents obtained from X-ray diffraction method giving in Tables 5.5 through 5.10 and specific gravity (S.G.) of each mineral.

$$n = (V_v / V_{total}) \times 100 \tag{5.1}$$

$$V_v = (W_{sat} - W_{dry}) / \rho_{water} \tag{5.2}$$

$$V_{total} = W_{dry} / \rho_{rock} \tag{5.3}$$

where $V_v$ is pore volume of specimen ($cm^3$), $V_{total}$ is specimen volume ($cm^3$), and $W_{sat}$ is weight of the soaked and surface-dried specimen (g).

$$n = (V_{total} - \%V / V_{total}) \times 100 \tag{5.4}$$

$$\%V = \sum_{i=1}^{n} \left( \frac{W_i}{S.G._i} \right) \tag{5.5}$$

$$\%W = W_{total} \times \%A \tag{5.6}$$

where $\%V$ is percentage of mineral content by volume of specimen ($cm^3$), $W_{total}$ is weight of specimen (g), and $\%A$ is the mineral amount (%)

Table V.4 Rock porosity.

| Group | Rock type | Porosity (%) |
|---|---|---|
| Clastic | Phu Phan Sandstone | 7.29 ± 0.82 |
| | Sao Khua Sandstone | 4.38 ± 2.19 |
| | Phra Wihan Sandstone | 10.13 ± 2.13 |
| | Phu Kradung Sandstone | 5.34 ± 1.25 |
| Plutonic | Rayong-Bang Lamung Granodiorite | 0.75 ± 0.36 |
| | Tak Granite | 0.75 ± 0.50 |
| | Haad Som Pan Granite | 1.84 ± 0.77 |
| Carbonate | Khao Khad Marble | 0.18 ± 0.03 |
| | Khao Khad Limestone | 0.74 ± 0.17 |
| | Khao Khad Travertine | 1.50 ± 0.45 |
| Sulfate and Chloride | Tak Fa Gypsum | 4.44 ± 0.35 |
| | Tak Fa Anhydrite | 3.47 ± 1.30 |
| | Maha Sarakham Salt | 4.66 ± 0.08 |
| Silicate | Pyrophyllite | 1.30 ± 0.46 |
| | Dickite | 2.06 ± 0.01 |
| | Skarn | 0.33 ± 0.02 |
| Volcanic | Khao Kradong Basalt | 0.76 ± 0.11 |
| | Khao Kradong Vesicular Basalt | 6.58 ± 0.21 |
| | Khao Yai Rhyolite | 0.56 ± 0.10 |
| | Khao Yai Andesite | 0.89 ± 0.30 |
| | Khao Yai Tuff | 1.15 ± 0.40 |

## 5.5    Mean groove volumes

After 10 mm scratching, the grooves on the specimen surface are examined by laser-scanning with a 0.2 mm line scan interval and the vertical precision in ± 1 micron. The data of scanning are used to calculate the groove volume of each groove by using SURFER software 16.6 (Golden Software, 2019). Table 5.4 presents the mean groove volume (V) and standard deviation for all rocks.

Table V.5 Mean groove volumes.

| Group | Rock type | V (mm$^3$) |
|---|---|---|
| Clastic | Phu Phan Sandstone | 2.712 ± 0.803 |
| | Sao Khua Sandstone | 3.988 ± 0.820 |
| | Phra Wihan Sandstone | 3.561 ± 0.778 |
| | Phu Kradung Sandstone | 2.593 ± 0.583 |
| Plutonic | Rayong-Bang Lamung Granodiorite | 1.244 ± 0.122 |
| | Tak Granite | 1.204 ± 0.274 |
| | Haad Som Pan Granite | 2.628 ± 0.461 |
| Carbonate | Khao Khad Marble | 4.554 ± 1.495 |
| | Khao Khad Limestone | 2.480 ± 0.834 |
| | Khao Khad Travertine | 1.722 ± 0.451 |
| Sulfate and Chloride | Tak Fa Gypsum | 10.795 ± 4.949 |
| | Tak Fa Anhydrite | 4.811 ± 1.559 |
| | Maha Sarakham Salt | 3.072 ± 1.501 |
| Silicate | Pyrophyllite | 1.981 ± 0.245 |
| | Dickite | 3.071 ± 1.036 |
| | Skarn | 2.995 ± 0.918 |
| Volcanic | Khao Kradong Basalt | 1.696 ± 0.192 |
| | Khao Kradong Vesicular Basalt | 1.818 ± 0.382 |
| | Khao Yai Rhyolite | 1.847 ± 0.353 |
| | Khao Yai Andesite | 1.828 ± 0.495 |
| | Khao Yai Tuff | 5.369 ± 0.839 |

## 5.6    X-ray diffraction analysis

The specimens after the compression test are finely ground to obtain a powder with less than 0.25 mm particle size (pass through mesh #60) as following the ASTM E1426-14e1 (2019) standard practice. The representative specimens, maximum and minimum density values, are used to determine the average weight percentage of mineral compositions by using the X-ray diffraction method (XRD). The results are shown in Tables 5.5 through 5.10.

Table V.6 Mineral compositions of rock specimens in clastic group.

| Clastic group | | Rock Type | | | |
| --- | --- | --- | --- | --- | --- |
| | | Phu Phan Sandstone (Kpp) | Sao Khua Sandstone (Ksk) | Phra Wihan Sandstone (JKpw) | Phu Kradung Sandstone (Jpk) |
| Mineral Compositions (%) | Quartz | 86.13 ± 0.81 | 71.89 ± 16.21 | 83.50 ± 0.01 | 38.35 ± 2.35 |
| | Kaolinite | 6.27 ± 1.05 | 5.29 ± 3.52 | 3.94 ± 0.09 | 2.94 ± 0.04 |
| | Muscovite | 1.65 ± 1.05 | 13.77 ± 9.34 | 0.66 ± 0.20 | 11.87 ± 0.53 |
| | Albite | 3.46 ± 0.48 | 6.06 ± 3.39 | 3.91 ± 0.30 | 22.05 ± 1.39 |
| | Anorthite | 0.00 | 0.23 ± 0.12 | 1.03 ± 0.02 | 2.39 ± 0.59 |
| | Microcline | 0.60 ± 0.14 | 1.66 ± 0.10 | 3.23 ± 0.13 | 4.43 ± 0.23 |
| | Calcite | 0.00 | 0.00 | 0.27 ± 0.08 | 0.24 ± 0.02 |
| | Oligoclase | 0.00 | 1.04 ± 0.04 | 0.00 | 9.53 ± 0.69 |
| | Chlorite | 1.90 ± 0.48 | 0.08 ± 0.02 | 3.48 ± 0.06 | 8.23 ± 0.52 |

Table V.7 Mineral compositions of rock specimens in plutonic group.

| Plutonic group | | Rock Type | | |
|---|---|---|---|---|
| | | Rayong-Bang Lamung Granodiorite (Trgr) | Tak Granite (Cgr) | Haad Som Pan Granite (Kgr) |
| Mineral Compositions (%) | Quartz | 44.82 ± 0.01 | 27.71 ± 12.04 | 27.04 ± 16.73 |
| | Muscovite | 33.04 ± 0.02 | 7.97 ± 3.44 | 14.50 ± 4.89 |
| | Chlorite | 20.96 ± 0.01 | 1.42 ± 0.41 | 0.86 ± 0.18 |
| | Albite | 22.59 ± 0.01 | 18.76 ± 2.24 | 28.62 ± 15.31 |
| | Orthoclase | 15.30 ± 0.01 | 31.63 ± 6.15 | 13.75 ± 3.14 |
| | Anorthite | 3.66 ± 0.04 | 8.99 ± 1.83 | 10.23 ± 1.14 |
| | Diopside | 3.69 ± 0.05 | 3.54 ± 2.45 | 5.01 ± 1.29 |

Table V.8 Mineral compositions of rock specimens in carbonate group.

| Carbonate group | | Rock Type | | |
|---|---|---|---|---|
| | | Khao Khad Marble (Pkd) | Khao Khad Limestone (Pkd) | Khao Khad Travertine (Pkd) |
| Mineral Compositions (%) | Calcite | 93.50 ± 2.29 | 92.24 ± 4.08 | 93.48 ± 5.24 |
| | Quartz | 0.46 ± 0.35 | 0.00 | 0.05 ± 0.07 |
| | Dolomite | 4.35 ±1.57 | 5.05 ± 4.00 | 6.02 ± 5.80 |
| | Chalcopyrite | 1.70 ± 0.37 | 0.00 | 0.46 ± 0.49 |
| | Fluorite | 0.00 | 0.22 ± 0.10 | 0.00 |
| | Microcline | 0.00 | 1.79 ± 0.14 | 0.00 |
| | Actinolite | 0.00 | 0.71 ± 0.04 | 0.00 |

Table V.9 Mineral compositions of rock specimens in sulfate group.

| Sulfate and Chloride group | | Rock Type | | |
|---|---|---|---|---|
| | | Tak Fa Gypsum (Tkb) | Tak Fa Anhydrite (Tkb) | Maha sarakham Salt (KTms) |
| Mineral Compositions (%) | Anhydrite | 0.00 | 99.08 ± 0.66 | 0.28 ± 0.05 |
| | Fluorite | 1.53 ± 1.17 | 0.93 ± 0.66 | 0.00 |
| | Gypsum | 98.47 ± 1.17 | 0.00 | 1.83 ± 0.19 |
| | Halite | 0.00 | 0.00 | 95.50 ± 0.03 |
| | Sylvite | 0.00 | 0.00 | 0.31 ± 0.07 |
| | Dickite | 0.00 | 0.00 | 0.16 ± 0.21 |

Table V.10 Mineral compositions of rock specimens in silicate group.

| Silicate group | | Rock Type | | |
|---|---|---|---|---|
| | | Pyrophyllite (PTRv) | Dickite (PTRv) | Skarn (PTRv) |
| Mineral Compositions (%) | Dickite | 30.35 ± 15.22 | 84.18 ± 1.05 | 35.89 ± 1.26 |
| | Kaolinite | 26.16 ± 15.85 | 15.26 ±1.22 | 19.19 ±1.18 |
| | Quartz | 43.49 ± 31.07 | 0.57 ± 0.17 | 32.55 ± 1.85 |
| | Nacrite | 0.00 | 0.00 | 6.22 ±1.23 |
| | Alunite | 0.00 | 0.00 | 3.30 ±1.63 |
| | Pyrite | 0.00 | 0.00 | 2.87 ± 1.36 |

55

Table V.11 Mineral compositions of rock specimens in volcanic group.

| Volcanic group | | Rock Type | | | | |
|---|---|---|---|---|---|---|
| | | Khao Kradong Basalt (Qbs) | Khao Kradong Vessicular Basalt (Qbs) | Khao Yai Ryorite (PTRv) | Khao Yai Andesite (PTRv) | Khao Yai Tuff (PTRv) |
| Mineral Compositions (%) | Quartz | 0.69 ± 0.97 | 0.13 ± 0.18 | 30.99 ± 5.56 | 43.59 ± 0.82 | 7.57 ± 7.06 |
| | Muscovite | 9.46 ± 0.75 | 18.14 ± 0.87 | 26.19 ± 0.29 | 4.48 ± 0.67 | 22.49 ± 1.06 |
| | Chlorite | 3.89 ± 0.33 | 1.19 ± 0.32 | 18.69 ± 11.82 | 4.28 ± 0.05 | 34.42 ± 1.95 |
| | Albite | 19.45 ± 2.04 | 43.53 ± 0.08 | 6.21 ± 2.64 | 2.91 ± 0.57 | 16.73 ± 6.26 |
| | Orthoclase | 0.00 | 6.15 ± 0.59 | 6.29 ± 0.81 | 0.80 ± 0.25 | 1.97 ± 0.33 |
| | Anorthite | 18.68 ± 5.83 | 29.90 ± 2.13 | 5.61 ± 0.87 | 0.46 ± 0.30 | 2.60 ± 0.33 |
| | Diopsite | 31.70 ± 6.08 | 0.00 | 3.66 ± 1.12 | 0.00 | 0.00 |
| | Microcline | 16.14 ± 0.90 | 0.00 | 1.70 ± 1.32 | 0.00 | 0.00 |
| | Kaolinite | 0.00 | 0.99 ± 0.26 | 2.65 ± 0.19 | 43.50 ± 0.32 | 0.00 |
| | Hematite | 0.00 | 0.00 | 1.15 ± 0.34 | 0.00 | 5.57 ± 1.31 |
| | Calcite | 0.00 | 0.00 | 0.00 | 0.00 | 8.66 ± 12.25 |

## 5.7 Equivalent quartz content and Volumetric hardness

Equivalent quartz content (EQC) is estimated by using the mineral compositions obtain from XRD multiplied by Rosiwal hardness as shown in Eq. 5.7. Volumetric hardness ($H_V$) is one of mineral parameter calculated from mineral contents and Mohs hardness ($H_M$). The important thing of volumetric hardness different from other mineral parameters is percentage of mineral content by volume (%V), which calculate from the weight percentage of mineral contents (%W) obtained from XRD (Table 5.5 to 5.10) divided by their specific gravity (S.G.) as shown in Equation. (5.8). Equation. (5.9) is the volumetric hardness calculated by using the summation of %V of each mineral multiplied by their Mohs hardness ($H_M$) divide by summation of %V of all minerals composed in the rock. From the result of EQC and $H_V$ given in Table 5.11, it can be observed that the distribution of the $H_V$ is significantly less than the EQC.

$$EQC = \sum_{i=1}^{n} \%A_i \times R_i \qquad (5.7)$$

$$\%V = \sum_{i=1}^{n} \left( \frac{\%W_i}{S.G._i} \right) \qquad (5.8)$$

$$H_V = \frac{\left( \sum_{i=1}^{n} \%V_i \times H_M \right)}{\sum \%V} \qquad (5.9)$$

where EQC is equivalent quartz content (%), %A is the mineral amount (%), R is Rosiwal hardness (%), and n is the number of minerals.

Table V.12 Equivalent quartz content and volumetric hardness.

| Group | Rock type | EQC (%) | $H_V$ |
|---|---|---|---|
| Clastic | Phu phan sandstone | 88.26 | 6.52 |
| | Sao khua sandstone | 76.04 | 6.03 |
| | Phra wihan sandstone | 87.58 | 6.56 |
| | Phu kradung sandstone | 52.89 | 5.30 |
| Plutonic | Rayong-Bang Lamung Granodiorite | 63.52 | 6.19 |
| | Tak Granite | 52.11 | 6.04 |
| | Haad Som Pan Granite | 51.88 | 5.86 |
| Carbonate | Khao Khad Marble | 4.21 | 3.06 |
| | Khao Khad Limestone | 4.66 | 3.12 |
| | Khao Khad Travertine | 3.82 | 3.05 |
| Sulfate and chloride | Tak Fa Gypsum | 1.09 | 2.02 |
| | Tak Fa Anhydrite | 3.86 | 3.26 |
| | Maha Sarakham Salt | 2.32 | 2.49 |
| Silicate | Pyrophyllite | 44.46 | 4.30 |
| | Dickite | 2.28 | 2.28 |
| | Skarn | 35.11 | 3.55 |
| Volcanic | Khao Kradong Basalt | 36.87 | 5.68 |
| | Khao Kradong Vesicular Basalt | 37.83 | 5.50 |
| | Khao Yai Rhyolite | 41.76 | 4.73 |
| | Khao Yai Andesite | 46.38 | 4.50 |
| | Khao Yai Tuff | 19.94 | 3.79 |

# CHAPTER VI

# ANALYSIS OF RESULTS

## 6.1    Introduction

This chapter correlates the CERCHAR abrasivity index (CAI) value with physical and mechanical properties, rock hardness determined by mineral volume, and equivalent quartz contents based on mineral compositions. The correlations between CAI value and groove volume, obtained from rock surfaces scratching, are also examined. Additionally, the chapter introduces the calculation methods for CERCHAR specific energy (CSE), which is derived from the work done and groove volume.

The analysis determines the correlations between CSE and several properties, such as CAI, mechanical properties, and mineral properties. These correlations are examined separately for all clastic rocks, and crystalline rocks. The findings reveal distinct responses between clastic and crystalline rocks, as detailed in the subsequent sections.

## 6.2    Mathematical relationships

Relationships between CAI value and physical properties including density and rock porosity are presented in Figures 6.1 and 6.2. However, it is notable that these relationships exhibit no significant correlation, as indicated by the coefficient of correlation ($R^2$) being less than 0.1 for all rocks. This lack of correlation has received limited attention from other researchers, particularly in terms of the CAI value and density correlation. Testing results conducted by Lee et al. (2012) and Ozdogan et al. (2018) have further confirmed the absence of any relationship between CAI value and rock porosity.

This study reveals a correlation between CAI value and rock porosity in clastic rocks, with a high $R^2$ of 0.948. Figure 6.2 illustrates that CAI increases as porosity increases in the clastic rock correlation. It suggests that only the clastic rocks exhibit a relationship between CAI value and rock porosity. The observed correlation is likely attributed to the formation process of clastic rocks, which involves the sedimentation of pre-existing rock fragments. Consequently, the porosity values of each rock within the clastic rock group are more distinct compared to other rock groups.
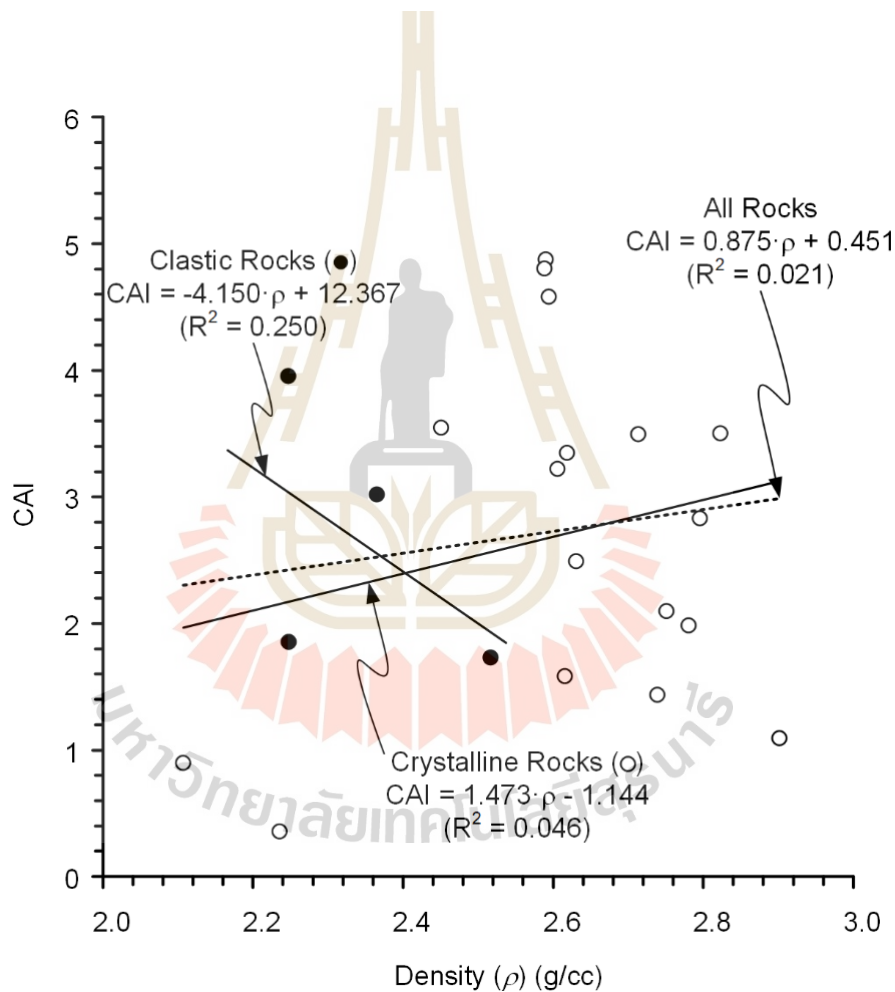


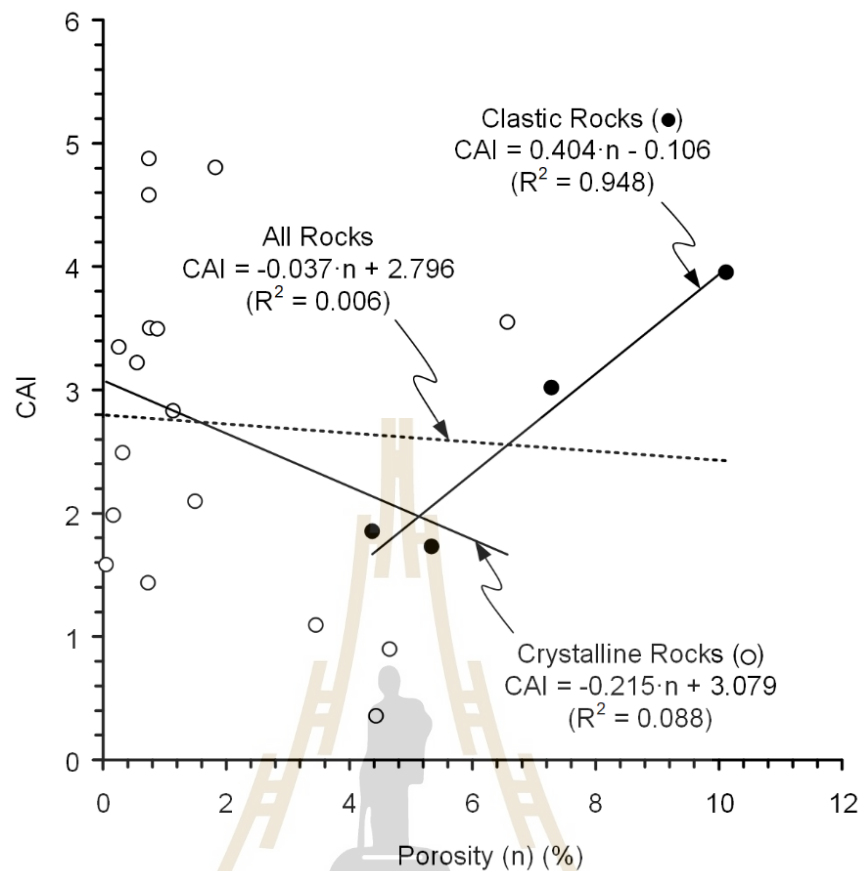Figure VI.1 Correlation between CAI value and density.

Figure VI.2 Correlation between CAI value and rock porosity (n).

Figure 6.3(a) presents the correlation between CAI value and uniaxial compressive strength ($\sigma_c$), which is fitted using linear regression. The data reveals a tendency for CAI value to increase linearly as $\sigma_c$ increases. However, the correlations are found to be poor, with $R^2$ of 0.247. This finding is consistent with previous research conducted by Ko et al. (2016), Ozdogan et al. (2018); and Zhang, Konietzky, and Frühwirt (2020), where no significant linear correlation was observed between CAI value and $\sigma_c$. It is noted that both clastic and crystalline rocks demonstrate poor correlations, particularly clastic rocks that exhibit no correlation for this relationship. However, among all rock types, crystalline rocks display a relatively better suitability for this correlation. Figure 6.3(b) compares the linear equation obtained here with those presented by other investigators, as quoted in the figure. They also obtain poor to fair correlations ($R2 < 0.5$) between the two parameters.
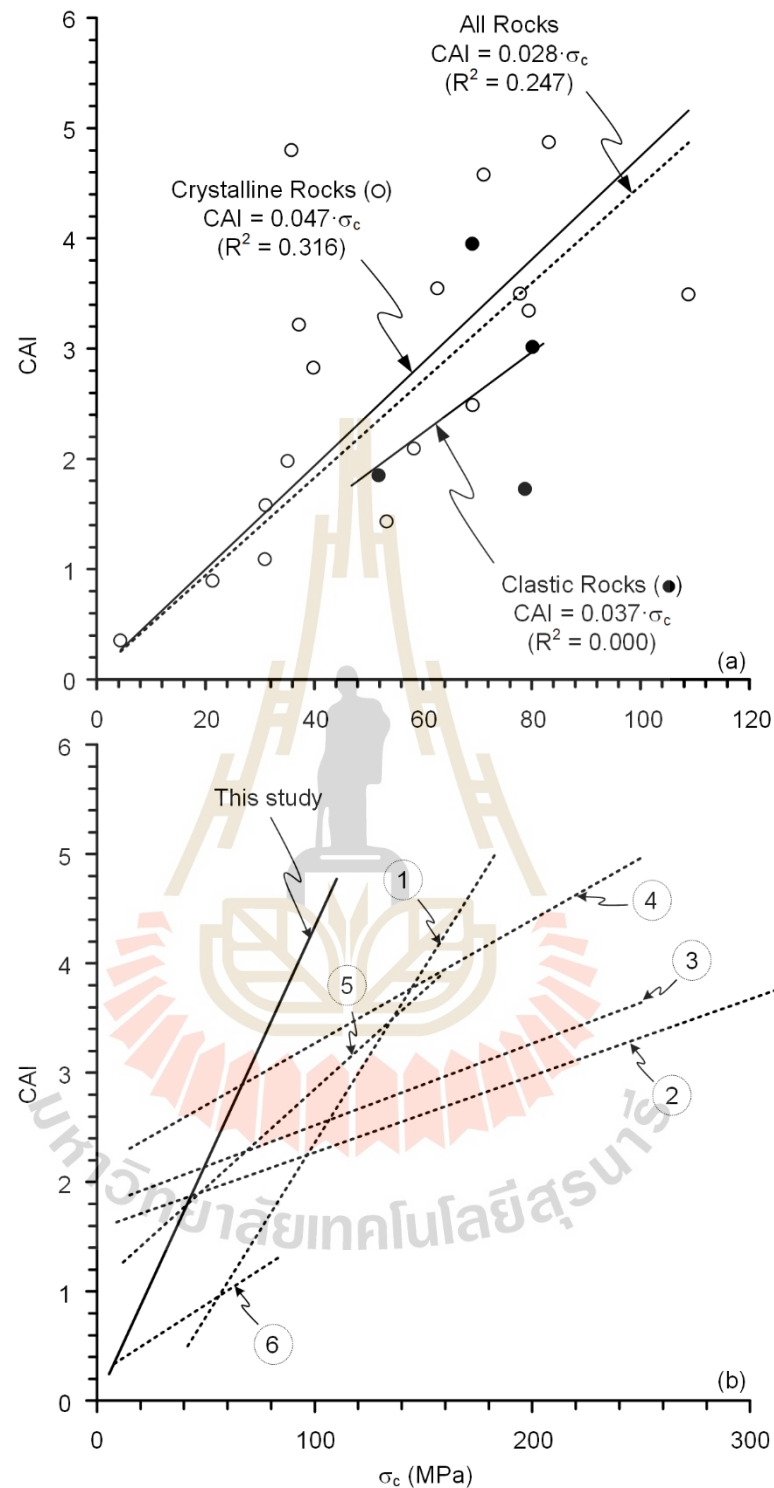
Figure VI.3  Correlation between CAI value and uniaxial compressive strength ($\sigma_c$) (a).
comparison of the linear correlation of this study with those obtained
elsewhere (b). ① Altindag et al. (2009), ② He et al. (2016), ③-④ Ko et
al. (2016), ⑤ Hamzaban et al. (2018), ⑥ Kotsombat et al. (2020).

Figure 6.4 illustrates the correlation between CAI value and Young's modulus (E), fitted with linear regression. However, the correlation of all rock types is found to be poor, with $R^2$ of 0.259. This finding agrees with the research conducted by He et al. (2016) and Zhang, Konietzky, and Frühwirt (2020), where similarly poor correlations between CAI value and E were observed, with $R^2$ lower than 0.3. He et al. (2016) mentioned that CAI value interpretation solely based on single mechanical properties, including Young's modulus, is not viable. However, interestingly, a significant correlation is observed within clastic rocks, where the CAI value exhibits a linear increase with increasing Young's modulus, with a high $R^2$ of 0.859. On the other hand, the correlation in crystalline rocks do not exhibit similar significance.
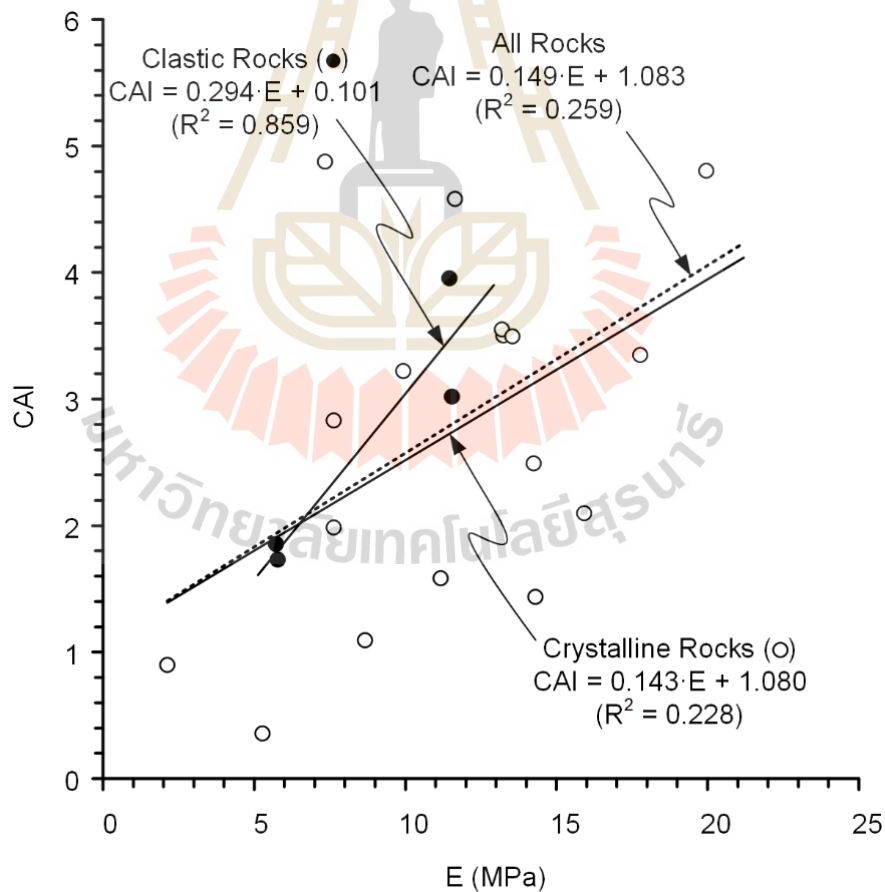


Figure VI.4 Correlation between CAI value and Young's modulus (E).

The data analysis reveals that there is no significant correlation ($R^2$ = 0.010) between the CAI value and Poisson's ratio, as illustrated in Figure 6.5. This finding is consistent with the results conducted by Lee et al. (2012), where they found no correlation between CAI and Poisson's ratio. Even though, the investigation considered clastic and crystalline rocks separately, revealing that there is also no correlation between CAI and Poisson's ratio for crystalline rocks. whereas a moderately strong correlation ($R^2$ = 0.593) is observed for clastic rocks, indicating that as Poisson's ratio increases, the CAI value also tends to increase.
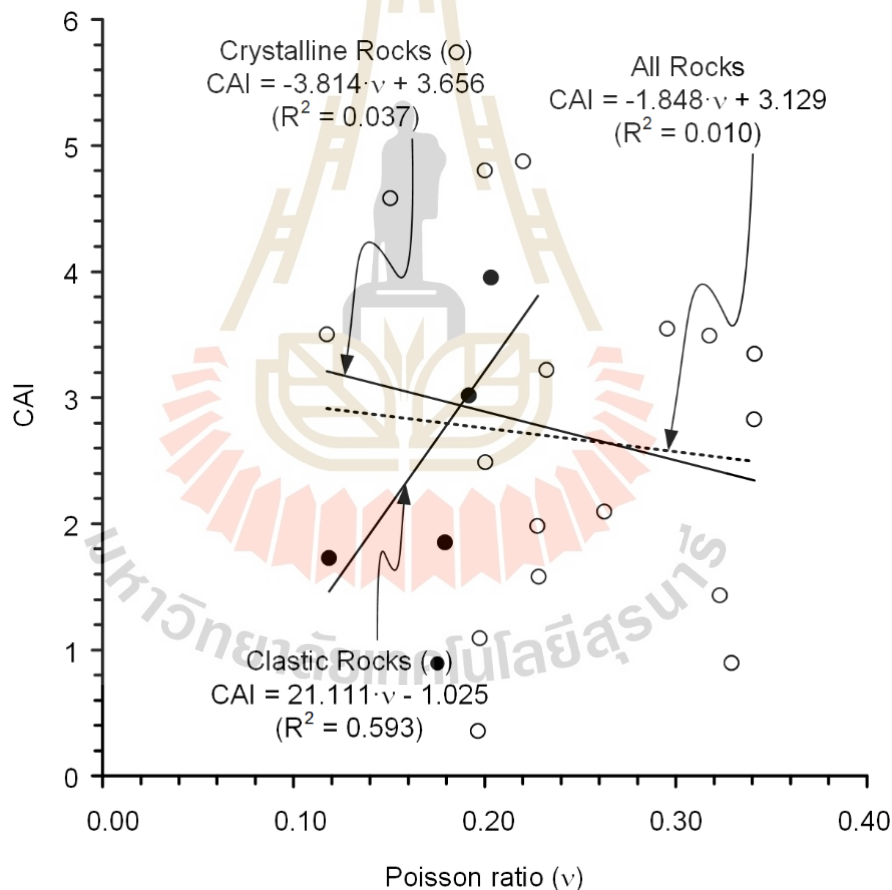


Figure VI.5 Correlation between CAI value and Poisson's ratio ($\nu$).

Limited research has been conducted regarding the correlation between the CAI value and cohesion (c), as well as friction angle ($\phi$). Figure 6.6 illustrates the correlation between the CAI value and cohesion. Overall, there is a poor correlation observed between CAI value and rock cohesion across all rocks ($R^2$ = 0.135). However, when analyzing clastic rocks separately, a stronger linear regression is found in this correlation, resulting in higher $R^2$ (0.839). This indicates a negative correlation, where an increase in rock cohesion corresponds to the decrease in CAI value. Nevertheless, in the crystalline rocks, although the correlation improves compared to all rocks, it remains a fair correlation with an $R^2$ of 0.320.
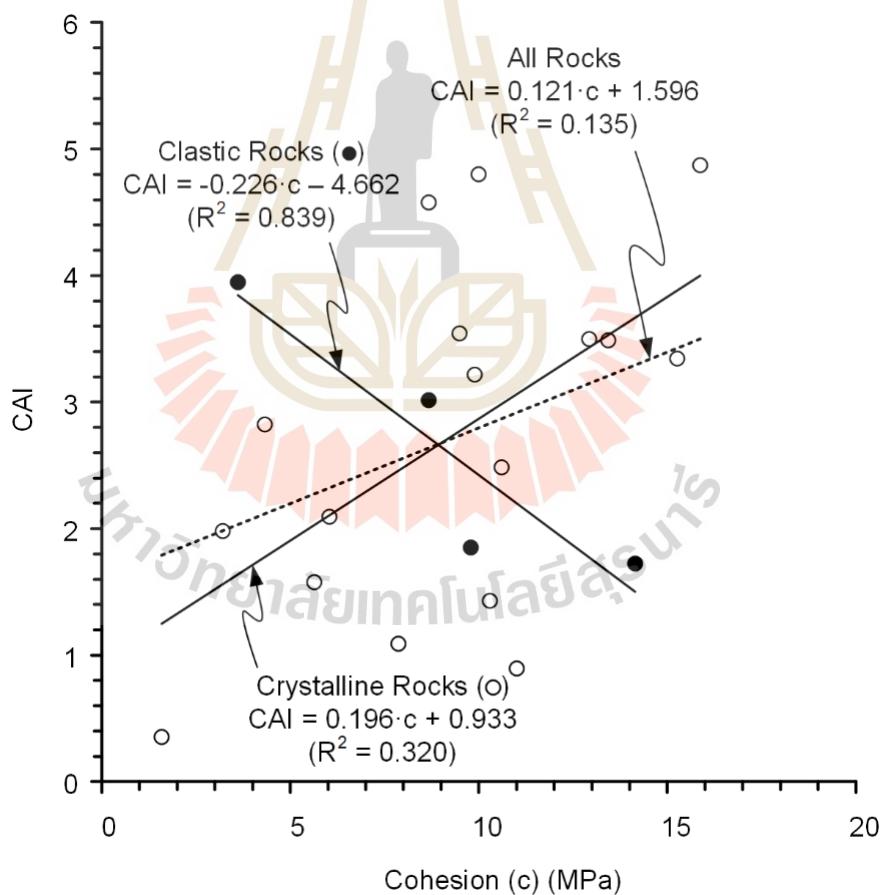


Figure VI.6 Correlation between CAI value and rock cohesion (c).

In Figure 6.7, the linear correlation between CAI value and friction angle is presented. For all rocks, the correlation shows an $R^2$ of 0.337, indicating that CAI value tends to increase with an increase of friction angles. Similar trends are observed when analyzing only crystalline rocks, although with a slightly lower $R^2$ (0.331). However, it is important to note that clastic rocks exhibit a more significant correlation, with an $R^2$ of 0.656, indicating a stronger relationship between CAI value and friction angle compared to all rocks group and crystalline rocks.
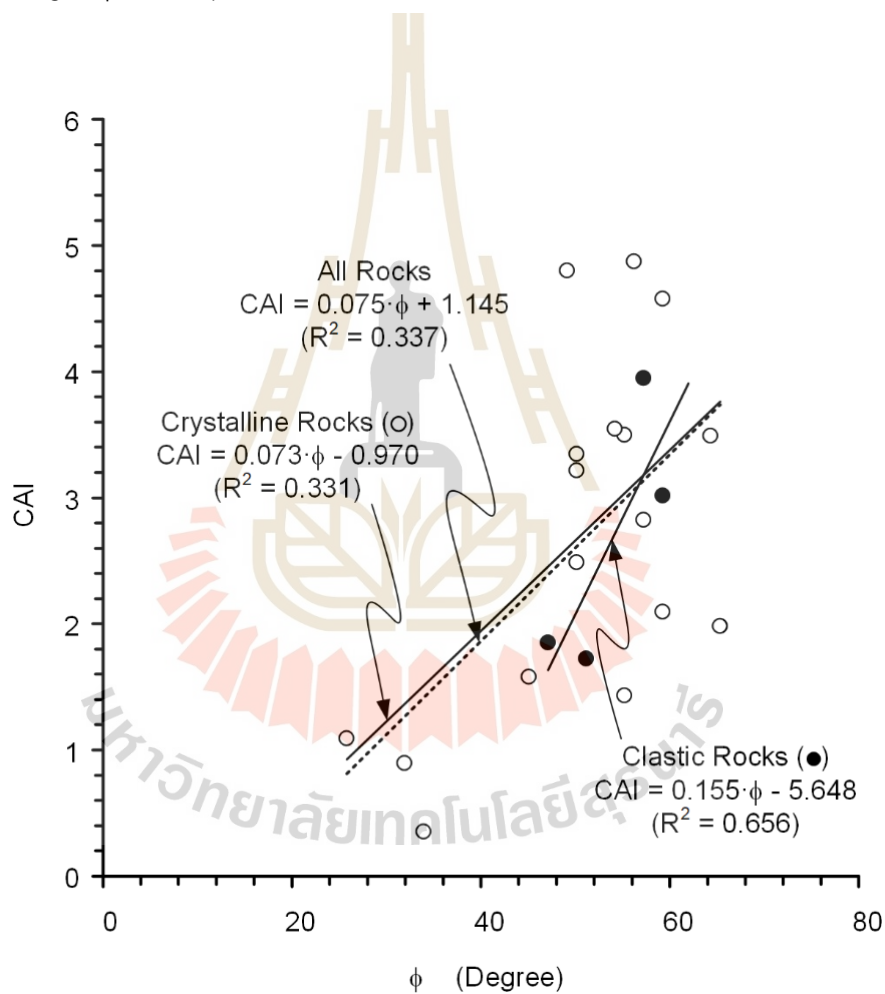


Figure VI.7 Correlation between CAI value and friction angle ($\phi$).

The relationship between the CAI value and mineral parameters, specifically equivalent quartz contents (EQC) and volumetric hardness ($H_V$), has been examined and analyzed. The findings indicate that a linear regression model best describes these relationships, revealing that as EQC and $H_V$ increase, the CAI also increases. Figure 6.8 illustrates the correlation between CAI and EQC, with an $R^2$ of 0.413 for all rocks. Notably, clastic rocks exhibit a more suitable correlation between CAI and EQC, with an $R^2$ of 0.623, while crystalline rocks demonstrate the highest $R^2$ of 0.877.
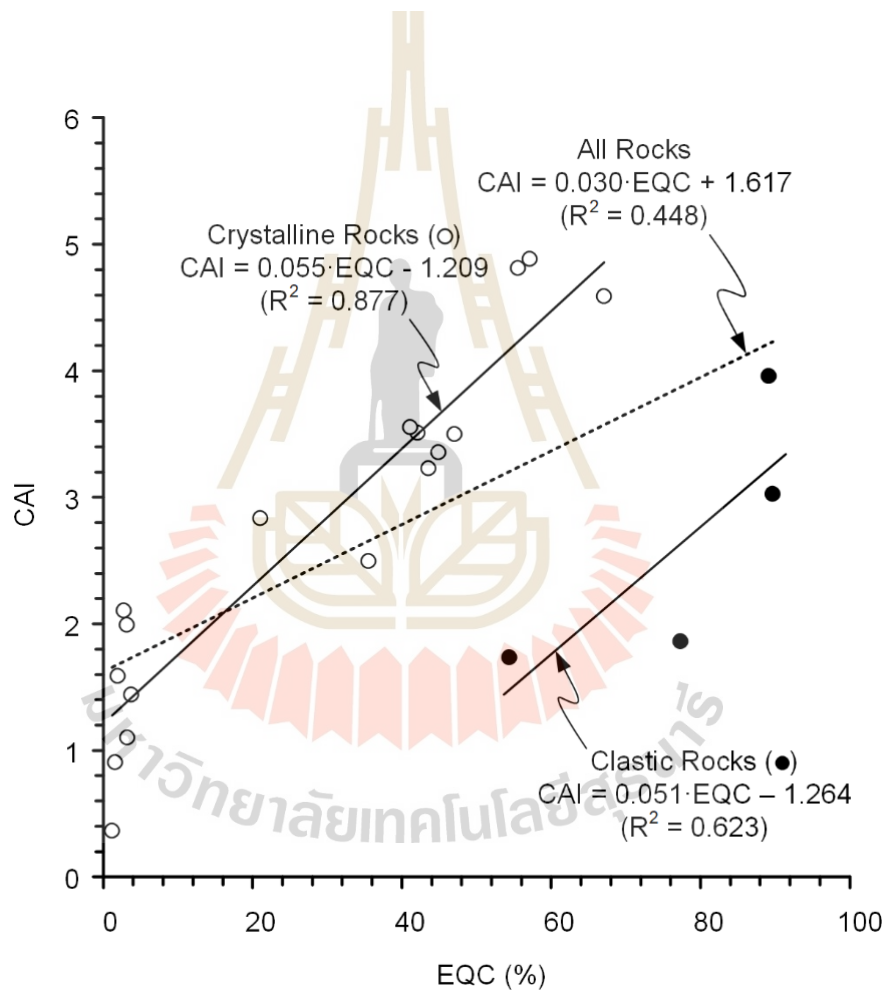


Figure VI.8 Correlation between CAI value and equivalent quartz contents (EQC).

In contrast, the correlation between CAI and $H_V$ is found to be more appropriate than the correlation between CAI and EQC, as depicted in Figure 6.9. The fitting curves indicate that when the $H_V$ of a rock is lower, the CAI remains correspondingly lower or even zero. For all rocks, when the CAI is zero, the $H_V$ value is approximately 0.4. This trend is consistent for both clastic and crystalline rocks. However, there is a distinction from the CAI correlation with EQC, where for all rocks and crystalline rocks, when the EQC is zero, the CAI value exceeds 1.2. The correlation between CAI and $H_V$ exhibits a significantly higher $R^2$ compared to the correlation between CAI and EQC, with $R^2$ of 0.591, 0.623, and 0.893 for all rocks, clastic rocks, and crystalline rocks, respectively.
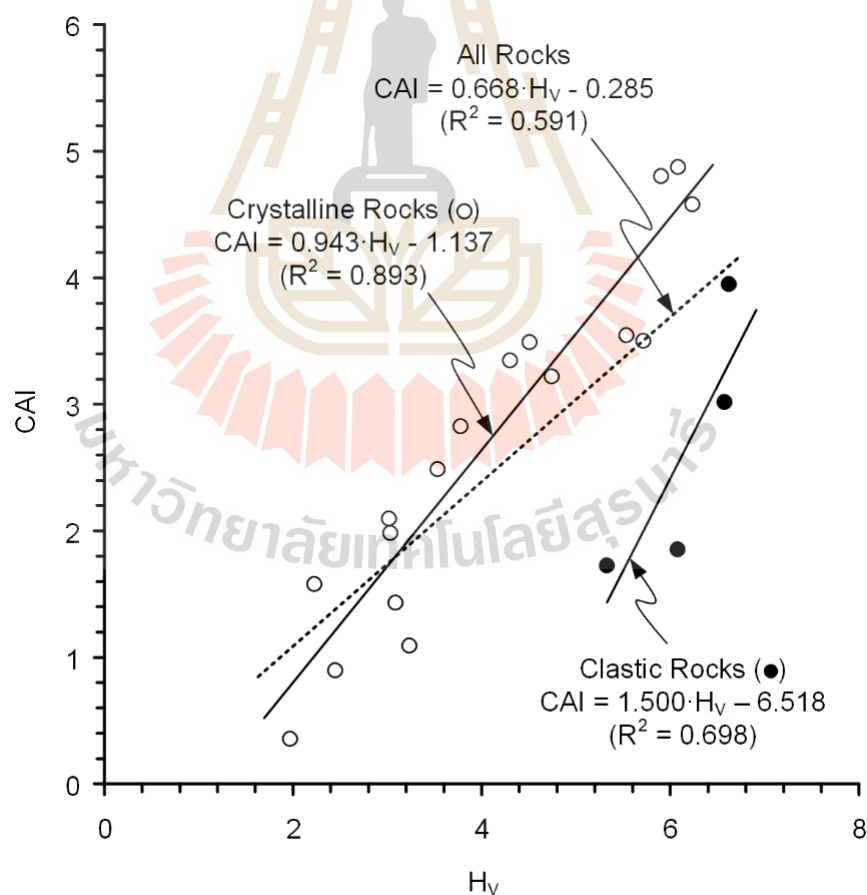


Figure VI.9 Correlation between CAI value and volumetric hardness ($H_V$).

A stronger relationship between CAI and $H_V$ compared to the relationship with EQC, is not supported by the results of Zhang et al. (2021). They found that the relationship between CAI and weighted mineral hardness is less suitable than the relationship with EQC. They specifically examined only limestone and granite rocks, whereas the finding obtained from this study covered a wider range of rock types.

The CAI values are plotted as a function of mean groove volume (V), and the correlations have been analyzed separately for each rock type, as illustrated in Figure 6.10(a). Figure 6.10(b) shows the correlations for clastic and crystalline rocks individually. The best fitting curve for the CAI-V correlation can be represented by a power equation, as indicated below:

$$CAI = \alpha \cdot (V)^{\beta} \tag{6.1}$$

where $\alpha$ and $\beta$ are empirical constants that determine the relationship between CAI and V.

There is an inverse relationship between the mean groove volume and CAI, indicating that as the CAI decreases, the mean groove volume tends to increase. Among 21 rock types studied here, approximately 13 of them exhibit an $R^2$ greater than 0.7. Rhyolite demonstrates the highest $R^2$ for this correlation, with a value of 0.983, while tuff shows the lowest $R^2$ of 0.063, as illustrated in Figure 6.10(a). Only vesicular basalt (line with circle number 18) shows a different pattern, where the CAI increases with an increase in mean groove volume. This behavior could be attributed to the surface roughness caused by air bubbles during the rock formation process. It can be noticed with the porosity data presented in Table 5.3 in Chapter 5 that the vesicular basalt exhibits higher porosity compared to other rocks, except for the clastic group, where porosity regularly occurs from the bonding process of sedimentary rock. Data of empirical counts and $R^2$ of each rock type are presented in Table 6.1.

Figure 6.10(b) presents the correlation between CAI and V, separated into all rocks, clastic rocks, and crystalline rocks. Through this grouping analysis, it is observed that crystalline rocks exhibit slightly higher $R^2$ compared to the correlation observed in all rocks combined, with $R^2$ of 0.452 and 0.391, respectively. On the other hand, the correlation for clastic rocks demonstrates no significant relationship, as indicated by an $R^2$ of 0.039. Suggesting that the mean groove volume and CAI have minimal association within this rock group.
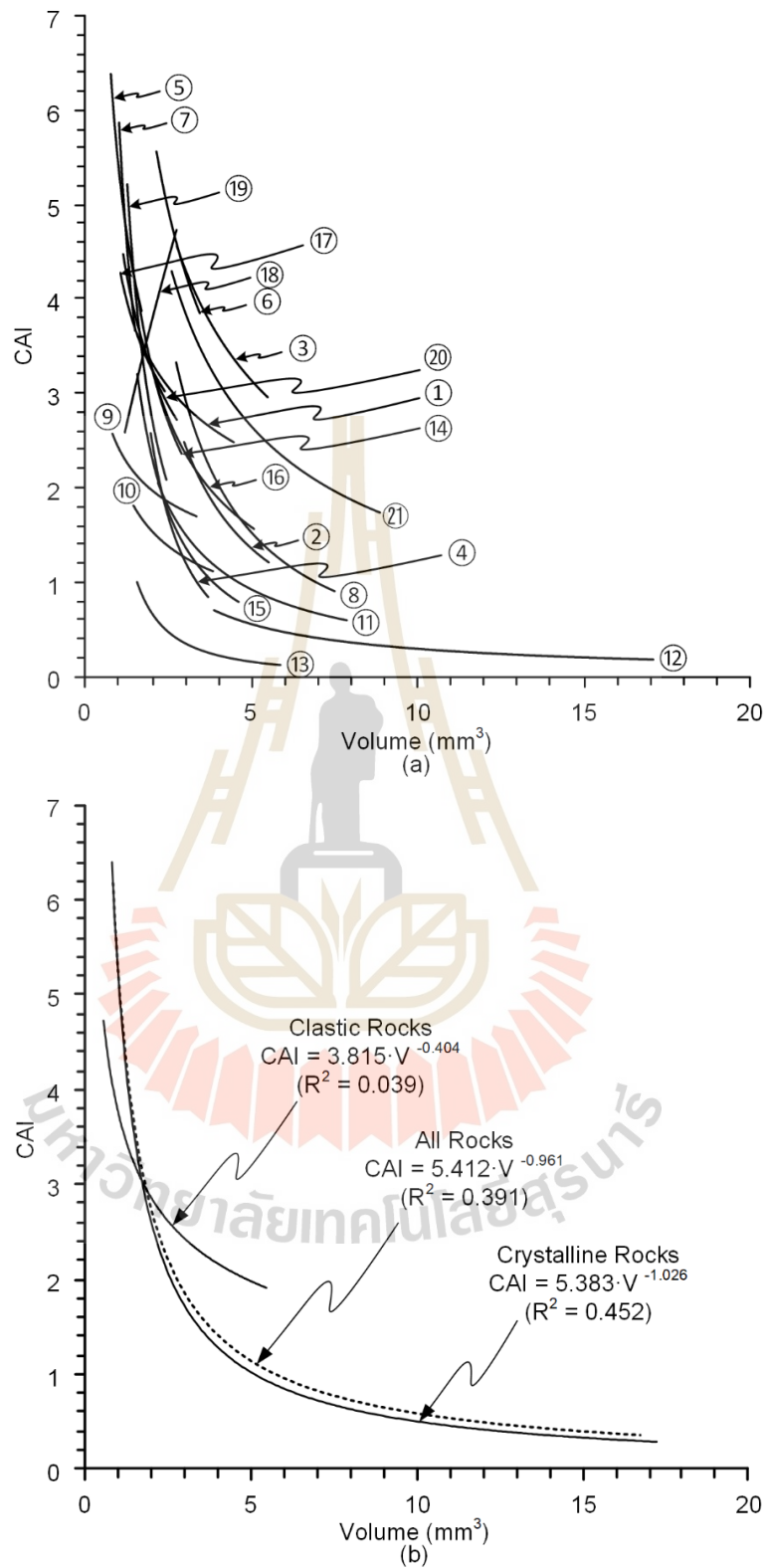
Figure VI.10 Correlation between CAI value and mean groove volume separated by rock types (a) and rock groups (b).

Table VI.1 Empirical constants and coefficient of correlations of power equation fitting curve of CAI correlation with mean groove volume group by rock types.

| Rock type | $\alpha$ | $\beta$ | $R^2$ |
|---|---|---|---|
| ① Phu Phan Sandstone | 4.263 | -0.362 | 0.890 |
| ② Sao Khua Sandstone | 8.723 | -1.158 | 0.619 |
| ③ Phra Wihan Sandstone | 8.559 | -0.625 | 0.724 |
| ④ Phu Kradueng Sandstone | 8.405 | -1.765 | 0.959 |
| ⑤ Tak Granite | 5.351 | -0.624 | 0.919 |
| ⑥ Haad Som Pan Granite | 9.948 | -0.770 | 0.859 |
| ⑦ Granodiorite | 5.886 | -1.197 | 0.980 |
| ⑧ Khao Khad Marble | 12.024 | -1.285 | 0.750 |
| ⑨ Khao Khad Travertine | 2.414 | -0.292 | 0.174 |
| ⑩ Khao Khad Limestone | 2.166 | -0.494 | 0.860 |
| ⑪ Tak Fa Anhydrite | 4.321 | -0.961 | 0.236 |
| ⑫ Tak Fa Gypsum | 2.417 | -0.914 | 0.563 |
| ⑬ Maha Sarakham Salt | 1.983 | -1.575 | 0.745 |
| ⑭ Pyrophyllite | 5.985 | -0.879 | 0.376 |
| ⑮ Dickite | 5.628 | -1.286 | 0.968 |
| ⑯ Skarn | 5.604 | -0.787 | 0.835 |
| ⑰ Khao Kradong Basalt | 4.348 | -0.420 | 0.349 |
| ⑱ Khao Kradong Vesicular Basalt | 2.308 | 0.716 | 0.628 |
| ⑲ Khao Yai Rhyolite | 7.077 | -1.380 | 0.983 |
| ⑳ Khao Yai Andesite | 4.779 | -0.559 | 0.921 |
| ㉑ Khao Yai Tuff | 8.628 | -0.735 | 0.063 |

## 6.3    Work and energy

Work and energy required to scratch the surfaces of rocks during CERCHAR testing have been initially presented in the research conducted by Hamzaban et al. (2018). The issue has been reviewed in Chapter 2, section 2.4. The concept of specific energy in the rock drilling process has been studied since 1965 by Teale (1965). To determine the work done, correlations between the lateral force (F) and scratching distance ($d_s$) from the findings discussed in Topic 5.4 in Chapter 5 were used. Equation (5.1) in Chapter 5 represents the best-fitting equation for the F-ds correlations. Equation (5.1) in Chapter 5 represents the best-fitting equation for the F-ds correlations.

To calculate the work done for the steel stylus scratching on the rock surfaces, the area under the F-ds correlations curve is considered. This can be determined by integrating the force equation over the entire scratching length. The calculation equation is as follows:

$$W = \int_{d_s=0}^{10} F \cdot d_S \qquad (6.2)$$

where W denotes the work done of steel stylus for scratching rock surface. The stylus energy using for scratching the rock surface is referred to as CERCHAR specific energy (CSE), as presented by Zhang, Konietzky, and Frühwirt (2020). The calculation of CSE is determined using Equation (6.3), which is expressed as follows:

$$CSE = \frac{W}{V} = \frac{\int_{d_s=0}^{10} F \cdot d_s}{V} \qquad (6.3)$$

where V is mean groove volume. The determination and mean value of the groove volume can be found in Topic 5.5 and Table 5.4 in Chapter 5.

Figure 6.11 illustrates the correlations between CSE and CAI value, for all rock groups, a linear correlation is observed, with an $R^2$ of 0.450. The correlation is, however, stronger for crystalline rocks, where the $R^2$ equal to 0.512. These groups demonstrate a linear increase in CSE as the CAI value increases. These correlations indicate that as the CAI value increases, the CSE value also shows a linear increase for both all rocks and crystalline rocks. On the contrary, clastic rocks exhibit no significant correlation between CSE and CAI, with an $R^2$ of 0.002.

This finding differs from the CSE and CAI relationship studied by Zhang, Konietzky, and Frühwirt (2020), where only nine different rock types are considered. They find an exponential increase in CSE as the CAI value increases, with an $R^2$ of 0.680.
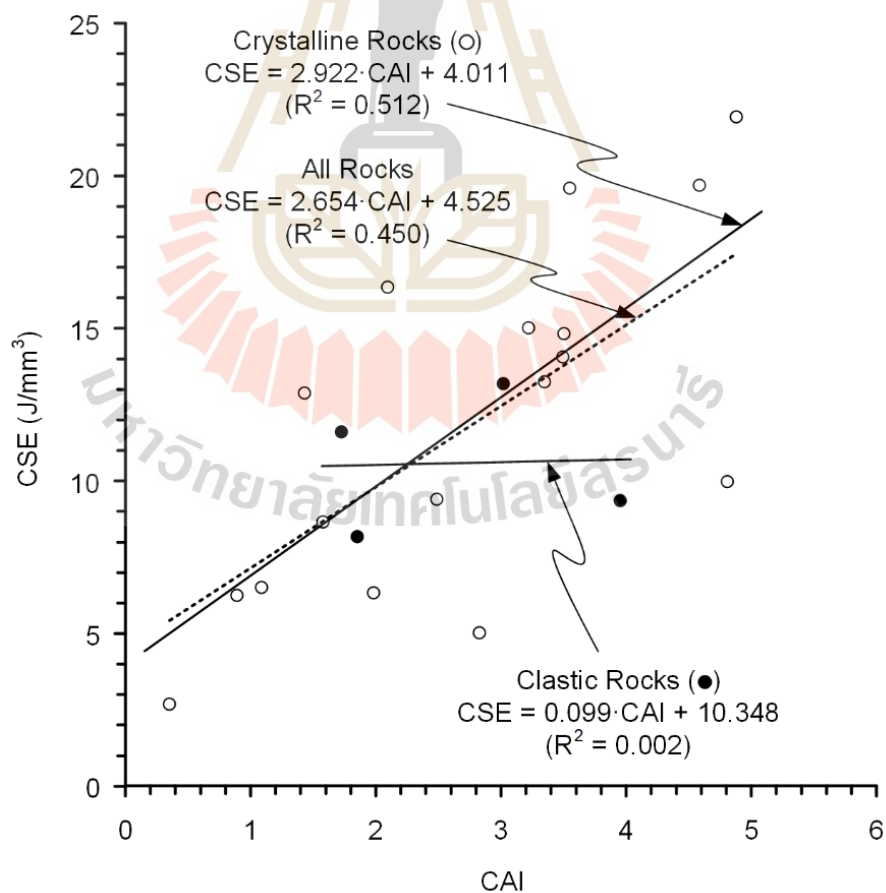


Figure VI.11 Correlation between CSE and CAI.

Figure 6.12 displays the relationship between CSE and $\sigma_c$. The plot reveals a positive linear correlation between CSE and $\sigma_c$ for all rocks, with an $R^2$ of 0.436. When examining the correlation within specific rock groups, it is observed that the correlation for crystalline rocks exhibits a slightly higher $R^2$ of 0.508 as compared to the correlation among all rocks. Furthermore, a finding is the strong correlation observed in clastic rocks, indicated by a high $R^2$ of 0.833.

This suggests that in rocks with low strength, there is an initiation of energy utilization, specifically around 4 J/mm$^3$, particularly for crystalline rocks. However, for the case of clastic rocks, no energy is required for initiation even in rocks with no strength.
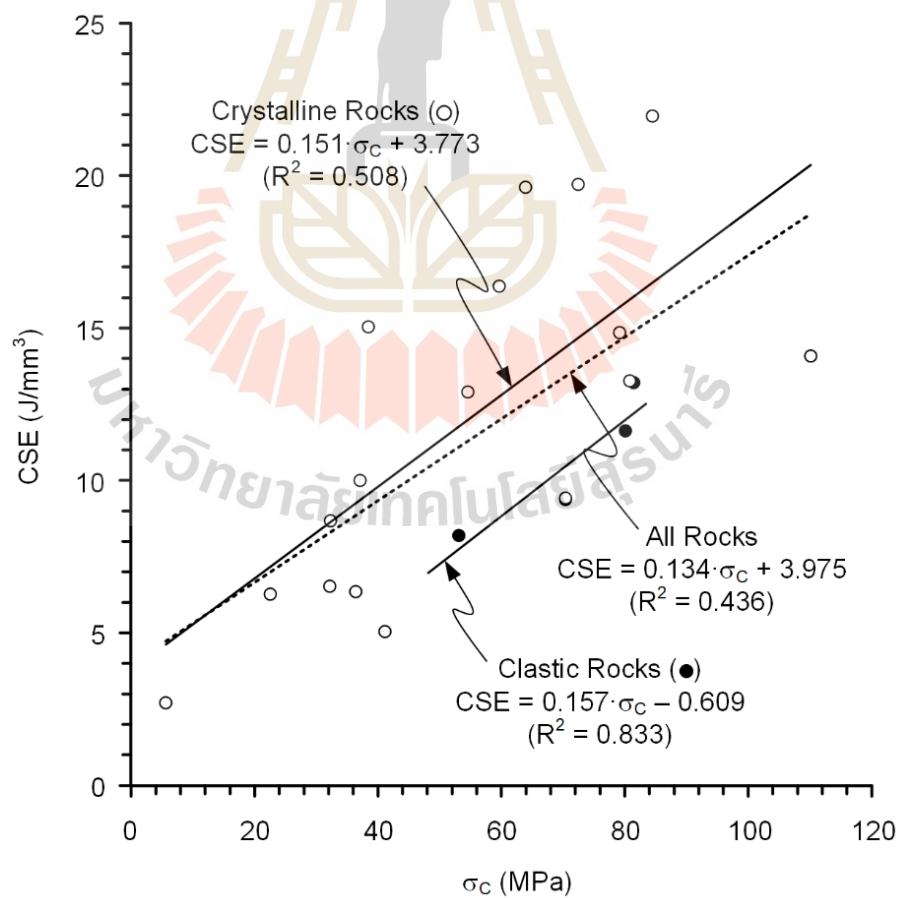


Figure VI.12 Correlation between CSE and $\sigma_c$.

The relations between CAI and rock cohesion in Figure 6.6, as well as friction angle in Figure 6.7, reveal fair correlations with $R^2$ below 0.350 for all rocks and for crystalline rocks. Similar analyses are performed for the correlations between CSE and rock cohesion, as well as friction angle, as shown in Figure 6.13 and Figure 6.14, respectively.

Figure 6.13 demonstrates the correlation between CSE and rock cohesion, revealing a fair correlation for all rocks with an $R^2$ of 0.319. When analyzing crystalline rocks separately, a slightly stronger correlation is observed, resulting in an $R^2$ of 0.370. These trends suggest that CSE tends to increase with an increase in rock cohesion. However, for clastic rocks, a weaker correlation is observed, with a lower $R^2$ of 0.099.
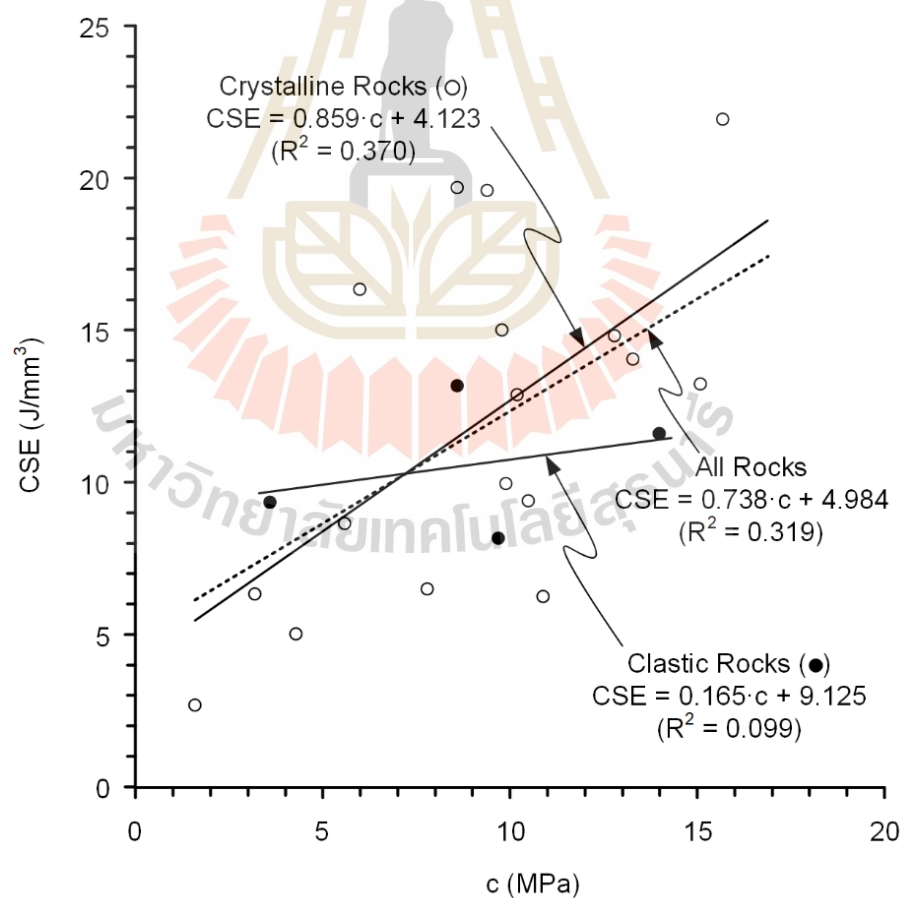


Figure VI.13 Correlation between CSE and rock cohesion.

The linear correlation between CSE and friction angle is presented in Figure 6.14. For all rocks, the correlation shows an $R^2$ of 0.257, suggesting that CSE tends to increase as friction angles increase. Similar trends are observed when analysing clastic and crystalline rocks separately, with a slightly improved correlation observed for crystalline rocks ($R^2$ = 0.273). The clastic rocks exhibit a stronger correlation, with an $R^2$ of 0.387, suggesting a more significant relationship between CSE and friction angle compared to all rocks and crystalline rocks only.



Figure VI.14 Correlation between CSE and friction angle.

# CHAPTER VII

# DISCUSSIONS AND CONCLUSIONS

## 7.1    Discussions

Various correlations with CERCHAR abrasivity index (CAI) reveals that correlation between CAI and rock density does not show any relation. Similarly, the correlation between CAI and rock porosity has received limited attention from researchers, with only a few studies investigating this relationship. It has been, however, discovered that CAI is influenced by rock porosity, specifically for the clas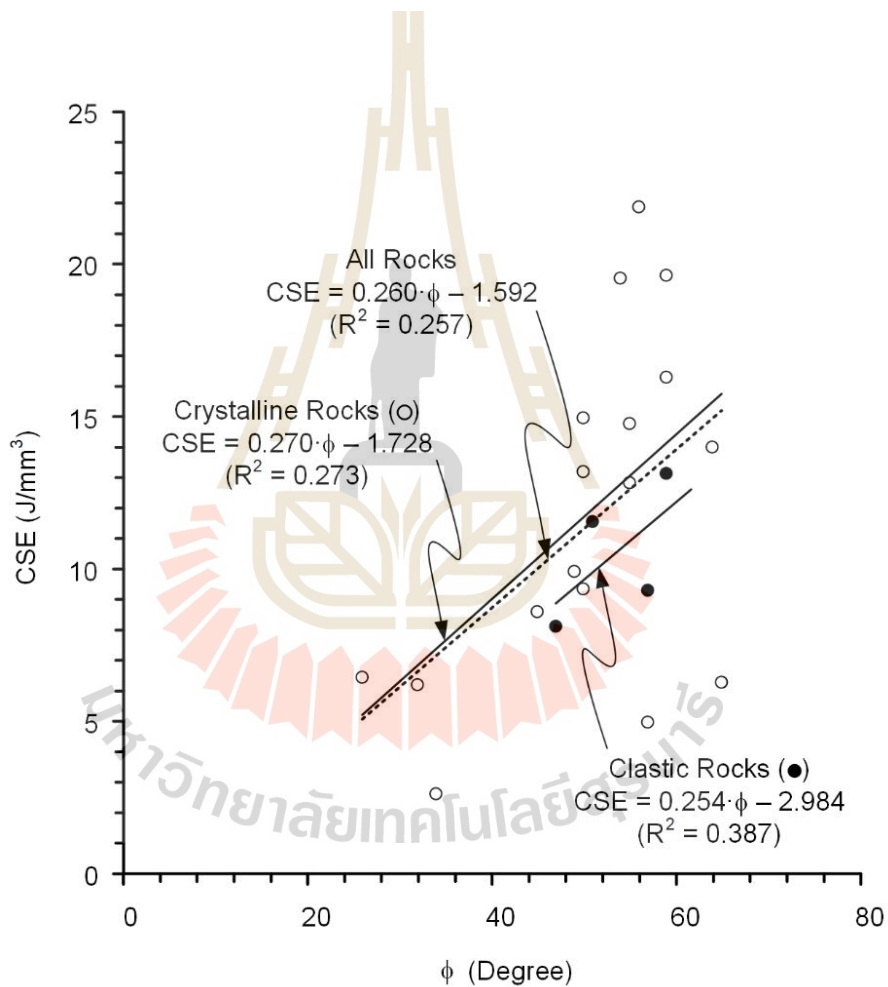tic rocks. Crystalline rocks, seem to be unaffected by porosity in relation to CAI, as experimentally shown by Ozdogan et al. (2018) and Yasar and Yilmaz (2016). This distinction suggests that the relationship between CAI and rock porosity is valid only for clastic rocks, which may be attributed to the unique formation processes, failure behavior, and cementing materials characteristic of clastic rocks.

Several investigators (Altindag et al., 2009; Hamzaban et al., 2018; He et al., 2016; Ko et al., 2016; Kotsombat et al., 2020) have recognized that only fair correlations can be obtained between uniaxial compressive strength and CERCHAR abrasivity index. Such correlation, however, has been widely performed. This is primarily because the rock strengths are readily available for most geological and mining engineering projects. Some investigators (Capik and Yilmaz, 2017; Er and Tuğrul, 2016; Teymen, 2020) can obtain their correlation coefficients of greater than 0.8. They however compare only few rock types with similar characteristics (e.g., sandstone, siltstone). In general rock strengths and CAI can not be correlated well because the two parameters are derived from different mechanisms of failure or breakage. The failure of uniaxial test specimen is induced by the initiation and propagation of microcracks, fissures, intercrystalline boundaries, pore spaces and cleavage. When the applied stress reaches an ultimate

value, these defects are connected, and compressive shear failure is induced (Jaeger et al., 2007). The wear of stylus tip (CAI) is produced by shearing process controlling by abrasiveness and hardness of the minerals composing rock which may not have a direct relation with their strength. The mechanisms induce the wear of stylus tip are complex. The stress distribution in rock at and around the stylus tip also shows very high gradient under macroscopic scale, as demonstrated by numerical simulations by Balani, et al. (2017)

Correlations between CAI and other mechanical properties, such as Young's modulus and Poisson's ratio, show that Young's modulus and Poisson's ratio affect CAI only in clastic rocks, whereas crystalline rocks do not exhibit any impact on CAI in relation to these mechanical properties. This discrepancy emphasizes the distinct behavior of clastic rocks in relation to CAI and suggests that the factors influencing CAI in clastic rocks may differ from those in crystalline rocks.

Correlations between CAI and triaxial properties, specifically cohesion and friction angle (Figures 6.6 and 6.7), show that CAI is affected by cohesion and friction angle only on clastic rocks. While crystalline rocks exhibit a slight influence on CAI value. The correlations between CAI and triaxial properties (cohesion and friction angle) suggests a limited influence of these factors on CAI. However, it is important to note that these initial findings may not conclusively establish any relationship, as extensive study on these specific correlations has not been undertaken.

The diagrams in Figures 6.8 and 6.9 show that clastic rocks tend to show higher EQC and $H_V$ values than the crystalline rocks do, even though CAI values for the two rock groups are within the same range. This results in a low correlation coefficient when only one equation is applied to describe their relation. The high EQC and $H_V$ values are due to that grains of the tested sandstones are mainly quartz, albite and anorthite with a combined weight percent between 65% and 90% (see Tables 5.5 to 5.10). Even though these minerals are highly abrasive and abundant in clastic rocks, they tend to have small impact on the wear of stylus tip. This is because the tested

surface also contains much softer and lower abrasive minerals (e.g., kaolinite, muscovite, calcite and chloride). The stylus tip ploughs through the softer materials and induces dislodging of the harder grains with a small interaction between the grains and stylus tip. As a result, these highly abrasive grains have small impact on the stylus tip wear. For crystalline rocks, however, the stylus tip likely scratches through all crystals that are more densely packed (regardless of high or low abrasivity). All minerals on the tested surface are, therefore, responsible to the wear of stylus tip.

Correlations between CAI and mineral compositions of rocks (Figures 6.8 and 6.9) give a more promising approach to predict the wear of stylus tip, as compared to the CAI-$\sigma_c$ relations. For CAI-EQC and CAI-$H_V$ relations, the improvement of their correlation coefficients by analyzing clastic and crystalline rocks individually suggests that CAI is governed not only by hardness of minerals composing rocks, but also by rock characteristics.

The volumetric hardness ($H_V$) proposed in this study has a clear advantage over the EQC method when they are correlated with CAI. For soft rocks EQC can not distinguish the different responses of mineral compositions to CAI. As demonstrated in Figure 6.8, these soft rocks include those containing low hardness minerals, for example, travertine, dickite, salt and gypsum. This is because EQC uses multipliers given by Rosiwal abrasiveness ($R_i$) which places a main emphasis on hard minerals, as $R_i$ = 100 (%) for quartz. $R_i$ values are decreased rapidly toward soft minerals with hardness low than 7. The volumetric hardness proposed here, however, simply uses Mohs scale hardness as multipliers to the minerals. The Mohs scale has been designed with, more or less, equal intervals for mineral hardness variation. Hence, $H_V$ can distinguish the equivalent rock hardness gradually and continuously from low to high ranges of CAI better than EQC. This is, particularly, useful for soft to medium strong rocks that are commonly found in mining and construction projects in Thailand.

It is recognized here that CAI is also affected by grain (crystal) size and shape, as experimentally shown by Er and Tuğrul (2016) and Yaralı et al. (2008). These factors

can not be analyzed in this study due to the narrow range of rock characteristics and limited number of rock types.

The concept of CERCHAR specific energy (CSE) is relatively new. It excludes the wear of stylus tip while deriving the relation between the applied mechanical energy of stylus pin and the mechanical properties and characteristics of rock. Only fair correlations have been obtained here for CSE-CAI and CSE-$\sigma_c$ relations (Figures 6.11 and 6.12). This may be due to the different mechanisms that induce failure and breakage between the two tests, as discussed above for CAI-$\sigma_c$ relation. The correlation analysis between CSE and triaxial properties reveals differences compared to the correlations observed between CAI and triaxial properties. In the case of CSE, neither cohesion nor friction angle exhibit any significant influence on CSE for both clastic and crystalline rocks, as illustrated in Figures 6.13 and 6.14.

To correlate CAI with machine and tool wear during construction and excavation, practitioners and operators need to keep record and documentation on the rock characteristics and operating parameters during excavation process. These include, for example, rock type, mineral compositions, rotational speeds, weight on bits, penetration rates, and temperatures. The more accurate and detailed records, the better correlation between the tool wear and the CAI obtained from laboratory can be achieved.

## 7.2 Conclusions

To determine the wear of excavation tools as affected by rock characteristics, CERCHAR abrasivity index (CAI) tools have been performed to correlate the results with various aspects of mechanical and mineral properties of twenty rock types commonly encountered in mining and construction projects in Thailand. Conclusions drawn from this study can be summarized as follows.

1)	No significant correlation ($R^2 < 0.1$) between CAI and density for all rock types.

2)	A strong correlation ($R^2 = 0.948$) is presented between CAI and rock porosity only for clastic rocks.

3)	Poor correlation ($R^2 = 0.247$) is obtained between CAI and uniaxial compressive strengths of Thai rocks selected in this study, primarily due to the differences of mechanisms governing the results obtained from the two tests.

4)	Young's modulus and Poisson's ratio relate with CAI only for clastic rocks, while crystalline rocks show a fair correlation for Young's modulus and no correlation for Poisson's ratio.

5)	A positive linear equation can adequately describe relation between CAI and rock friction angle for all rock groups, while no correlation between CAI and rock cohesion has been found, except for clastic rocks, where a strong negative correlation is found.

6)	Equivalent quartz content (EQC) and volumetric hardness ($H_V$) can be correlated with CAI. Their correlations notably improve when clastic rocks and crystalline rocks are analyzed separately in the regression.

7)	CAI-$H_V$ relation gives a clear advantage over CAI-EQC relation, as it can provide a better correlation for rocks containing soft to medium hard minerals.

8)	Scratching groove volume reduces exponentially with increasing rock abrasiveness.

9)	CSE increases with CAI, suggesting that rocks with high abrasivity require higher energy to cut, and yield lower excavated volume than those with lower abrasivity. Except for the clastic rocks, where the energy required can be estimated based on their uniaxial compressive strength instead of abrasivity.

10)     No correlation has been found between CSE and rock cohesion and friction angle.

## 7.3     Recommendations for future studies

The suggestions for additional studies are as follows:

1)     More CAI testing is required on a variety of rock types with wider range of rock strength, the results would yield more rigorous conclusions.

2)     The mechanisms driving the correlations for the performance and properties for all rocks are needed.

3)     The mineral properties that play a role in abrasiveness should be further investigated.

4)     A variety of clastic rocks should be investigated, in particular, on those containing various types of cementing materials.

5)     The effects of water content, grain (crystal) size and temperature should be assessed as they are normally encountered under in-situ conditions.

# REFERENCES

Al-Ameen, S. I., & Waller, M. D. (1994). The influence of rock strength and abrasive mineral content on the Cerchar Abrasive Index. *Engineering Geology, 36*(3), 293-301.

Alber, M., Yaralı, O., Dahl, F., Bruland, A., Käsling, H., Michalakopoulos, T. N., ... Özarslan, A. (2014). ISRM Suggested method for determining the abrasivity of rock by the CERCHAR abrasivity test. *Rock Mechanics and Rock Engineering, 47*(1), 261-266.

Altindag, R., Sengun, N., Sarac, S., Mutluturk, M., & Guney, A. (2009). Evaluating the relations between brittleness and Cerchar abrasion index of rocks. *Proceedings of the ISRM Regional Symposium - EUROCK 2009* (pp. 195-200). Cavtat, Croatia: CRC Press.

American Society for Testing and Materials. (2014). *Annual Book of ASTM Standards: Standard Test Methods for Compressive Strength and Elastic Moduli of Intact Rock Core Specimens under Varying States of Stress and Temperatures* (Vol. 04.09). West Conshohocken, PA: ASTM International.

American Society for Testing and Materials. (2018). *Annual Book of ASTM Standards: Standard Test Methods for Absorption and Bulk Specific Gravity of Dimension Stone* (Vol. 04.07). West Conshohocken, PA: ASTM International.

American Society for Testing and Materials. (2019). *Annual Book of ASTM Standards: Standard Test Method for Determination of Relative Crystallinity of Zeolite Sodium A by X-ray Diffraction* (Vol. 05.06). West Conshohocken, PA: ASTM International.

American Society for Testing and Materials. (2022). *Annual Book of ASTM Standards: Standard Test Method for Laboratory Determination of Abrasiveness of Rock Using the CERCHAR Method* (Vol. 04.09). West Conshohocken, PA: ASTM International.

Atkinson, T., Cassapi, V. B., & Singh, R. N. (1986). Assessment of abrasive wear resistance potential in rock excavation machinery. *International Journal of Mining and Geological Engineering, 4*(2), 151-163.

Aydın, H. (2019). Investigating the effects of various testing parameters on Cerchar abrasivity index and its repeatability. *Wear, 418-419*(1), 61-74.

Aydın, H., Yaralı, O., & Duru, H. (2016). The effects of specimen surface conditions and type of test apparatus on Cerchar Abrasivity Index. *Karaelmas Fen ve Mühendislik Dergisi, 6*(2), 293-298.

Balani, A., Chakeri, H., Barzegari, G., & Ozcelik, Y. (2017). Investigation of various parameters effect on CERCHAR abrasivity index with PFC3D modeling. *Geotechnical and Geological Engineering, 35*(6), 2747-2762.

Beste, U., Lundvall, A., & Jacobson, S. (2004). Micro-scratch evaluation of rock types—a means to comprehend rock drill wear. *Tribology International, 37*(2), 203-210.

Bharti, S., Deb, D., & Das, P. (2017). Abrasivity investigation by physico-mechanical parameters and microscopic analysis of rock samples. *Proceedings of the International Conference on Deep Excavation, Energy Resource and Production*, IIT Kharagpur, India.

Capik, M., & Yilmaz, A. O. (2017). Correlation between CERCHAR abrasivity index, rock properties, and drill bit lifetime. *Arabian Journal of Geosciences, 10*(1), 10-15.

Cheshomi, A., & Moradizadeh, M. (2021). The relationship between strength and abrasion characterizations in granite building stones. *Quarterly Journal of Engineering Geology and Hydrogeology, 54*(4).

Deliormanlı, A. H. (2012). CERCHAR abrasivity index (CAI) and its relation to strength and abrasion test methods for marble stones. *Construction and Building Materials, 30*(1), 16-21.

Er, S., & Tuğrul, A. (2016). Correlation of physico-mechanical properties of granitic rocks with CERCHAR abrasivity index in Turkey. *Measurement, 91*(1), 114-123.

Gharahbagh, E., Rostami, J., Ghasemi, A. R., & Tonon, F. (2011). Review of rock abrasion testing. *Proceedings of the 45th U.S. Rock Mechanics/Geomechanics Symposium* (pp. 11-144). San Francisco, California: ARMA.

Hamzaban, M.-T., Memarian, H., & Rostami, J. (2014). Continuous monitoring of pin tip wear and penetration into rock surface using a new CERCHAR abrasivity testing device. *Rock Mechanics and Rock Engineering, 47*(2), 689-701.

Hamzaban, M., Karami, B., & Rostami, J. (2019). Effect of pin speed on Cerchar abrasion test results. *Journal of Testing and Evaluation, 47*(1), 121-139.

Hamzaban, M. T., Memarian, H., & Rostami, J. (2018). Determination of scratching energy index for CERCHAR abrasion test. *Journal of Mining and Environment, 9*(1), 73-89.

He, J., Li, S., Li, X., Wang, X., & Guo, J. (2016). Study on the correlations between abrasiveness and mechanical properties of rocks combining with the microstructure characteristic. *Rock Mechanics and Rock Engineering, 49*(7), 2945-2951.

Jacobs, N., & Hagan, P. (2009). The effect of stylus hardness and some test parameters on Cerchar abrasivity index. *Proceedings of the 43rd U.S. Rock Mechanics Symposium*. Asheville, North Carolina: ARMA.

Janc, B., Jovicic, V., & Vukelić, Ž. (2020). Laboratory test methods for assessing the abrasivity of rocks and soils in geotechnology and mining applications. *Materials and Geoenvironment, 67*(3), 103-118.

Käsling, H., & Thuro, K. (2010). Determining rock abrasivity in the laboratory. *Proceedings of the* European Rock Mechanics Symposium EUROCK 2010 (pp. 425-428). Lausanne, Switzerland: CRC Press.

Ko, T. Y., Kim, T. K., Son, Y., & Jeon, S. (2016). Effect of geomechanical properties on Cerchar Abrasivity Index (CAI) and its application to TBM tunnelling. *Tunnelling and Underground Space Technology, 57*(1), 99-111.

Kotsombat, T., Thongprapha, T., & Fuenkajorn, K. (2020). Scratching rate effects on CERCHAR abrasiveness index of sandstones. *Proceedings of the Academicsera International Conference*. Chiang Mai, Thailand.

Lassnig, K., Latal, C., & Klima, K. (2008). Impact of grain size on the CERCHAR abrasiveness test. *Geomechanics and Tunnelling, 1*(1), 71-76.

Latal, C., Bach, H., & Thuro, K. (2020). Application of test methods for tool wear in quality control of railway ballast. *Geomechanics and Tunnelling, 13*(3), 327-337.

Lee, S., Jeong, H.-Y., & Jeon, S. (2012). Determination of Rock Abrasiveness using Cerchar Abrasiveness Test. *Tunnelling and Underground Space Technology, 22*(4), 284-295.

Li, Q., Li, J., Duan, L., & Tan, S. (2021). Prediction of rock abrasivity and hardness from mineral composition. *International Journal of Rock Mechanics and Mining Sciences, 140*(1).

Liu, B., Schieber, J., Mastalerz, M., & Teng, J. (2020). Variability of rock mechanical properties in the sequence stratigraphic context of the Upper Devonian New Albany Shale, Illinois Basin. *Marine and Petroleum Geology, 112*(1).

Majeed, Y., & Abu Bakar, M. Z. (2016). Statistical evaluation of CERCHAR abrasivity index (CAI) measurement methods and dependence on petrographic and mechanical properties of selected rocks of Pakistan. *Bulletin of Engineering Geology and the Environment, 75*(3), 1341-1360.

Moradizadeh, M., Cheshomi, A., Ghafoori, M., & TrighAzali, S. (2016). Correlation of equivalent quartz content, slake durability index and Is50 with CERCHAR abrasiveness index for different types of rock. *International Journal of Rock Mechanics and Mining Sciences, 86*(1), 42-47.

Nilsen, B., Dahl, F., Holzhauser, J., & Raleigh, P. (2006). Abrasivity testing for rock and soil. *Tunnels and Tunnelling International, 38*(4), 47-49.

Ozdogan, M. V., Deliormanli, A. H., & Yenice, H. (2018). The correlations between the CERCHAR abrasivity index and the geomechanical properties of building stones. *Arabian Journal of Geosciences, 11*(20).

Plinninger, R., Käsling, H., Thuro, K., & Spaun, G. (2003). Testing conditions and geomechanical properties influencing the CERCHAR abrasiveness index (CAI) value. *International Journal of Rock Mechanics and Mining Sciences, 40*(2), 259-263.

Plinninger, R. J. (2010). Hardrock abrasivity investigation using the rock abrasivity index (RAI). *Proceedings of the Geologically Active: 11th IAEG Congress* (pp. 3445-3452). Auckland, NewZealand: CRC Press.

Prieto, L. (2012). The CERCHAR abrasivity index's applicability to dredging rock. *Proceedings of the Western Dredging Association (WEDA XXXII) Technical Conference and Texas A&M University (TAMU 43) Dredging Seminar* (pp. 212-219). San Antonio, Texas: WEDA.

Rostami, J., Ghasemi, A., Alavi Gharahbagh, E., Dogruoz, C., & Dahl, F. (2014). Study of dominant factors affecting CERCHAR abrasivity index. *Rock Mechanics and Rock Engineering, 47*(5), 1905-1919.

Rostami, J., Ozdemir, L., Bruland, A., & Dahl, F. (2005). Review of issues related to Cerchar abrasivity testing and their implications on geotechnical investigations and cutter cost estimates. *Proceedings of the Rapid Excavation and Tunnelling Conference (RETC)* (pp. 738-751). Seattle, Washington: SME.

Rostami, K., Hamidi, J. K., & Nejati, H. R. (2020). Use of rock microscale properties for introducing a cuttability index in rock cutting with a chisel pick. *Arabian Journal of Geosciences, 13*(18), 1-12.

Sirdesai, N. N., Aravind, A., & Panchal, S. (2021). Impact of rock abrasivity on TBM cutter-discs during tunnelling in various rock formations. *Proceedings of the Advances in Mechanical Engineering* (pp. 527-534). Singapore: Springer.

Sotoudeh, F., Memarian, H., Hamzaban, M. T., & Rostami, J. (2014). Improvement of testing accuracy by a new generation of Cerchar abrasivity testing device. *Proceedings of the North American Tunneling Conference* (pp. 211-217). Los Angeles, California: SME.

Suana, M., & Peters, T. (1982). The CERCHAR abrasivity index and its relation to rock mineralogy and petrography. *Rock Mechanics, 15*(1), 1-8.

Teale, R. (1965). The concept of specific energy in rock drilling. *International Journal of Rock Mechanics and Mining Sciences & Geomechanics Abstracts, 2*(1), 57-73.

Teymen, A. (2020). The usability of Cerchar abrasivity index for the estimation of mechanical rock properties. *International Journal of Rock Mechanics and Mining Sciences, 128*(1).

Thuro, K. (1997). Drillability prediction: geological influences in hard rock drill and blast tunnelling. *Geologische Rundschau, 86*(2), 426-438.

Thuro, K., & Käsling, H. (2009). Classification of the abrasiveness of soil and rock. *Geomechanics and Tunnelling, 2*(2), 179-188.

Torrijo, F. J., Garzón-Roca, J., Company, J., & Cobos, G. (2019). Estimation of Cerchar abrasivity index of andesitic rocks in Ecuador from chemical compounds and petrographical properties using regression analyses. *Bulletin of Engineering Geology and the Environment, 78*(4), 2331-2344.

Ündül, Ö., & Er, S. (2017). Investigating the effects of micro-texture and geo-mechanical properties on the abrasiveness of volcanic rocks. *Engineering Geology, 229*(1), 85-94.

Wengang, Z., Liang, H., Zixu, Z., & Yanmei, Z. (2021). Digitalization of mechanical and physical properties of Singapore Bukit Timah granite rocks based on borehole data from four sites. *Underground Space, 6*(5), 483-491.

West, G. (1986). A relation between abrasiveness and quartz content for some Coal Measures sediments. *International Journal of Mining and Geological Engineering, 4*(1), 73-78.

West, G. (1989). Rock abrasiveness testing for tunnelling. *International Journal of Rock Mechanics and Mining Sciences & Geomechanics Abstracts, 26*(2), 151-160.

Yaralı, O., & Duru, H. (2016). Investigation into effect of scratch length and surface condition on Cerchar abrasivity index. *Tunnelling and Underground Space Technology, 60*(1), 111-120.

Yarali, O., Duru, h., & Sakız, U. (2014). Evaluation of the relationships among drilling rate index (DRI), mechanical properties, Cerchar abrasivity index and specific energy for rocks. *Proceedings of the Aachen Sixth International Mining Symposium* (pp. 205-220). Germany.

Yaralı, O., Yaşar, E., Bacak, G., & Ranjith, P. G. (2008). A study of rock abrasivity and tool wear in coal measures rocks. *International Journal of Coal Geology, 74*(1), 53-66.

Yasar, S., & Yilmaz, A. (2016). Tool wear prediction with different models for medium strength rocks. *Proceedings of the 13th International Conference Underground Construction Prague 2016*. Prague.

Zhang, G., & Konietzky, H. (2020). Cerchar Abrasion Ratio (CAR) as a New Indicator for Assessing Rock Abrasivity, Rock–Stylus Interaction and Cutting Efficiency. *Rock Mechanics and Rock Engineering, 53*(7), 3363-3371.

Zhang, G., Konietzky, H., & Frühwirt, T. (2020). Investigation of scratching specific energy in the Cerchar abrasivity test and its application for evaluating rock-tool interaction and efficiency of rock cutting. *Wear, 448-449*(1).

Zhang, G., Konietzky, H., Song, Z., & Huang, S. (2020). Study of some testing condition-based factors affecting the Cerchar abrasivity index (CAI). *Arabian Journal of Geosciences, 13*(23).

Zhang, G., Konietzky, H., Song, Z., & Zhang, M. (2020). Study of Cerchar abrasive parameters and their relations to intrinsic properties of rocks for construction. *Construction and Building Materials, 244*(1).

Zhang, S.-R., She, L., Wang, C., Wang, Y.-J., Cao, R.-L., Li, Y.-L., & Cao, K.-L. (2021). Investigation on the relationship among the Cerchar abrasivity index, drilling parameters and physical and mechanical properties of the rock. *Tunnelling and Underground Space Technology, 112*(1).

APPENDIX A

UNIAXIAL AND TRIAXIAL COMPRESSIVE STRENGTH TEST RESULTS

Table A.1 Density, and uniaxial compressive strength, Young's modulus, and Poisson's ratio from uniaxial compression tests of clastic rock group.

| Sample No | Density (g/cc) | $\sigma_c$ (MPa) | E (Gpa) | n |
|---|---|---|---|---|
| Phu Phan sandstone – 1 | 2.33 | 83.0 | 9.9 | 0.21 |
| Phu Phan sandstone – 2 | 2.38 | 96.1 | 15.3 | 0.13 |
| Phu Phan sandstone – 3 | 2.37 | 76.3 | 11.3 | 0.21 |
| Phu Phan sandstone – 4 | 2.35 | 65.5 | 9.7 | 0.21 |
| Phu Phan sandstone – 5 | 2.34 | 86.3 | 11.6 | 0.20 |
| Mean ± SD | 2.35 ± 0.02 | 81.4 ± 11.4 | 11.5 ± 2.3 | 0.19 ± 0.04 |
| Sao Khua sandstone – 1 | 2.49 | 52.4 | 4.8 | 0.16 |
| Sao Khua sandstone – 2 | 2.46 | 48.1 | 6.6 | 0.18 |
| Sao Khua sandstone – 3 | 2.45 | 59.0 | 5.7 | 0.19 |
| Mean ± SD | 2.47 ± 0.02 | 53.1 ± 5.5 | 5.7 ± 0.9 | 0.18 ± 0.02 |
| Pha Wihan sandstone – 1 | 2.24 | 28.4 | 6.9 | 0.19 |
| Pha Wihan sandstone – 2 | 2.26 | 72.1 | 13.3 | 0.21 |
| Pha Wihan sandstone – 3 | 2.24 | 72.1 | 9.6 | 0.20 |
| Pha Wihan sandstone – 4 | 2.24 | 67.7 | 12.4 | 0.18 |
| Pha Wihan sandstone – 5 | 2.31 | 69.7 | 10.5 | 0.22 |
| Mean ± SD | 2.26 ± 0.03 | 70.4 ± 2.1 | 11.5 ± 1.7 | 0.20 ± 0.02 |
| Phu Kradung sandstone – 1 | 2.51 | 87.3 | 7.1 | 0.11 |
| Phu Kradung sandstone – 2 | 2.51 | 59.0 | 4.6 | 0.13 |
| Phu Kradung sandstone – 3 | 2.51 | 93.9 | 5.6 | 0.12 |
| Mean ± SD | 2.51 ± 0.00 | 80.1 ± 18.6 | 5.8 ± 1.2 | 0.12 ± 0.01 |

Table A.2 Density, and uniaxial compressive strength, Young's modulus, and Poisson's ratio from uniaxial compression tests of plutonic rock group.

| Sample No | Density (g/cc) | $\sigma_c$ (MPa) | E (Gpa) | n |
|---|---|---|---|---|
| Granodiorite – 1 | 2.66 | 73.7 | 21.2 | 0.19 |
| Granodiorite – 2 | 2.65 | 71.2 | 22.6 | 0.20 |
| Granodiorite – 3 | 2.67 | 87.1 | 20.8 | 0.22 |
| Granodiorite – 4 | 2.65 | 57.9 | 15.3 | 0.19 |
| Mean ± SD | 2.66 ± 0.01 | 72.5 ± 12.0 | 20.0 ± 3.2 | 0.20 ± 0.02 |
| Tak granite – 1 | 2.63 | 96.4 | 16.1 | 0.15 |
| Tak granite – 2 | 2.62 | 70.3 | 9.0 | 0.17 |
| Tak granite – 3 | 2.68 | 100.5 | 8.3 | 0.18 |
| Tak granite – 4 | 2.58 | 52.4 | 13.7 | 0.14 |
| Tak granite – 5 | 2.60 | 102.7 | 11.1 | 0.11 |
| Mean ± SD | 2.62 ± 0.04 | 84.5 ± 22.1 | 11.6 ± 3.2 | 0.15 ± 0.03 |
| Haad Som Pan granite – 1 | 2.61 | 51.4 | 11.7 | 0.20 |
| Haad Som Pan granite – 2 | 2.57 | 23.4 | 6.1 | 0.24 |
| Haad Som Pan granite – 3 | 2.53 | 36.5 | 4.3 | 0.23 |
| Mean ± SD | 2.57 ± 0.04 | 37.1 ± 14.0 | 7.3 ± 3.9 | 0.22 ± 0.02 |

Table A.3 Density, and uniaxial compressive strength, Young's modulus, and Poisson's ratio from uniaxial compression tests of carbonate rock group.

| Sample No | Density (g/cc) | $\sigma_c$ (MPa) | E (Gpa) | n |
|---|---|---|---|---|
| Khao Khad marble – 1 | 2.80 | 53.2 | 8.6 | 0.22 |
| Khao Khad marble – 2 | 2.77 | 29.8 | 7.6 | 0.24 |
| Khao Khad marble – 3 | 2.76 | 29.1 | 7.6 | 0.21 |
| Khao Khad marble – 4 | 2.73 | 40.4 | 9.5 | 0.23 |
| Khao Khad marble – 5 | 2.81 | 29.5 | 4.9 | 0.25 |
| Mean ± SD | 2.77 ± 0.03 | 36.4 ± 10.5 | 7.6 ± 1.7 | 0.23 ± 0.02 |
| Khao Khad limestone – 1 | 2.68 | 52.4 | 14.7 | 0.33 |
| Khao Khad limestone – 2 | 2.68 | 63.3 | 16.3 | 0.32 |
| Khao Khad limestone – 3 | 2.68 | 32.8 | 9.0 | 0.33 |
| Khao Khad limestone – 4 | 2.67 | 59.0 | 15.6 | 0.31 |
| Khao Khad limestone – 5 | 2.67 | 65.5 | 15.9 | 0.34 |
| Mean ± SD | 2.68± 0.00 | 54.6 ± 13.2 | 14.3 ± 3.0 | 0.33 ± 0.01 |
| Khao Khad travertine – 1 | 2.71 | 60.2 | 14.2 | 0.28 |
| Khao Khad travertine – 2 | 2.75 | 44.1 | 19.6 | 0.25 |
| Khao Khad travertine – 3 | 2.76 | 52.1 | 13.8 | 0.29 |
| Khao Khad travertine – 4 | 2.76 | 81.1 | 17.9 | 0.23 |
| Khao Khad travertine – 5 | 2.76 | 44.0 | 14.2 | 0.28 |
| Khao Khad travertine – 6 | 2.75 | 76.4 | 15.9 | 0.25 |
| Mean ± SD | 2.75 ± 0.02 | 59.6 ± 14.0 | 15.9 ± 2.4 | 0.26 ± 0.02 |

Table A.4 Density, and uniaxial compressive strength, Young's modulus, and Poisson's ratio from uniaxial compression tests of sulfate and chloride rock group.

| Sample No | Density (g/cc) | $\sigma_c$ (MPa) | E (Gpa) | n |
|---|---|---|---|---|
| Tak Fa gypsum – 1 | 2.24 | 6.5 | 1.7 | 0.19 |
| Tak Fa gypsum – 2 | 2.22 | 5.1 | 9.7 | 0.26 |
| Tak Fa gypsum – 3 | 2.24 | 5.3 | 4.4 | 0.14 |
| Mean ± SD | 2.23 ± 0.01 | 5.6 ± 0.8 | 5.3 ± 4.0 | 020 ± 0.02 |
| Tak Fa anhydrite – 1 | 2.96 | 24.9 | 9.4 | 0.19 |
| Tak Fa anhydrite – 2 | 2.96 | 44.5 | 10.6 | 0.21 |
| Tak Fa anhydrite – 3 | 2.94 | 24.5 | 5.9 | 0.18 |
| Tak Fa anhydrite – 4 | 2.90 | 34.9 | 8.8 | 0.21 |
| Mean ± SD | 2.94± 0.03 | 32.2 ± 9.5 | 8.7 ± 2.0 | 0.20 ± 0.01 |
| Maha Sarakham Salt – 1 | 2.12 | 30.0 | 3.3 | 0.29 |
| Maha Sarakham Salt – 2 | 2.13 | 27.1 | 1.6 | 0.27 |
| Maha Sarakham Salt – 3 | 2.12 | 23.8 | 1.6 | 0.29 |
| Maha Sarakham Salt – 4 | 2.13 | 20.6 | 1.5 | 0.30 |
| Mean ± SD | 2.13 ± 0.00 | 25.4 ± 4.1 | 2.0 ± 0.8 | 0.29 ± 0.02 |

Table A.5 Density, and uniaxial compressive strength, Young's modulus, and Poisson's ratio from uniaxial compression tests of silicate rock group.

| Sample No | Density (g/cc) | $\sigma_c$ (MPa) | E (Gpa) | n |
|---|---|---|---|---|
| Pyrophyllite – 1 | 2.60 | 89.8 | 19.6 | 0.37 |
| Pyrophyllite – 2 | 2.62 | 63.8 | 17.7 | 0.37 |
| Pyrophyllite – 3 | 2.60 | 89.9 | 15.3 | 0.36 |
| Pyrophyllite – 4 | 2.60 | 76.7 | 22.1 | 0.30 |
| Pyrophyllite – 5 | 2.60 | 83.6 | 14.2 | 0.32 |
| Mean ± SD | 2.60 ± 0.01 | 80.8 ± 10.9 | 17.8 ± 3.2 | 0.34 ± 0.03 |
| Dickite – 1 | 2.63 | 27.2 | 9.8 | 0.23 |
| Dickite – 2 | 2.60 | 38.1 | 13.4 | 0.23 |
| Dickite – 3 | 2.62 | 31.7 | 10.3 | 0.23 |
| Mean ± SD | 2.62± 0.01 | 32.3 ± 5.5 | 11.2 ± 2.0 | 0.23 ± 0.00 |
| Skarn – 1 | 2.63 | 83.6 | 18.9 | 0.20 |
| Skarn – 2 | 2.64 | 57.3 | 9.6 | 0.20 |
| Skarn – 3 | 2.63 | 70.5 | 14.4 | 0.20 |
| Mean ± SD | 2.63 ± 0.01 | 70.4 ± 13.2 | 14.3 ± 4.7 | 0.20 ± 0.00 |

Table A.6 Density, and uniaxial compressive strength, Young's modulus, and Poisson's ratio from uniaxial compression tests of volcanic rock group.

| Sample No | Density (g/cc) | $\sigma_c$ (MPa) | E (Gpa) | $\nu$ |
|---|---|---|---|---|
| Khao Kradong basalt – 1 | 2.82 | 85.1 | 15.0 | 0.10 |
| Khao Kradong basalt – 2 | 2.82 | 83.0 | 13.1 | 0.11 |
| Khao Kradong basalt – 3 | 2.82 | 61.2 | 13.8 | 0.11 |
| Khao Kradong basalt – 4 | 2.82 | 87.4 | 11.1 | 0.15 |
| Mean ± SD | 2.82 ± 0.00 | 79.2 ± 12.1 | 13.3 ± 1.6 | 0.12 ± 0.02 |
| Khao Kradong vesicular basalt – 1 | 2.36 | 65.6 | 9.4 | 0.30 |
| Khao Kradong vesicular basalt – 2 | 2.45 | 63.2 | 15.6 | 0.30 |
| Khao Kradong vesicular basalt – 3 | 2.50 | 68.0 | 13.5 | 0.29 |
| Khao Kradong vesicular basalt – 4 | 2.46 | 58.9 | 14.3 | 0.30 |
| Mean ± SD | 2.44± 0.06 | 63.9 ± 3.9 | 13.2 ± 2.7 | 0.30 ± 0.01 |
| Khao Yai rhyolite – 1 | 2.60 | 32.1 | 7.4 | 0.21 |
| Khao Yai rhyolite – 2 | 2.61 | 39.3 | 10.5 | 0.20 |
| Khao Yai rhyolite – 3 | 2.60 | 36.6 | 8.5 | 0.25 |
| Khao Yai rhyolite – 4 | 2.53 | 47.8 | 11.6 | 0.25 |
| Khao Yai rhyolite – 5 | 2.64 | 36.6 | 11.6 | 0.25 |
| Mean ± SD | 2.60 ± 0.04 | 38.5 ± 5.8 | 9.9 ± 1.9 | 0.23 ± 0.02 |
| Khao Yai andesite – 1 | 2.95 | 117.7 | 19.4 | 0.32 |
| Khao Yai andesite – 2 | 3.02 | 73.8 | 5.3 | 0.32 |
| Khao Yai andesite – 3 | 2.94 | 42.7 | 3.1 | 0.33 |
| Khao Yai andesite – 4 | 2.99 | 154.2 | 18.0 | 0.32 |
| Khao Yai andesite – 5 | 2.97 | 162.2 | 21.9 | 0.32 |
| Mean ± SD | 2.98 ± 0.03 | 110.1 ± 51.4 | 13.5 ± 8.7 | 0.32 ± 0.01 |
| Khao Yai tuff – 1 | 2.80 | 46.5 | 8.8 | 0.33 |
| Khao Yai tuff – 2 | 2.77 | 25.9 | 5.3 | 0.35 |
| Khao Yai tuff – 3 | 2.81 | 51.0 | 8.8 | 0.35 |
| Mean ± SD | 279 ± 0.02 | 41.1 ± 13.4 | 7.6 ± 2.0 | 0.34 ± 0.01 |
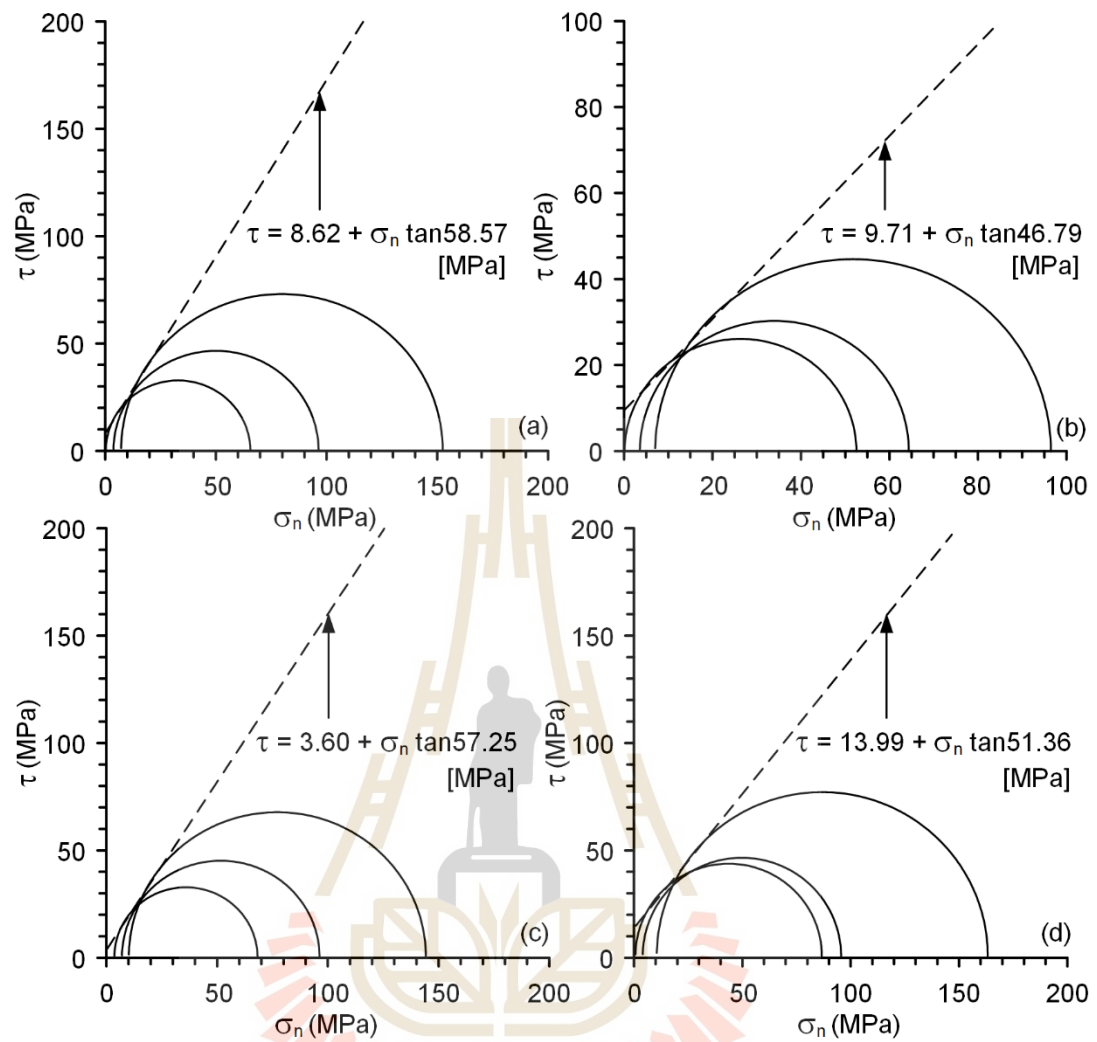
Figure A.1    Mohr's circles from triaxial compressive strength tests of clastic rock group; Phu Phan sandstone (a), Sao Khua sandstone (b), Pha Wihan sandstone (c) and Phu Kradung sandstone (d).
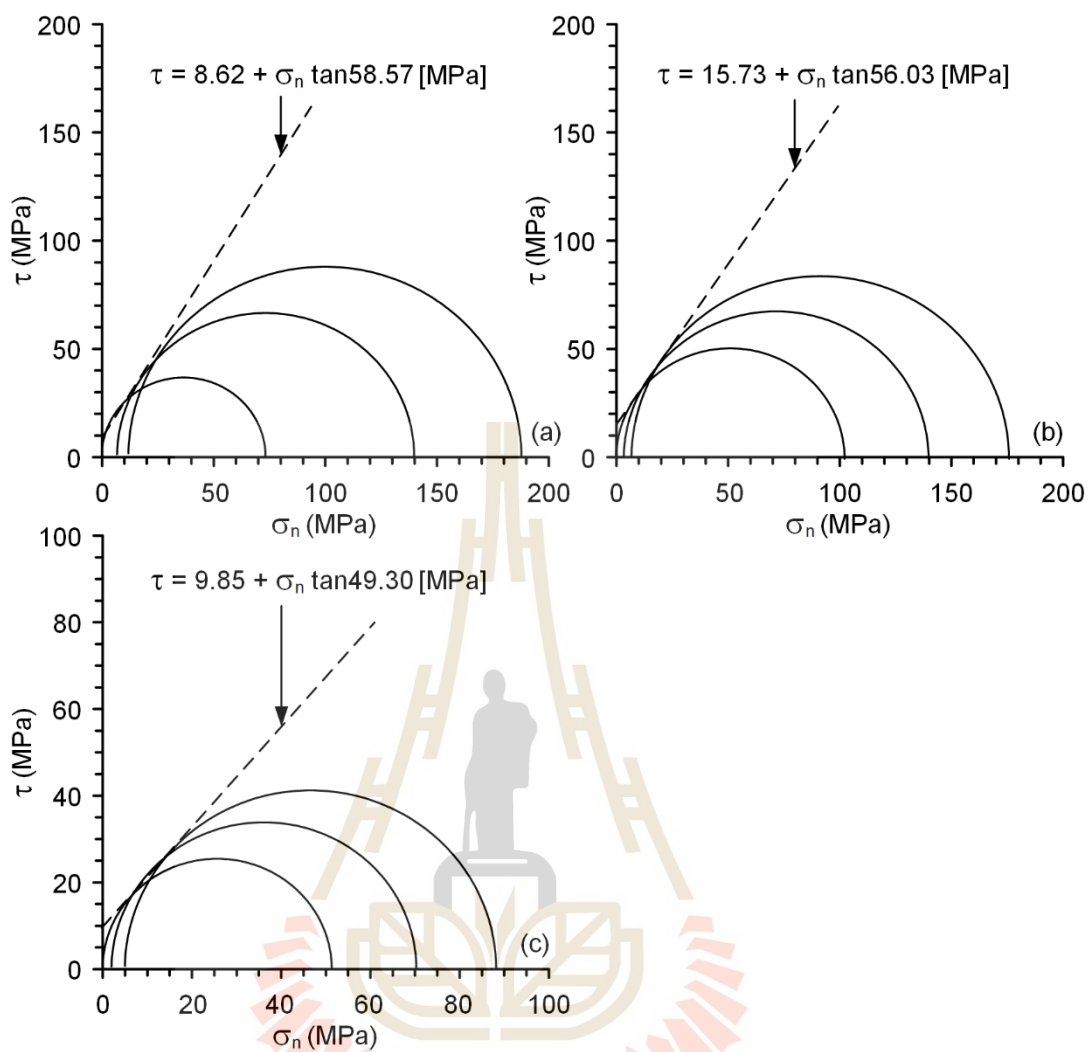
Figure A.2    Mohr's circles from triaxial compressive strength tests of plutonic rock group; granodiorite (a), Tak granite (b) and Haad Som Pan granite (c).
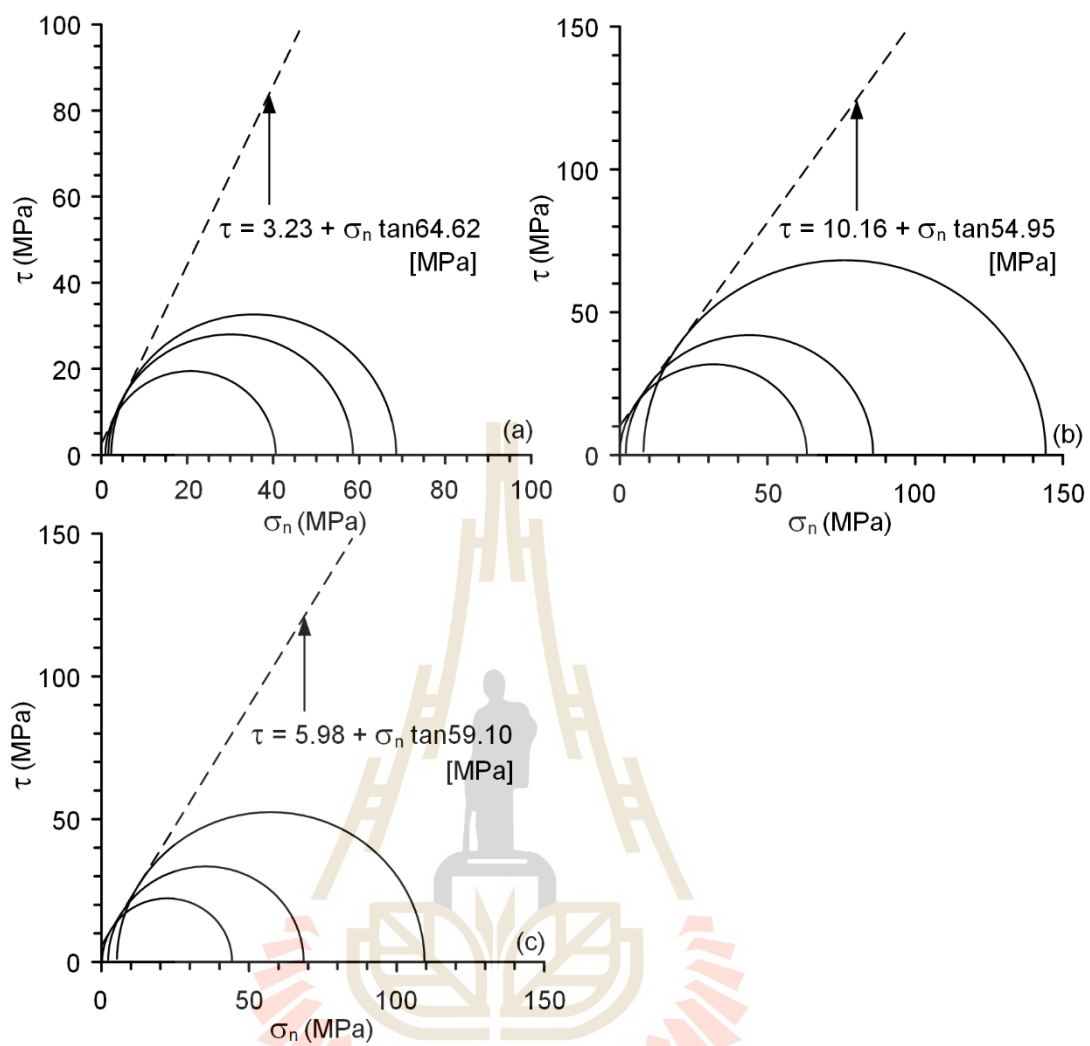
Figure A.3    Mohr's circles from triaxial compressive strength tests of carbonate rock group; Khao Khad marble (a), Khao Khad limestone (b) and Khao Khad travertine (c).
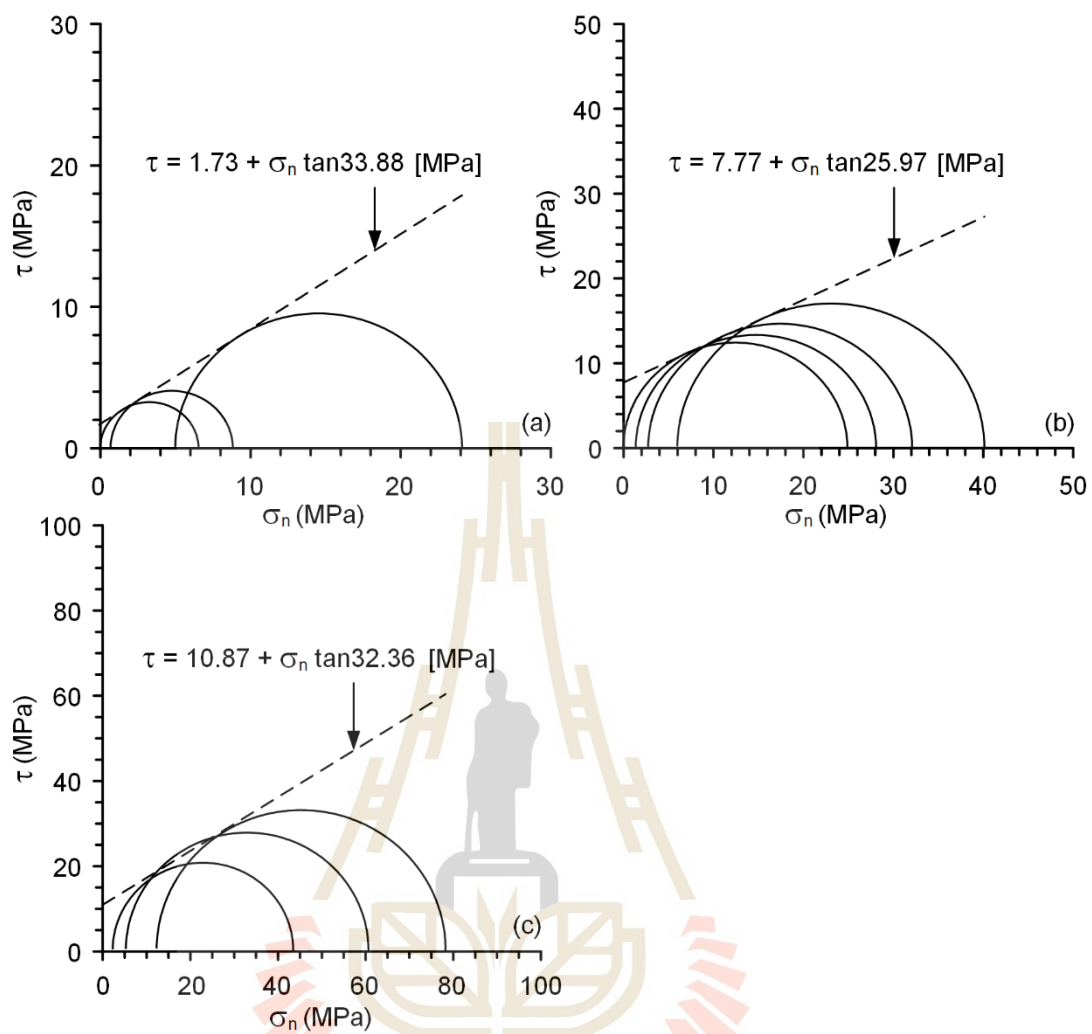
Figure A.4    Mohr's circles from triaxial compressive strength tests of sulfate & chloride rock group; Tak Fa gypsum (a), Tak Fa anhydrite (b) and Maha Sarakham salt (c).
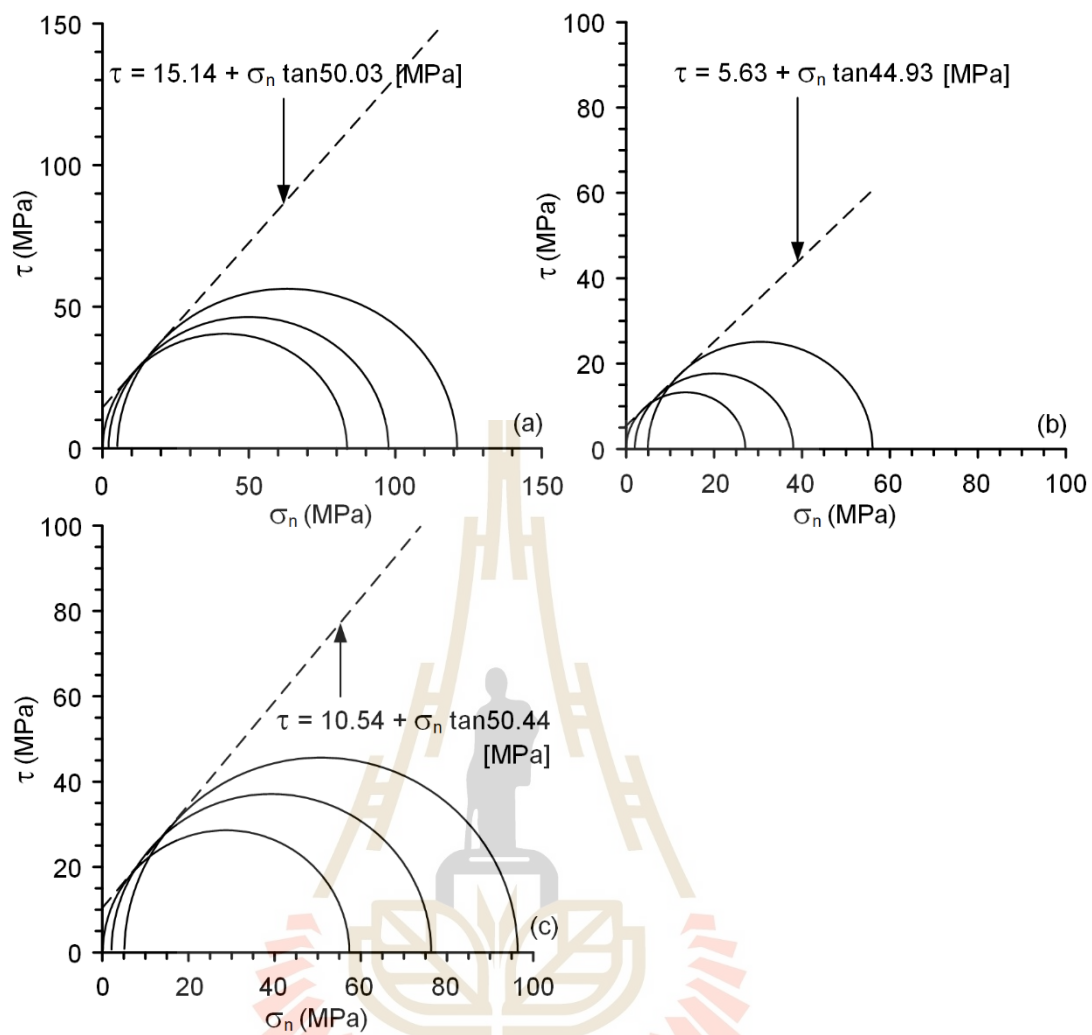
Figure A.5    Mohr's circles from triaxial compressive strength tests of silicate rock group; pyrophyllite (a), dickite (b) and skarn (c).
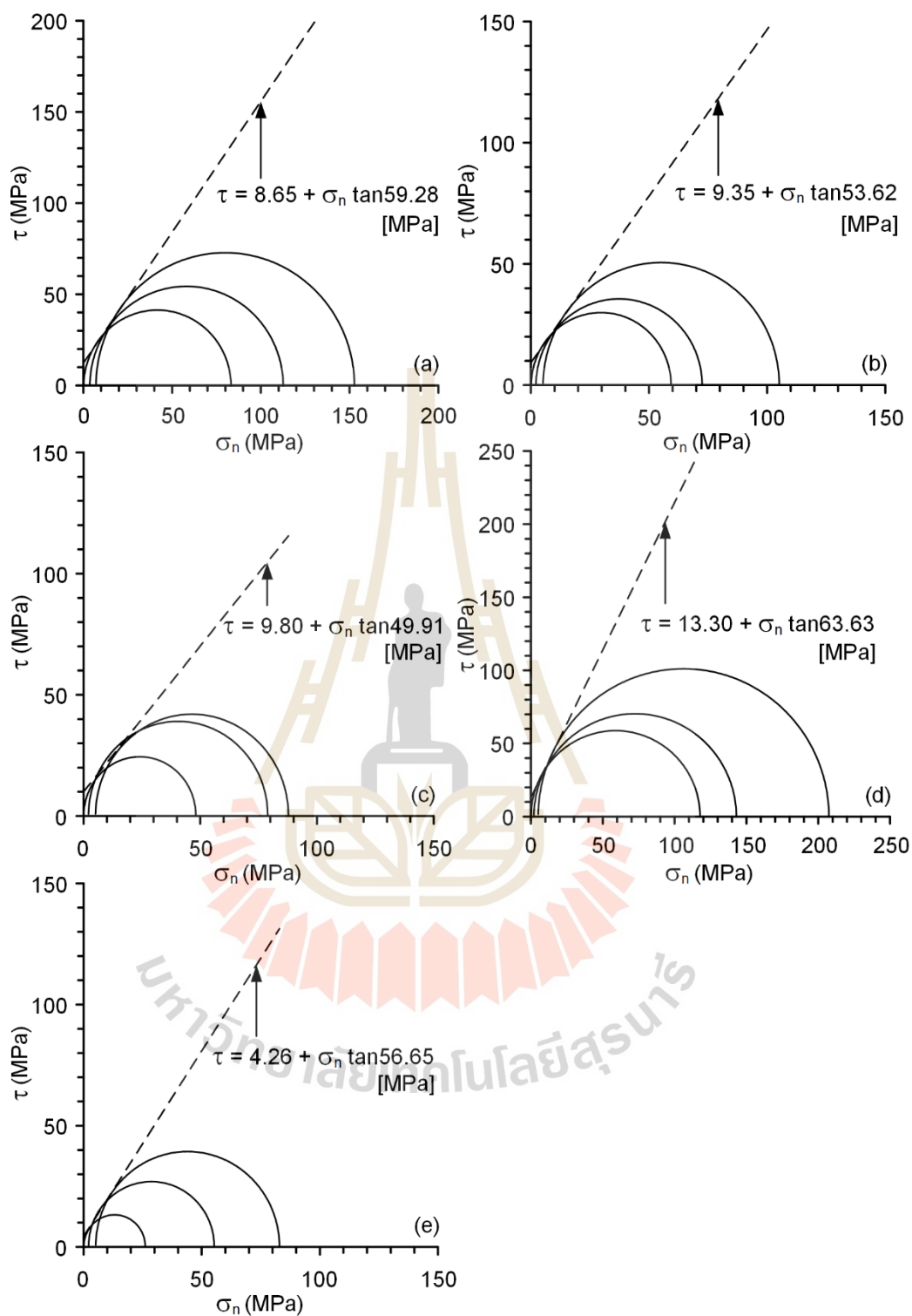
Figure A.6    Mohr's circles from triaxial compressive strength tests of volcanic rock

group; Khao Kradong basalt (a), Khao Kradong vesicular basalt (b), Khao

Yai rhyolite (c), Khao Yai andesite (d) and Khao Yai tuff (e)

APPENDIX B

IMAGES OF CERCHAR STYLUS TIPS AND THEIR CORRESPONDING

GROOVES ON ROCK SURFACE
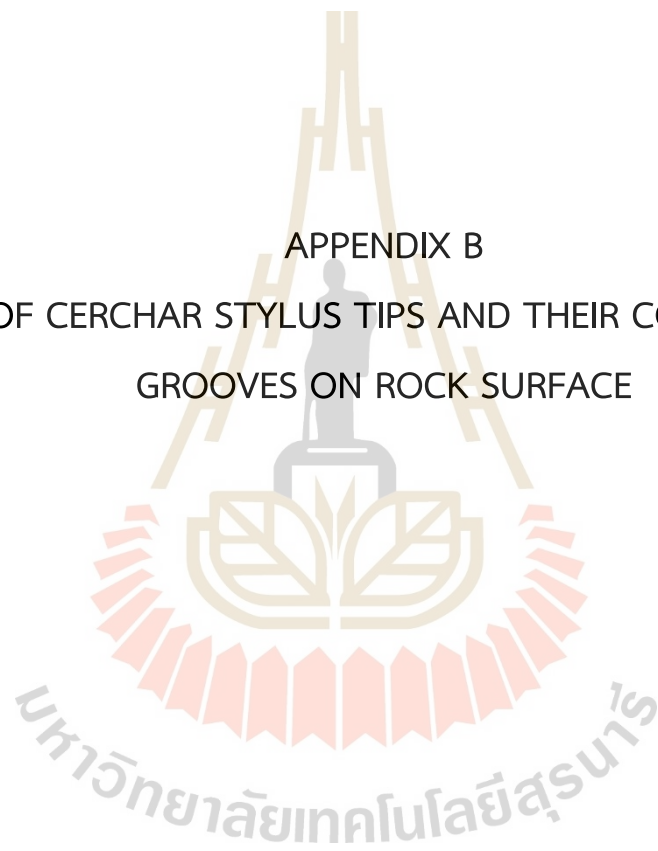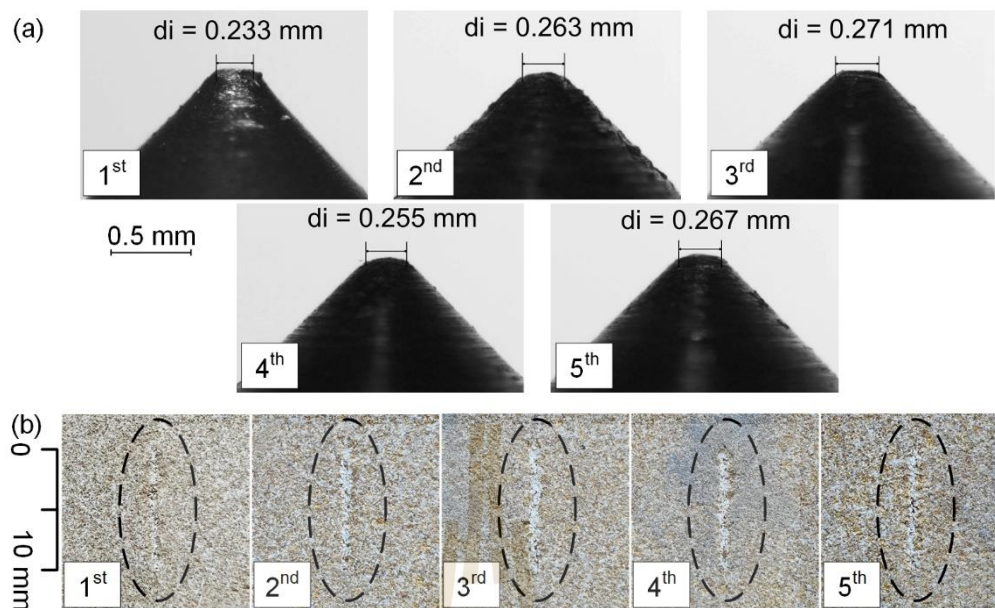
Figure B.1 (a) Steel stylus tips after CERCHAR testing on Phu Phan sandstone specimens and (b) their corresponding groove images.
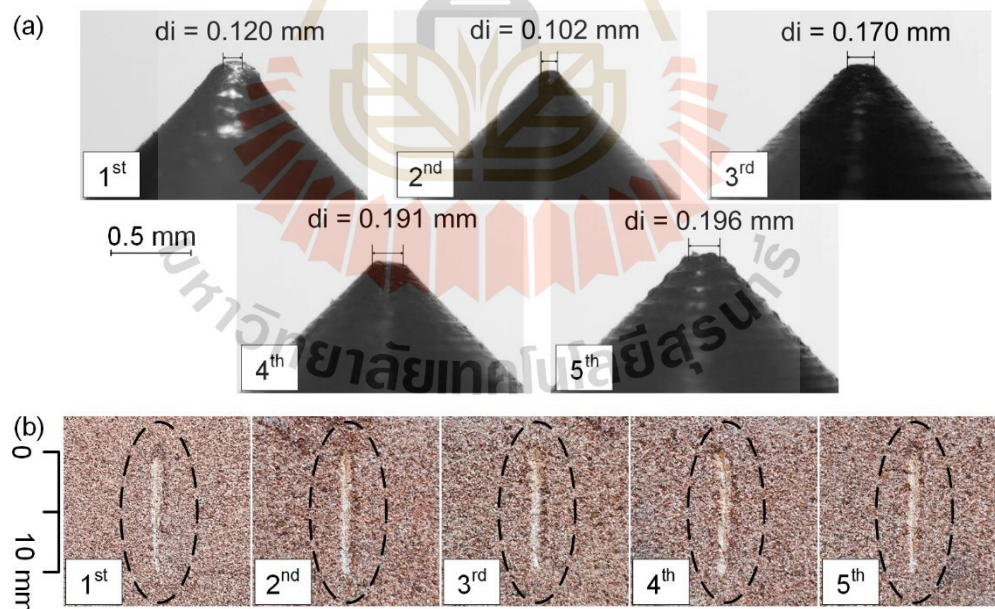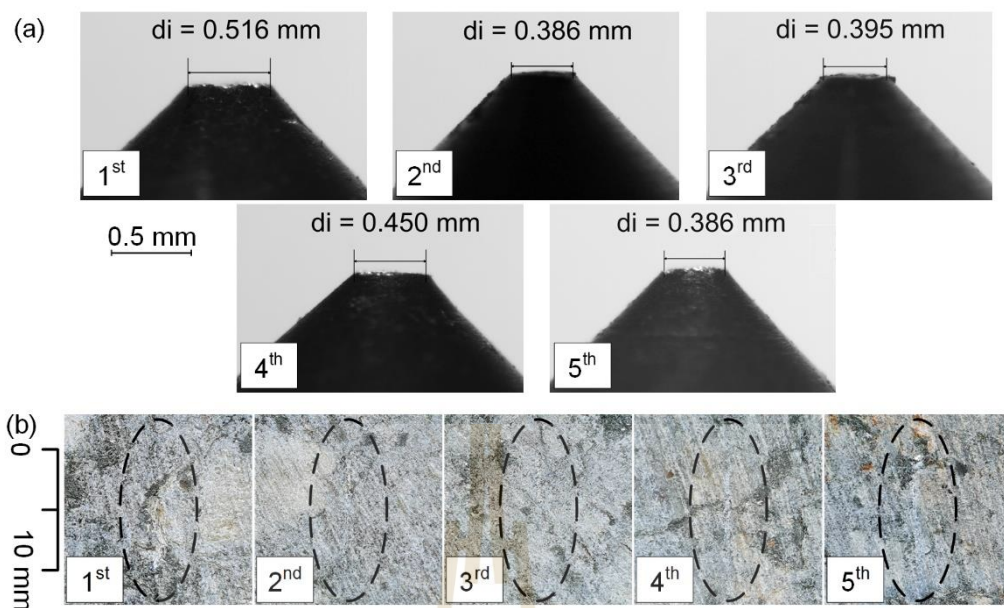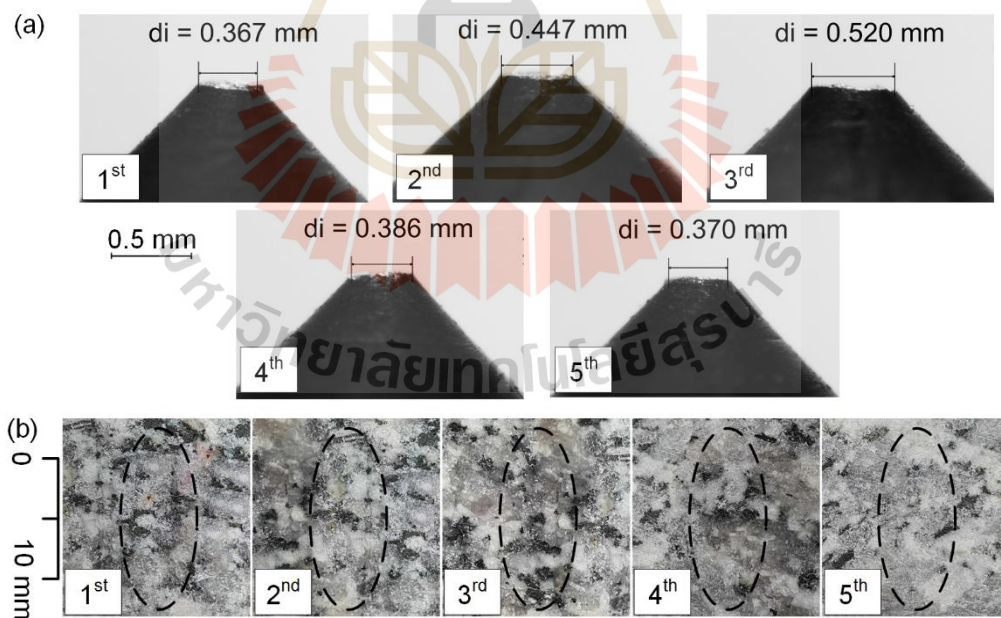


Figure B.2 (a) Steel stylus tips after CERCHAR testing on Sao Khua sandstone specimens and (b) their corresponding groove images.
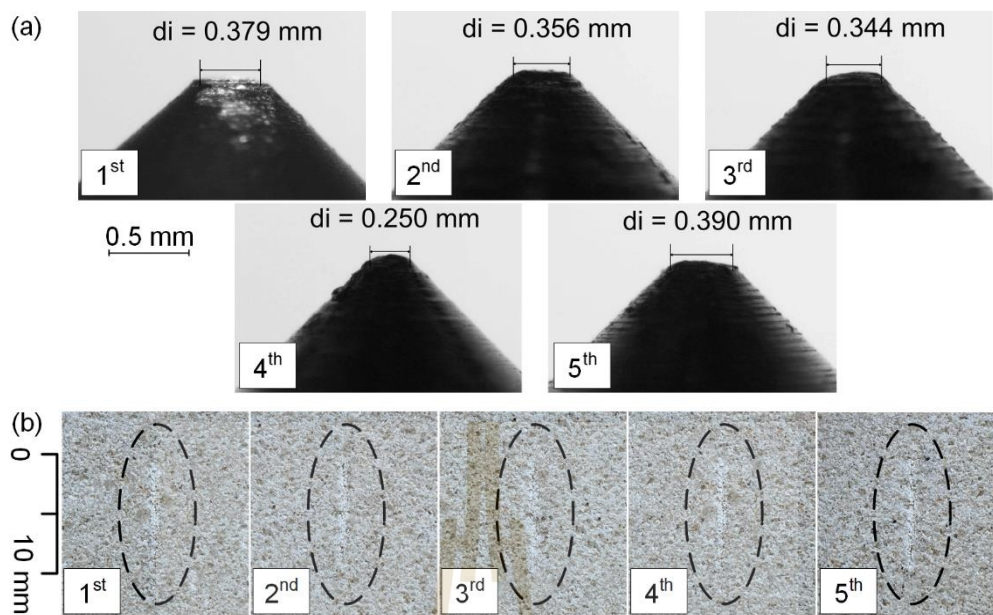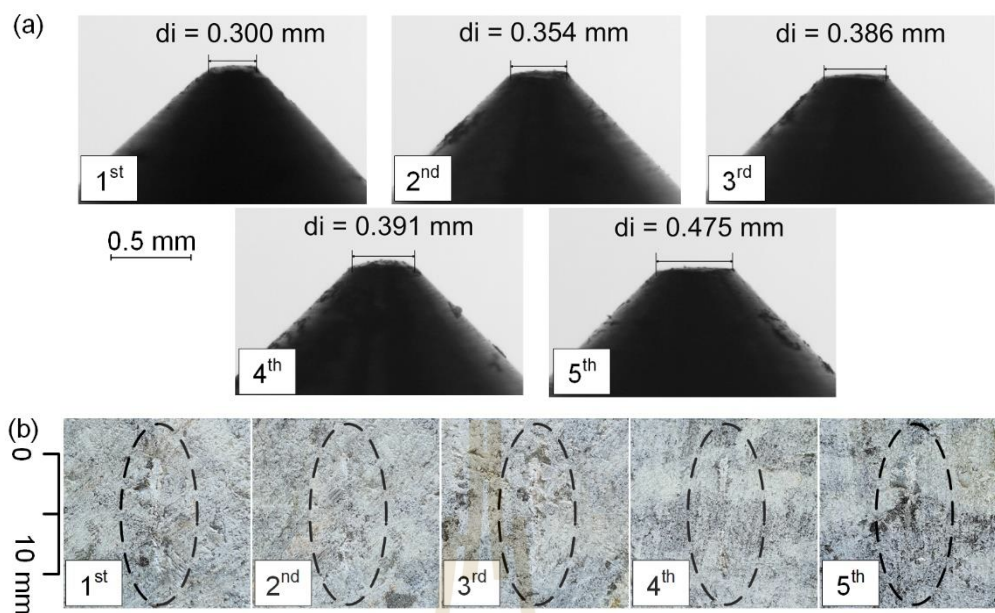
Figure B.3  (a) Steel stylus tips after CERCHAR testing on Phra Wihan sandstone specimens and (b) their corresponding groove images.
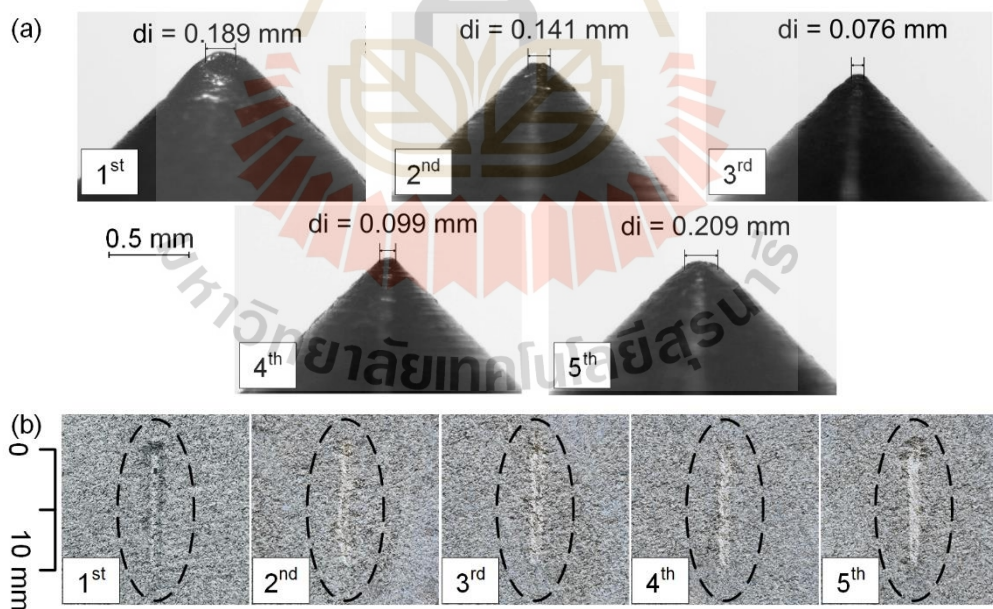


Figure B.4  (a) Steel stylus tips after CERCHAR testing on Phu Kradung sandstone specimens and (b) their corresponding groove images.

Figure B.5  (a) Steel stylus tips after CERCHAR testing on granodiorite specimens and (b) their corresponding groove images.



Figure B.6  (a) Steel stylus tips after CERCHAR testing on Tak granite specimens and (b) their corresponding groove images.

Figure B.7  (a) Steel stylus tips after CERCHAR testing on Haad Som Pan granite specimens and (b) their corresponding groove images.
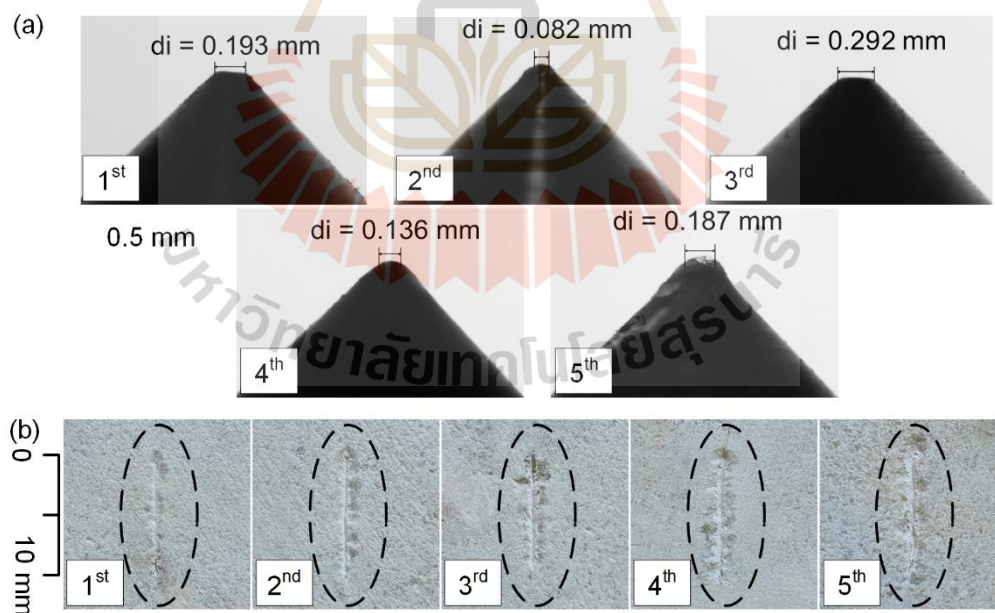


Figure B.8  (a) Steel stylus tips after CERCHAR testing on Khao Khad marble specimens and (b) their corresponding groove images.
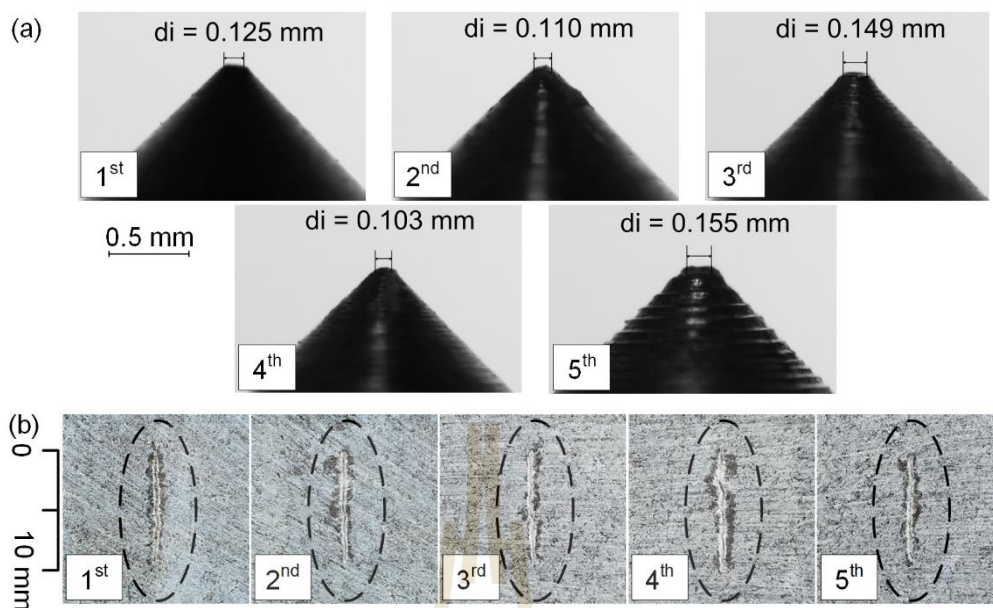
Figure B.9  (a) Steel stylus tips after CERCHAR testing on Khao Khad limestone specimens and (b) their corresponding groove images.
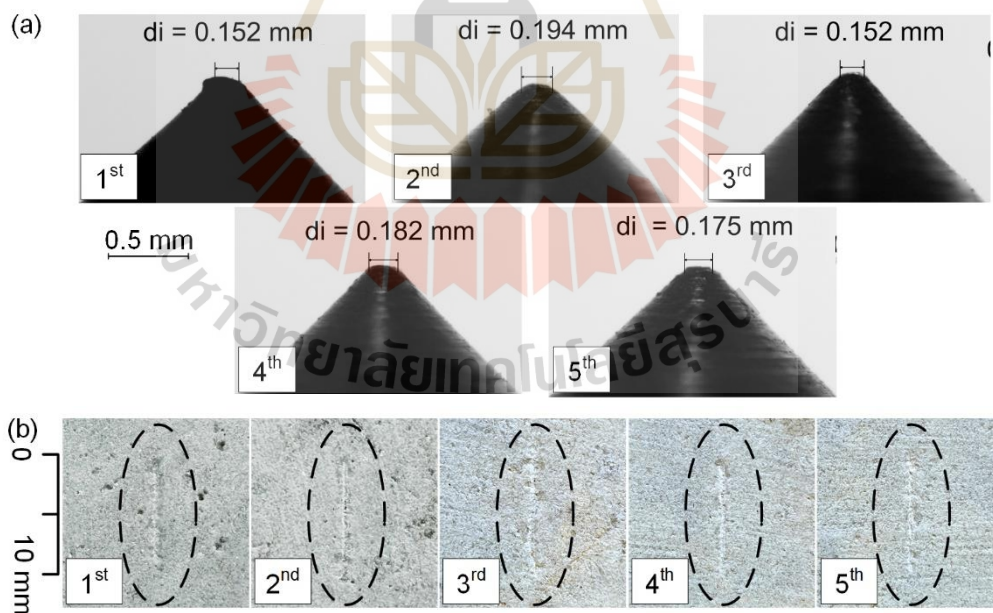


Figure B.10 (a) Steel stylus tips after CERCHAR testing on Khao Khad travertine specimens and (b) their corresponding groove images.
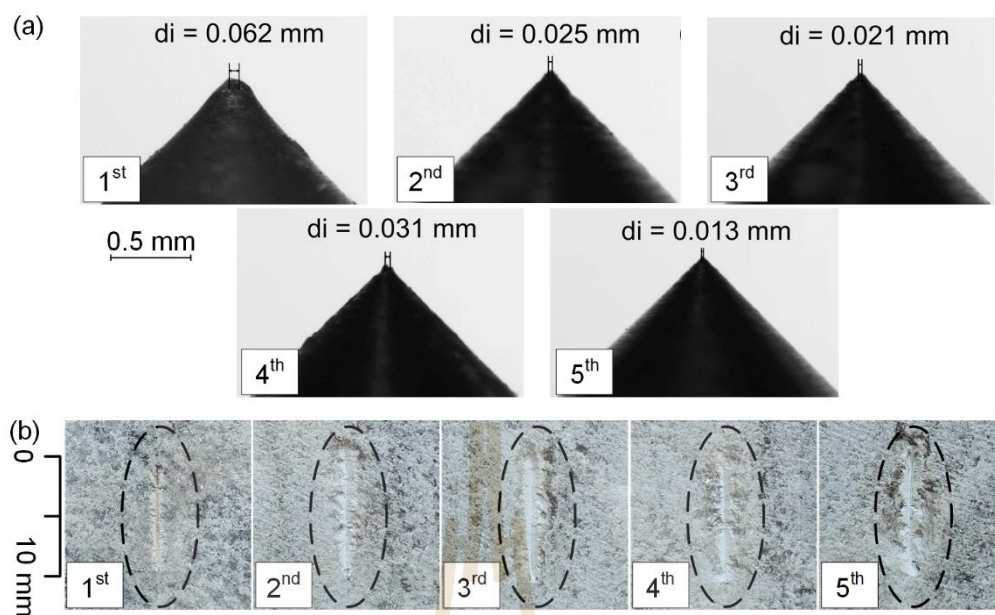
Figure B.11 (a) Steel stylus tips after CERCHAR testing on Tak Fa gypsum specimens and (b) their corresponding groove images.
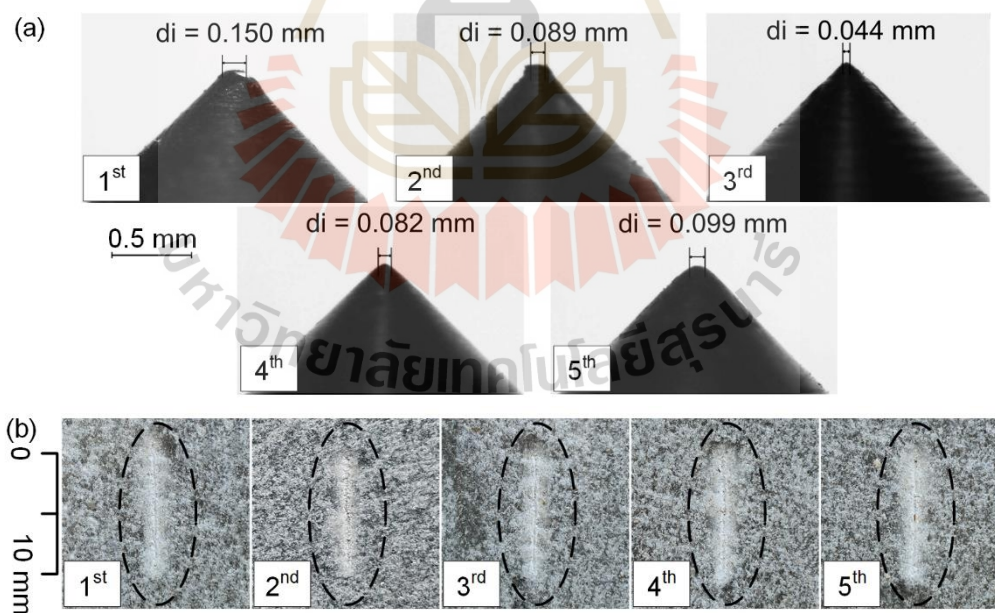


Figure B.12 (a) Steel stylus tips after CERCHAR testing on Tak Fa anhydrite specimens and (b) their corresponding groove images.
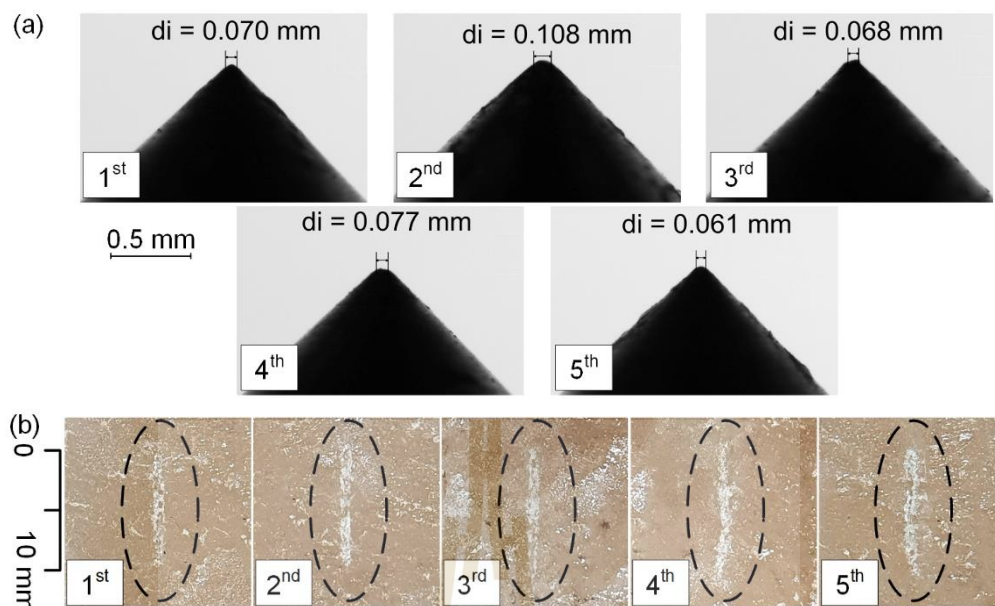
Figure B.13 (a) Steel stylus tips after CERCHAR testing on Maha Sarakham salt specimens and (b) their corresponding groove images.
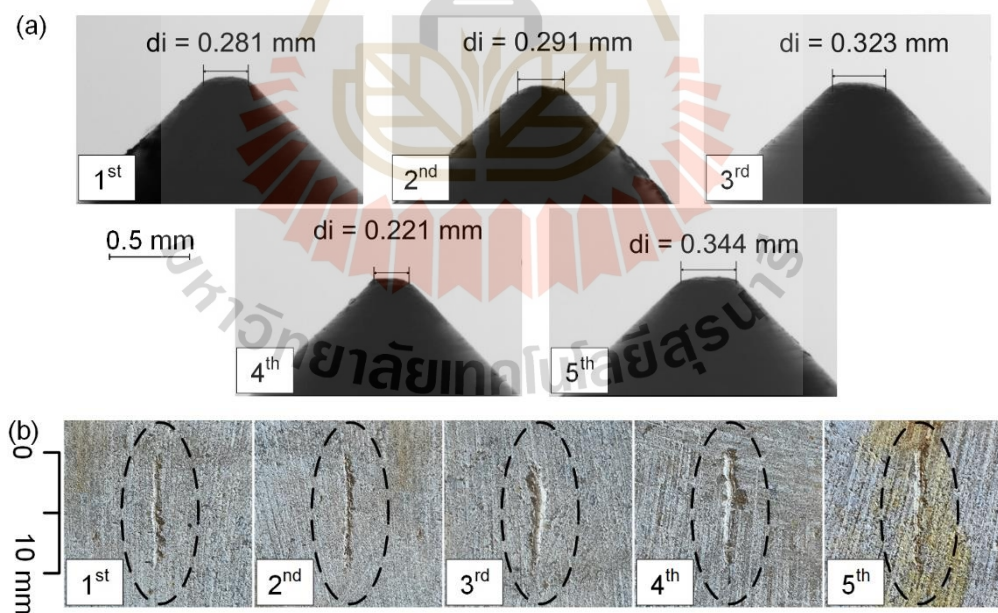


Figure B.14 (a) Steel stylus tips after CERCHAR testing on pyrophyllite specimens and (b) their corresponding groove images.

Figure B.15 (a) Steel stylus tips after CERCHAR testing on dickite specimens and (b) their corresponding groove images.

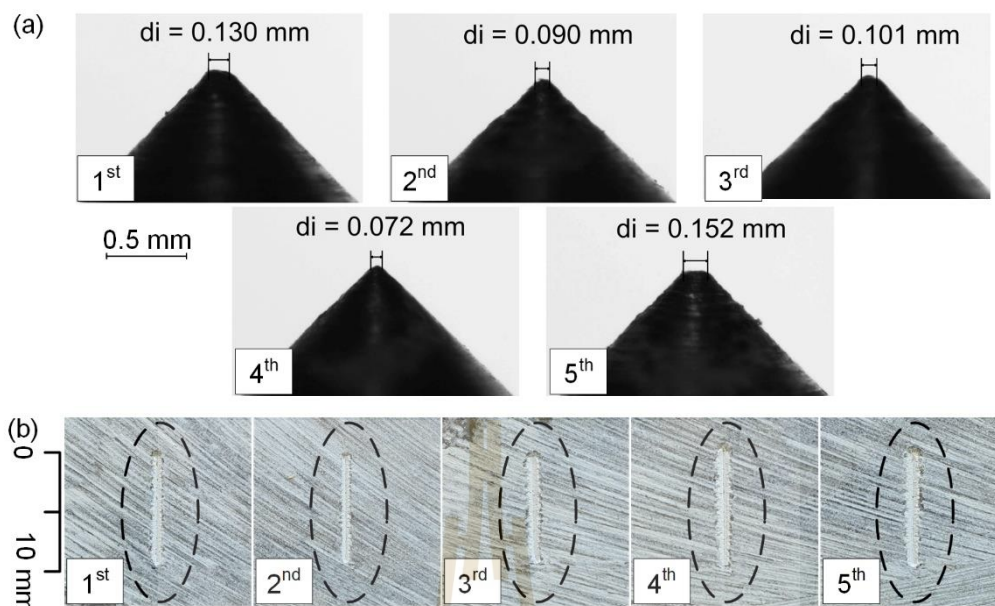

Figure B.16 (a) Steel stylus tips after CERCHAR testing on skarn specimens and (b) their corresponding groove images.

Figure B.17 (a) Steel stylus tips after CERCHAR testing on Khao Kradong basalt specimens and (b) their corresponding groove images.
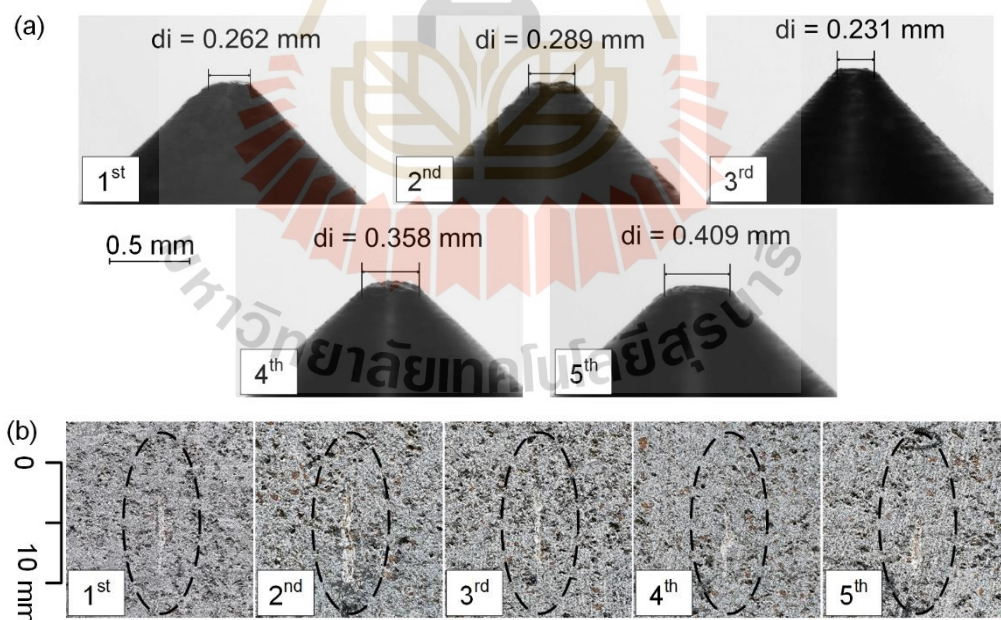


Figure B.18 (a) Steel stylus tips after CERCHAR testing on Khao Kradong vesicular basalt specimens and (b) their corresponding groove images.
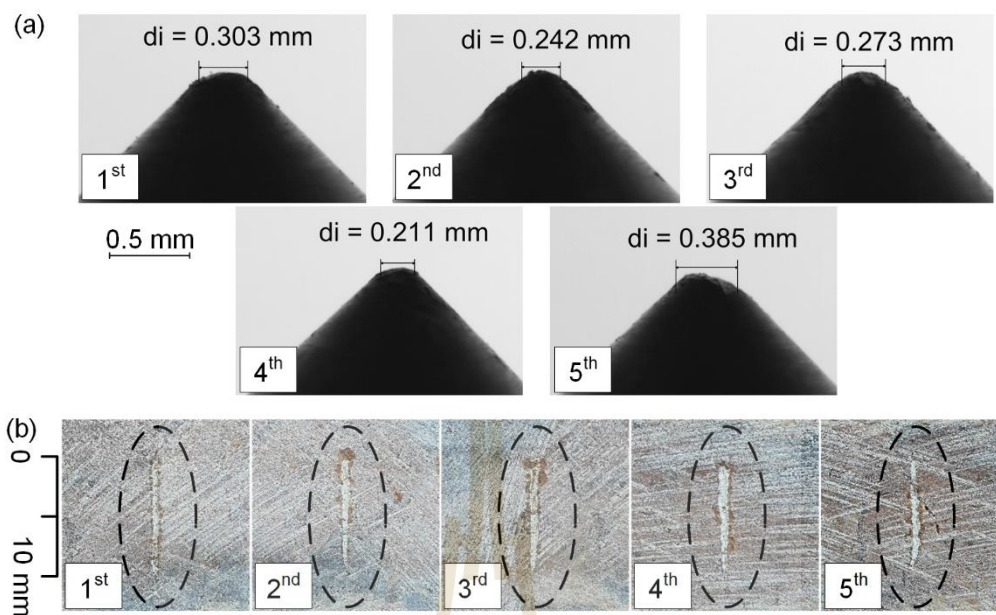
Figure B.19 (a) Steel stylus tips after CERCHAR testing on Khao Yai rhyolite specimens
and (b) their corresponding groove images.
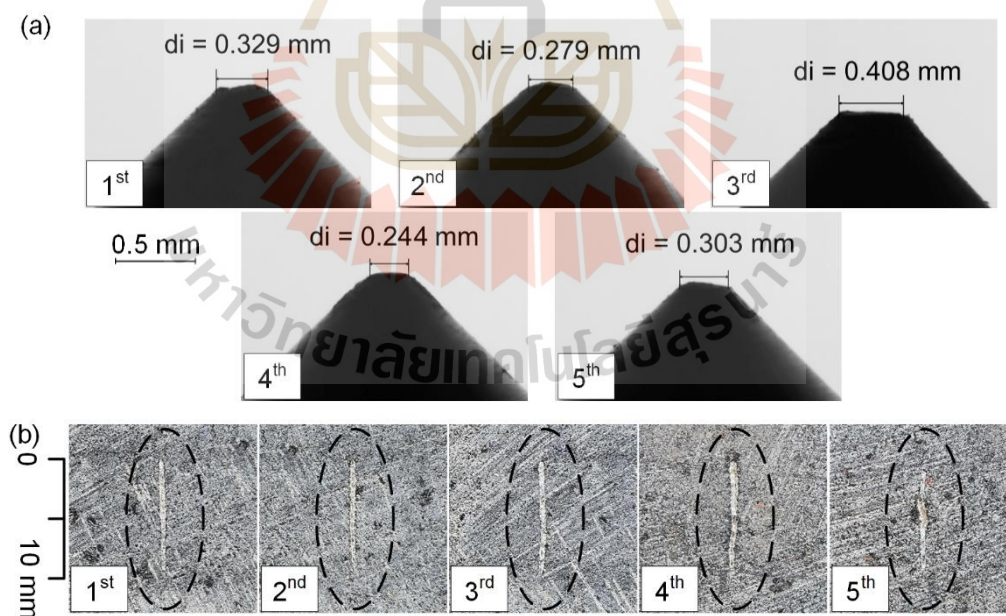


Figure B.20 (a) Steel stylus tips after CERCHAR testing on Khao Yai andesite specimens
and (b) their corresponding groove images.
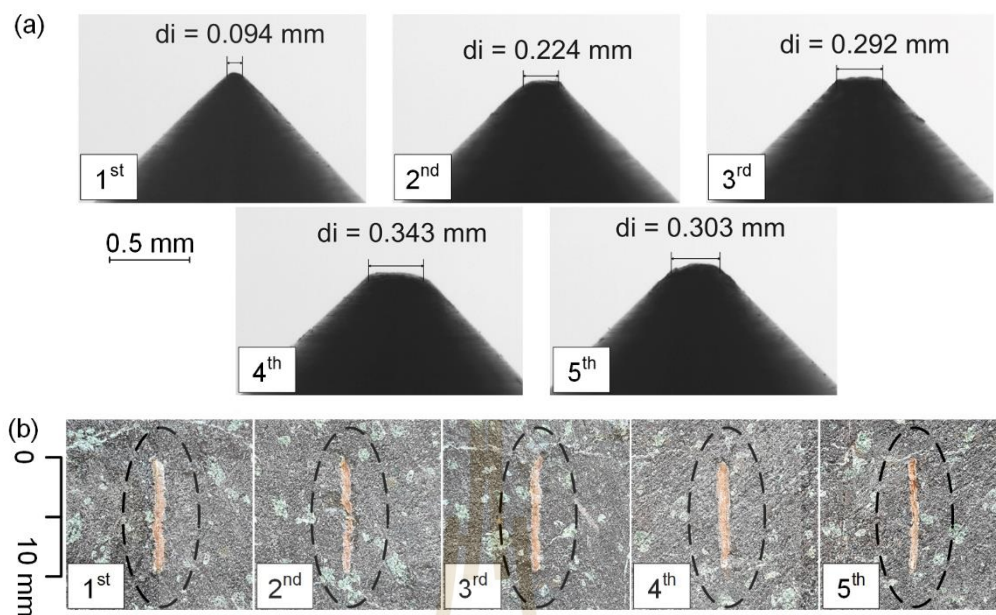
Figure B.21 (a) Steel stylus tips after CERCHAR testing on Khao Yai tuff specimens and
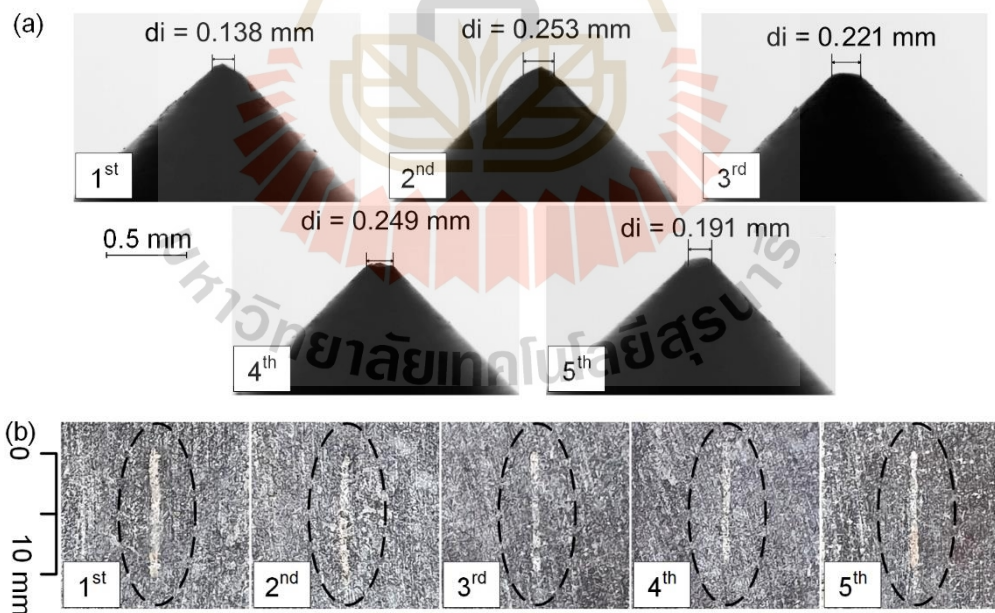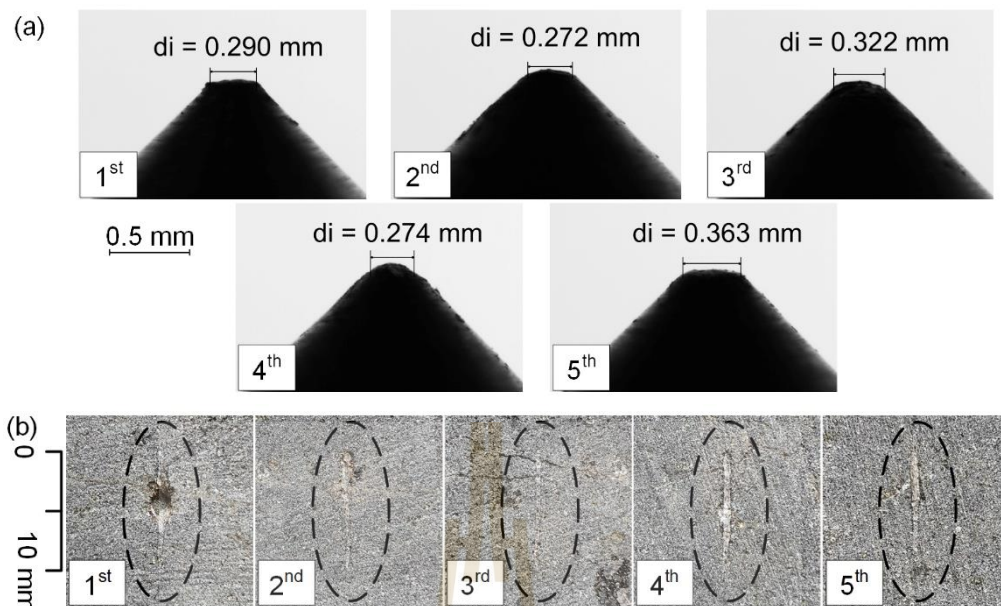(b) their corresponding groove images.

APPENDIX C

SCRATCHING FORCE – DISPLACEMENT CURVES
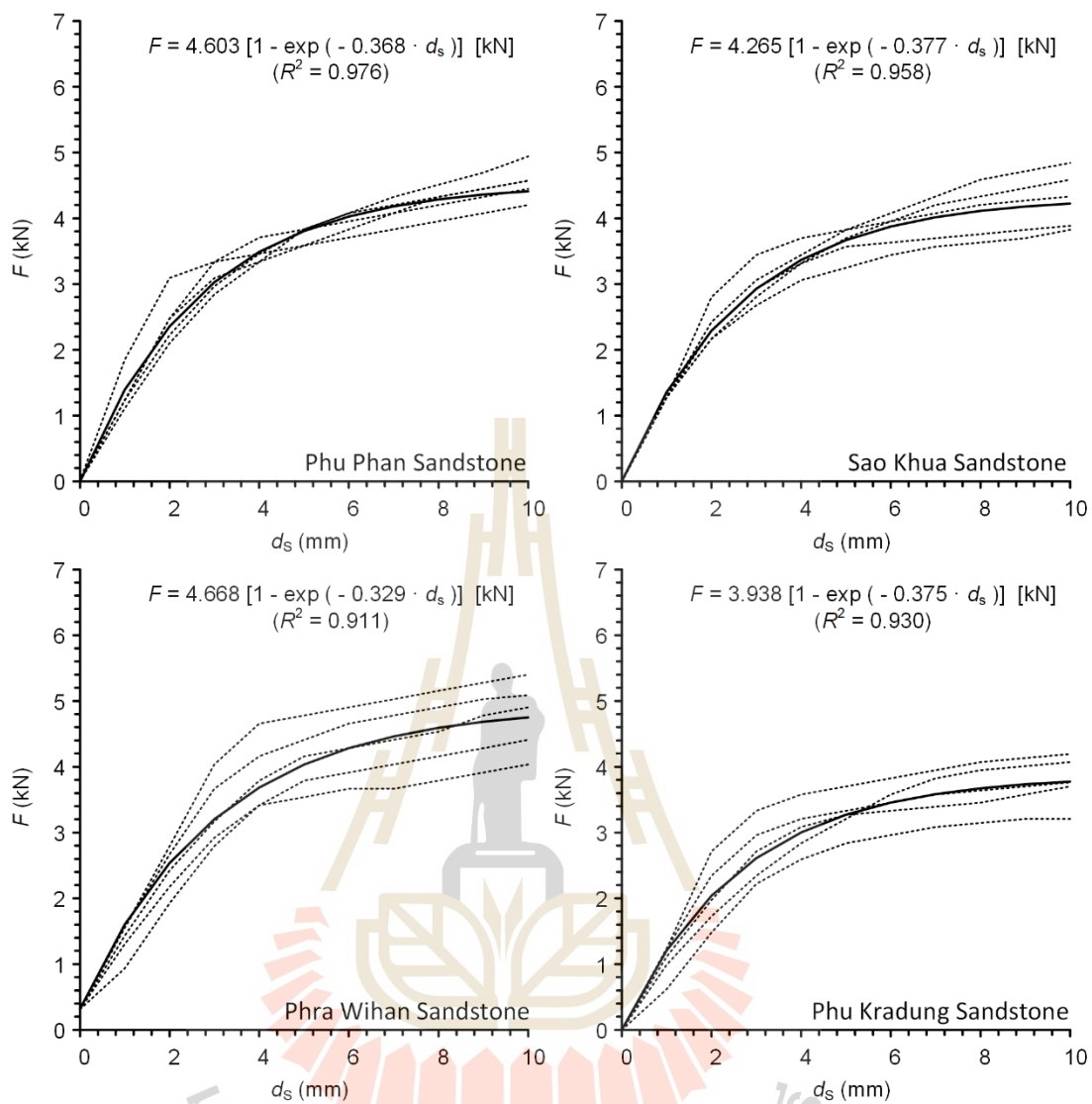
Figure C.1   Scratching forces (F) as a function of scratching displacement ($d_s$) for clastic rock group. Dash line represents each groove. Solid lines are their average.
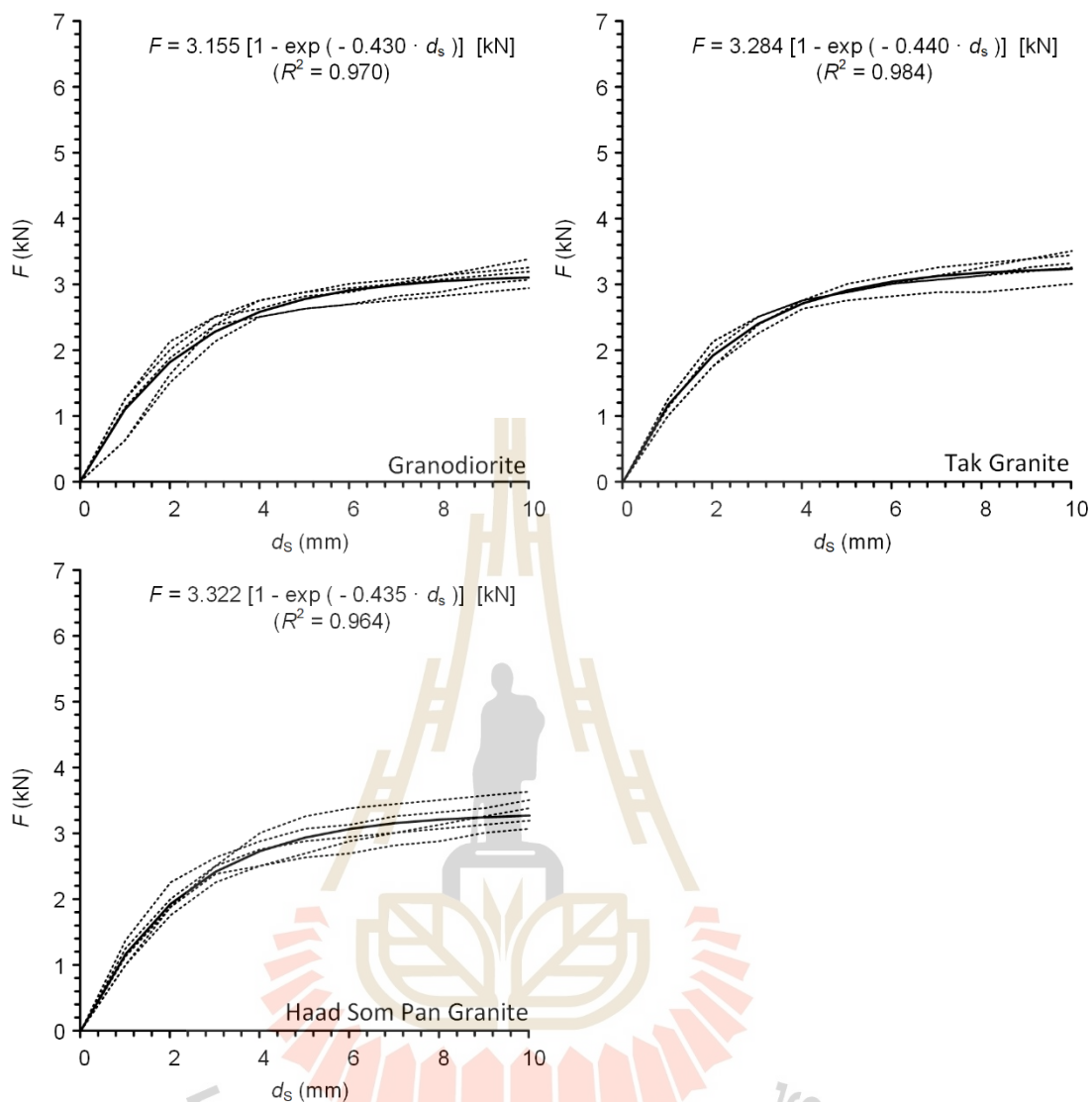
Figure C.2  Scratching forces (F) as a function of scratching displacement ($d_s$) for plutonic rock group. Dash line represents each groove. Solid lines are their average.
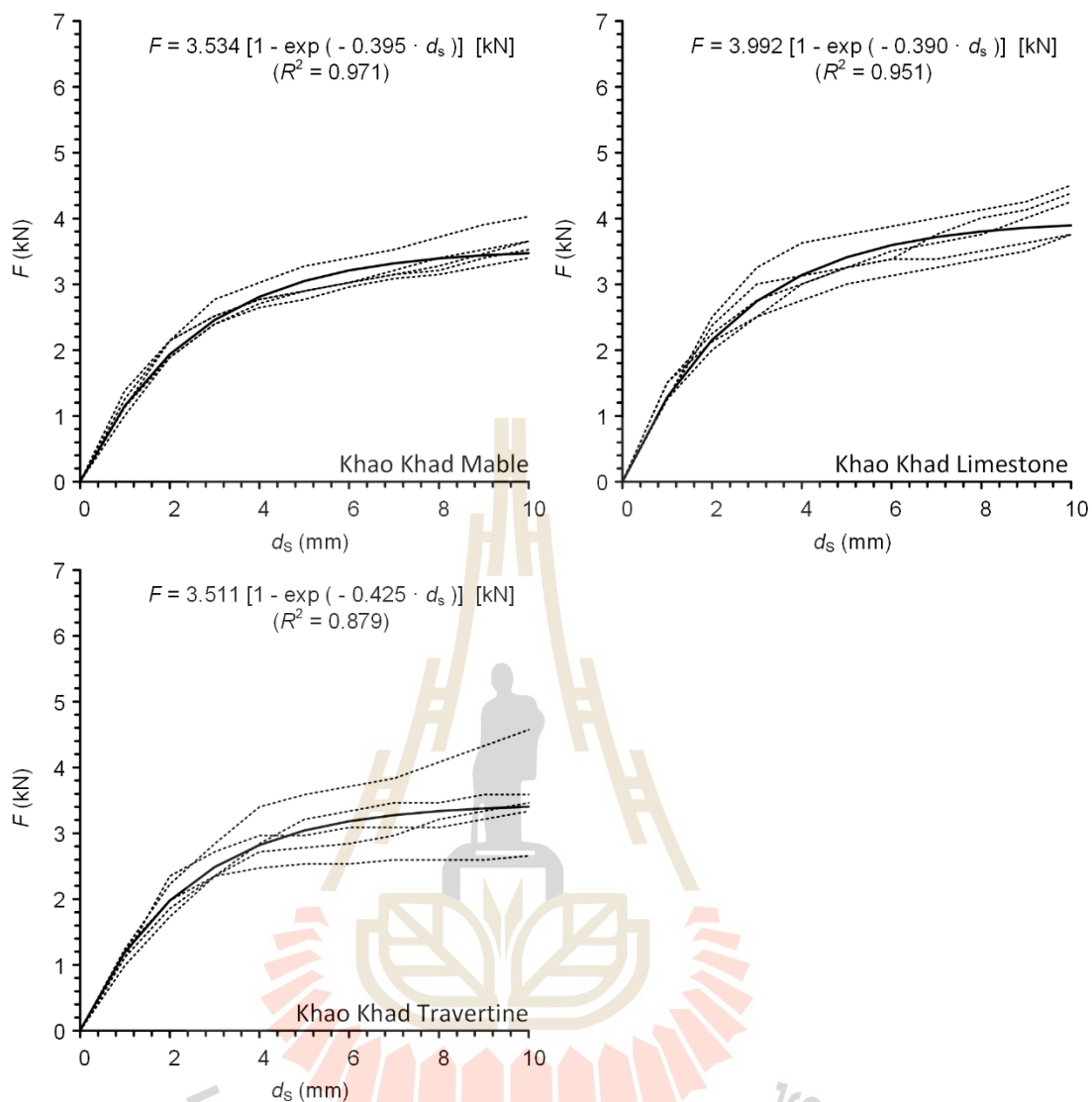
Figure C.3  Scratching forces (F) as a function of scratching displacement ($d_s$) for carbonate rock group. Dash line represents each groove. Solid lines are their average.
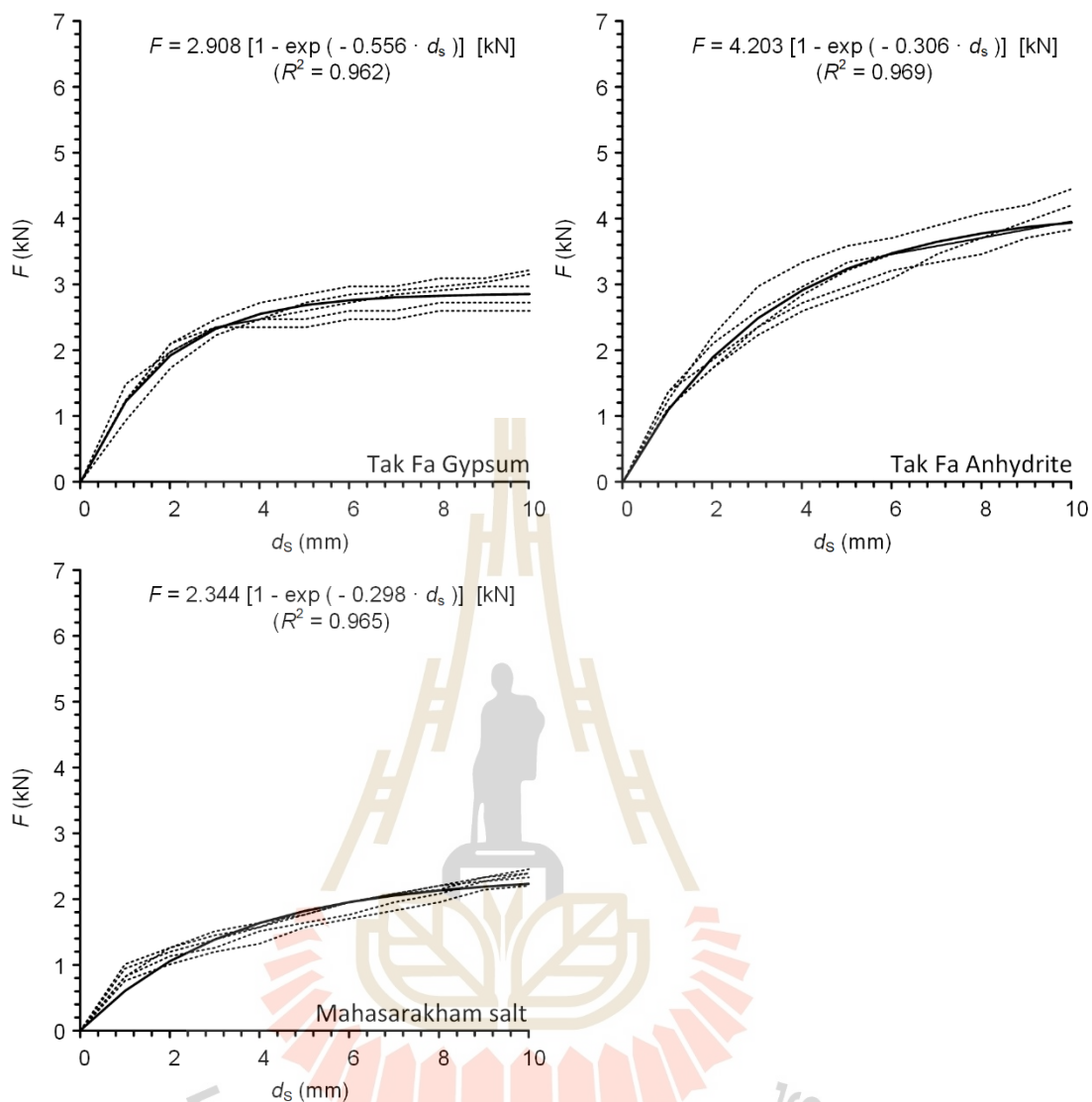
Figure C.4    Scratching forces (F) as a function of scratching displacement ($d_s$) for sulfate rock group. Dash line represents each groove. Solid lines are their average.
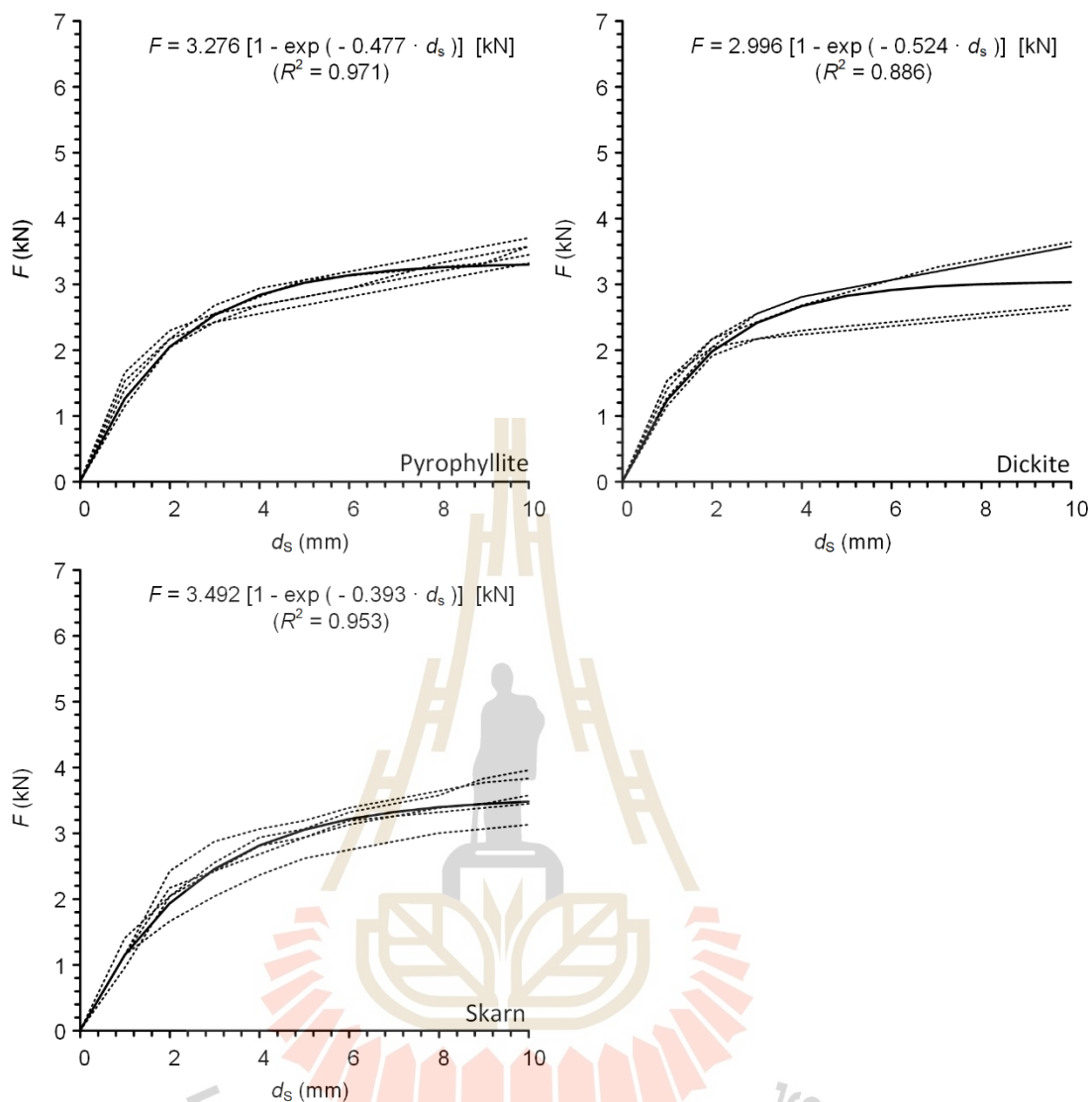
Figure C.5    Scratching forces (F) as a function of scratching displacement ($d_s$) for silicate rock group. Dash line represents each groove. Solid lines are their average.
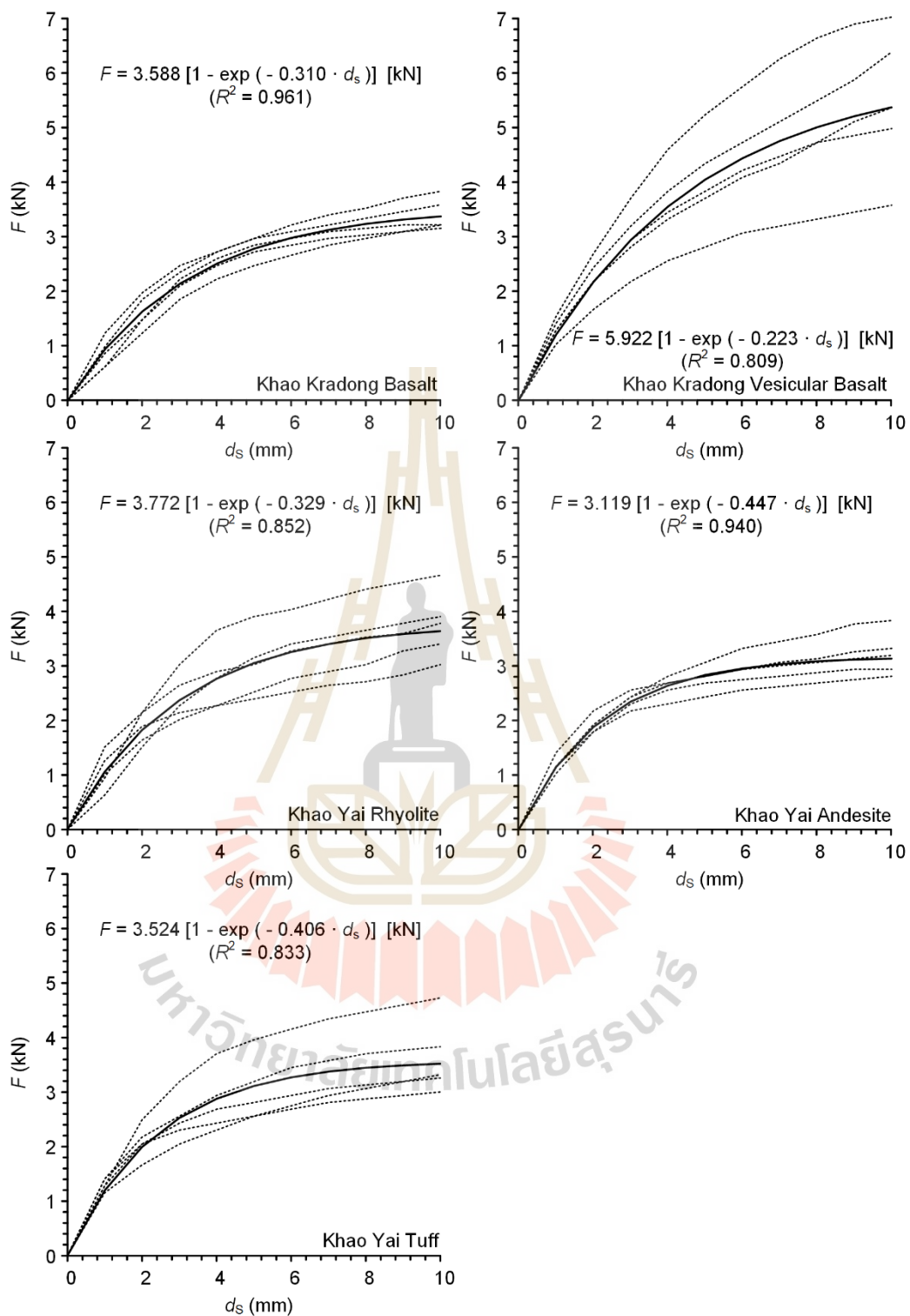
Figure C.6  Scratching forces (F) as a function of scratching displacement (ds) for volcanic rock group. Dash line represents each groove. Solid lines are their average.

APPENDIX D

LASER – SCANNED IMAGES
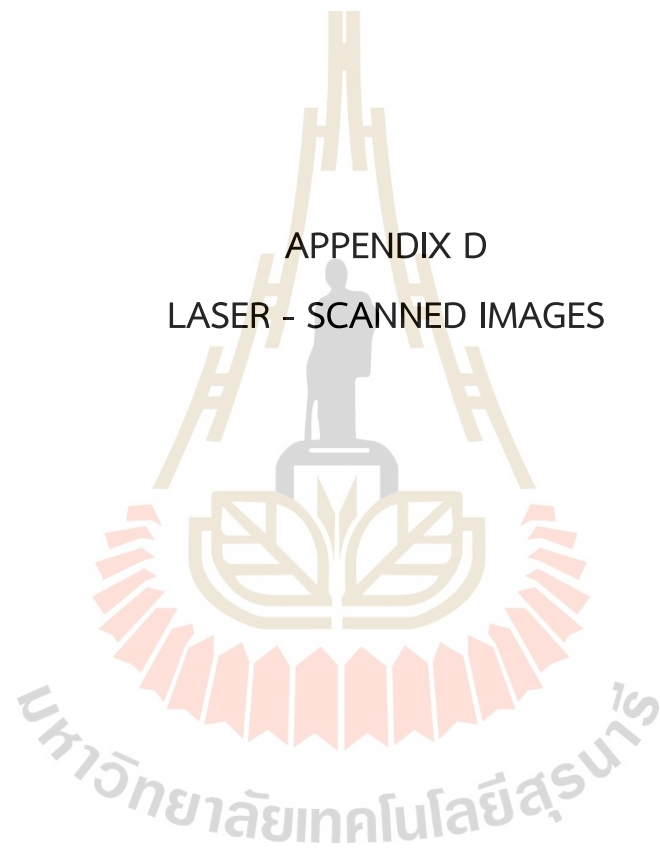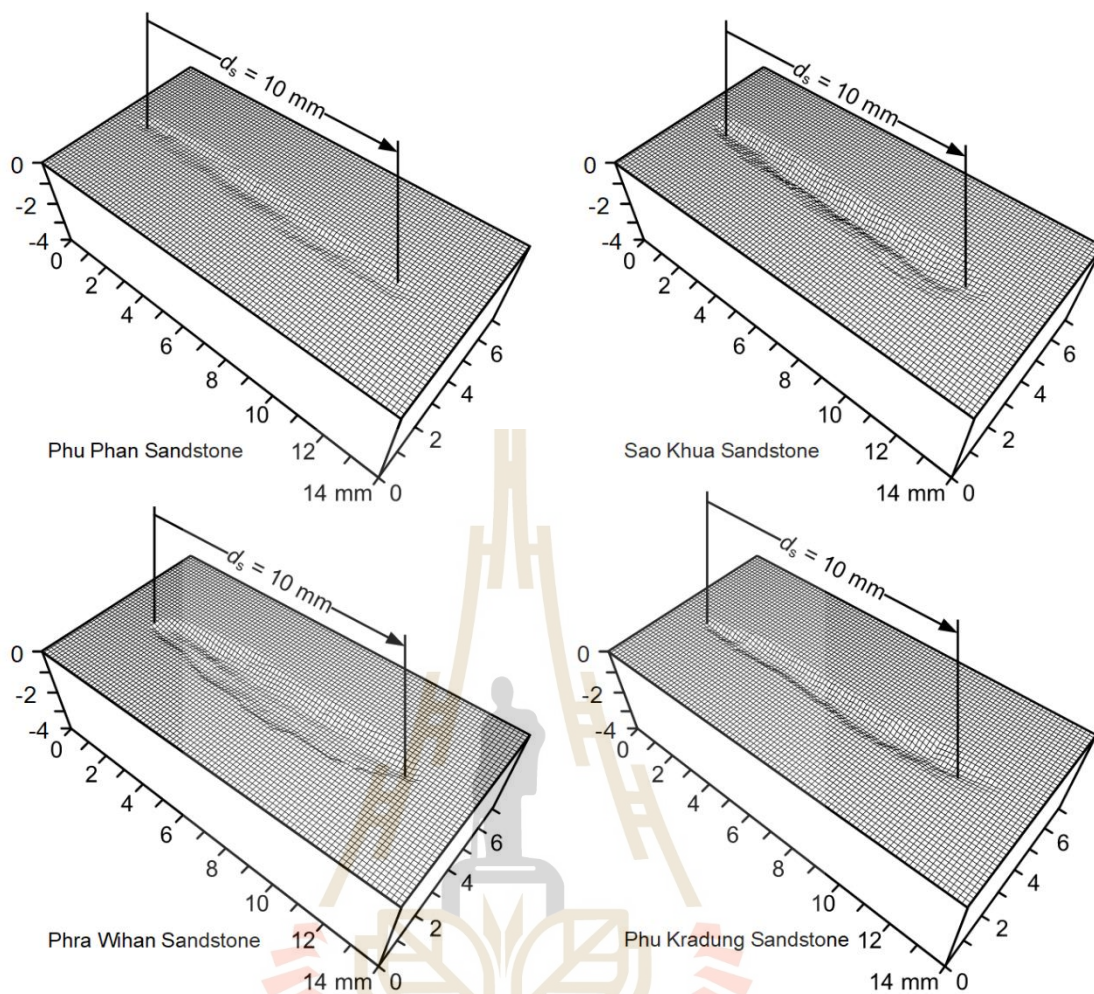
Figure D.1  Representative laser-scanned images of grooves on rock surfaces after CAI testing for clastic rock group. Arrow indicates scratching direction.
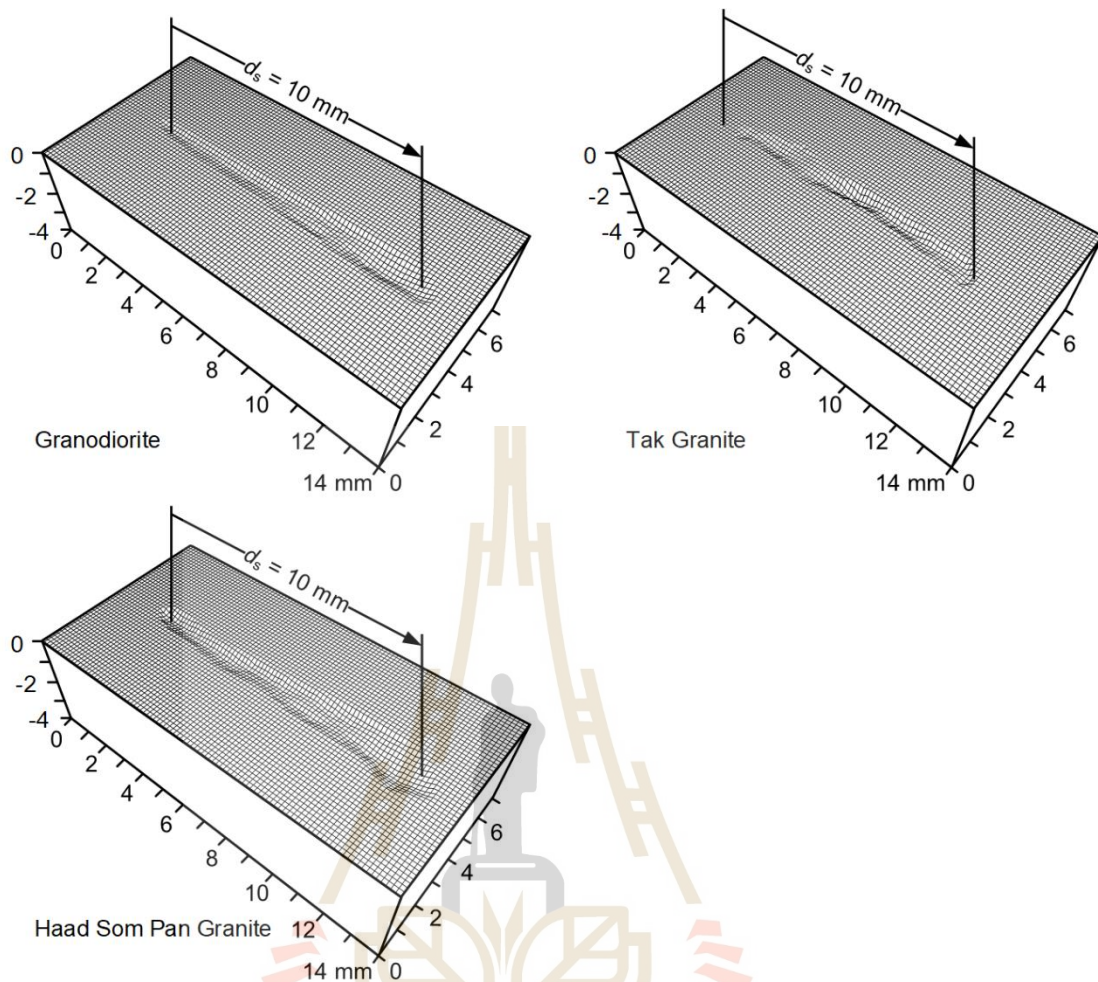
Figure D.2   Representative laser-scanned images of grooves on rock surfaces after CAI testing for plutonic rock group. Arrow indicates scratching direction.
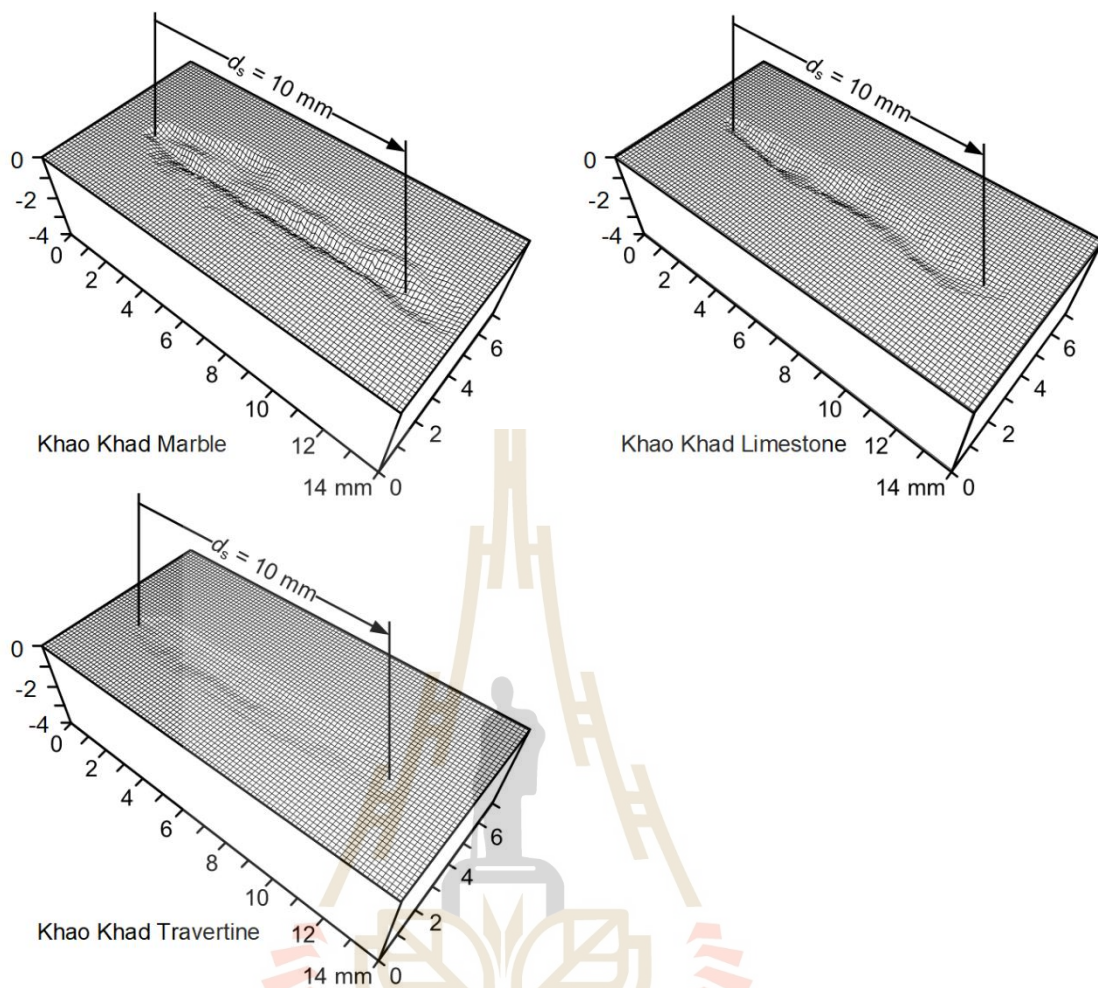
Figure D.3  Representative laser-scanned images of grooves on rock surfaces after CAI testing for carbonate rock group. Arrow indicates scratching direction.
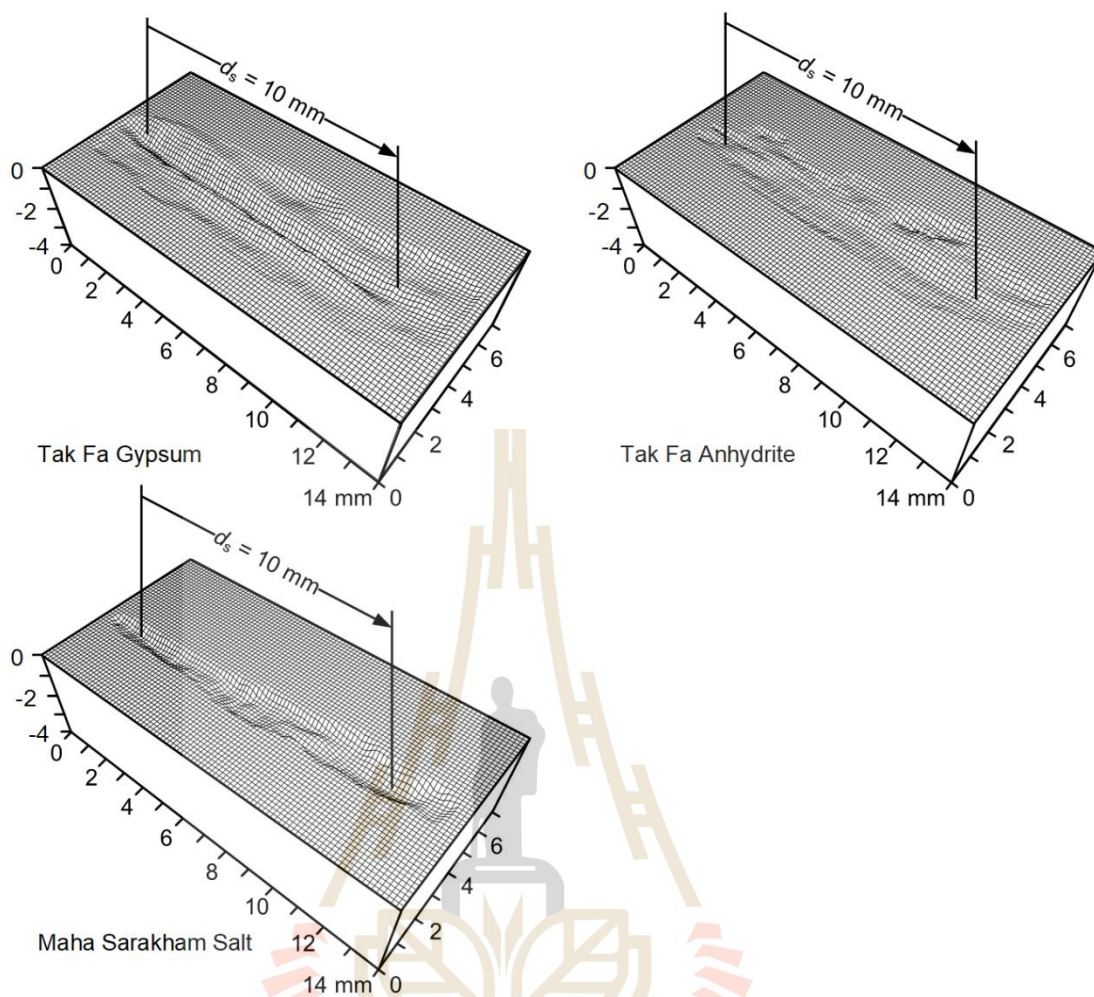
Figure D.4  Representative laser-scanned images of grooves on rock surfaces after CAI testing for sulfate & chloride rock group. Arrow indicates scratching direction.
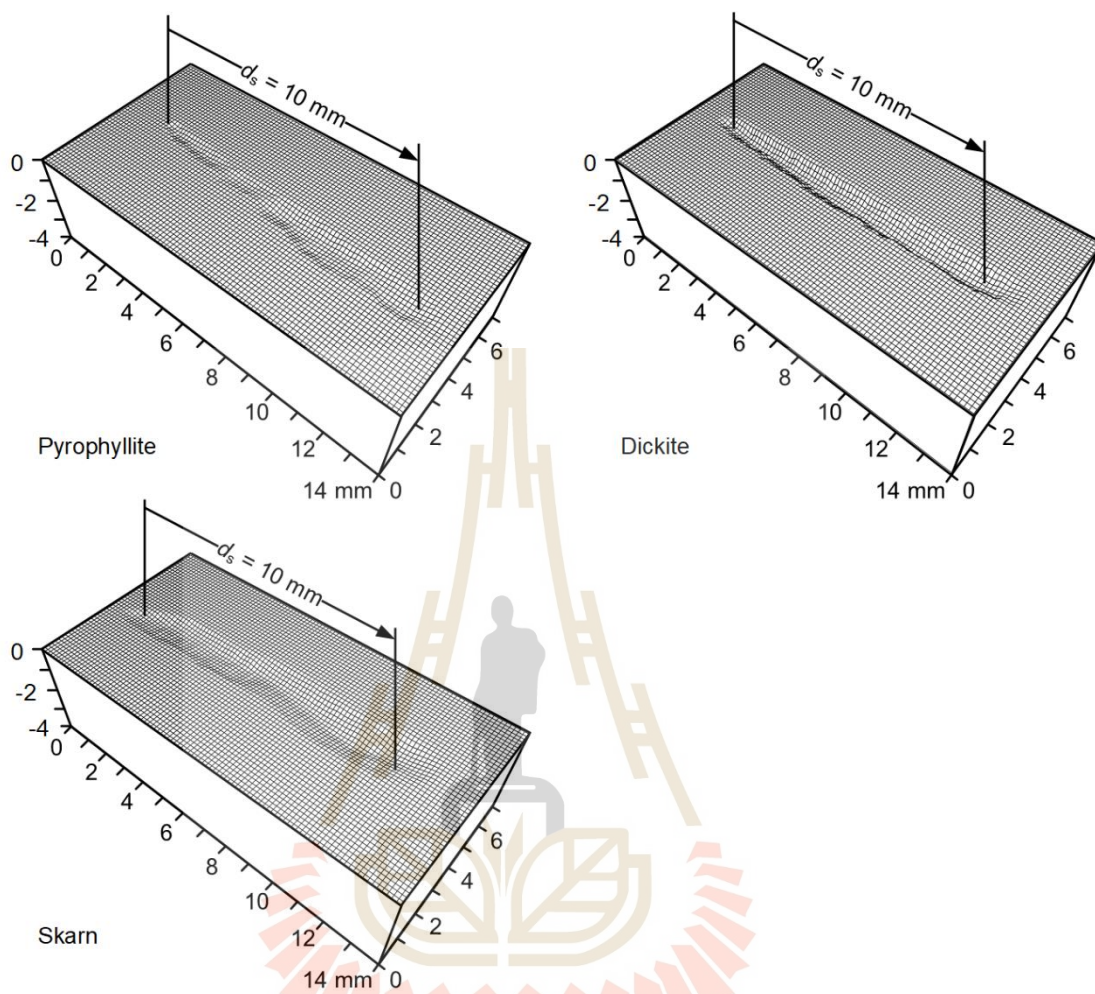
Figure D.5   Representative laser-scanned images of grooves on rock surfaces after CAI testing for silicate rock group. Arrow indicates scratching direction.
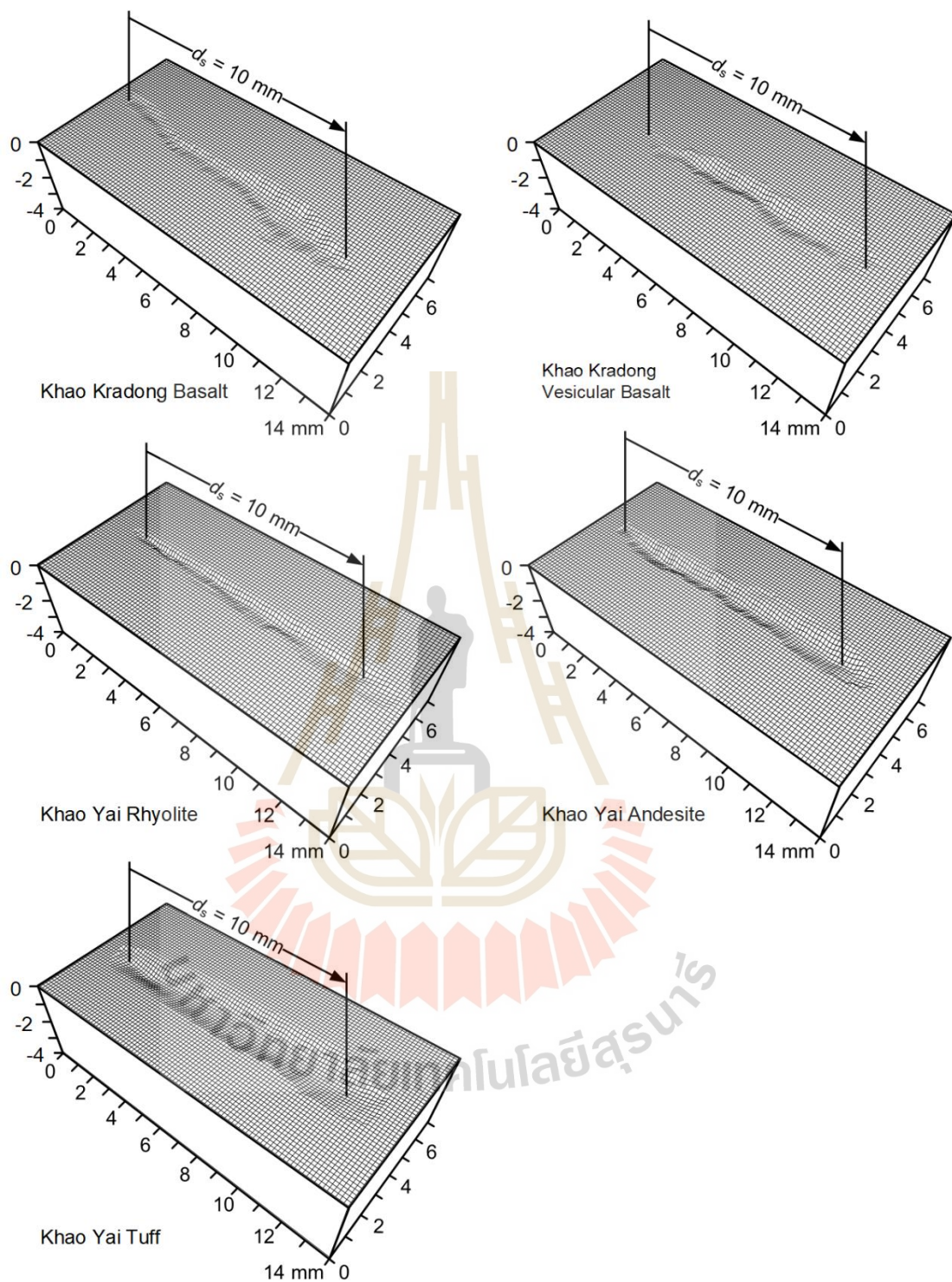
Figure D.6   Representative laser-scanned images of grooves on rock surfaces after CAI

testing for volcanic rock group. Arrow indicates scratching direction.

APPENDIX E

LIST OF PUBLICATION
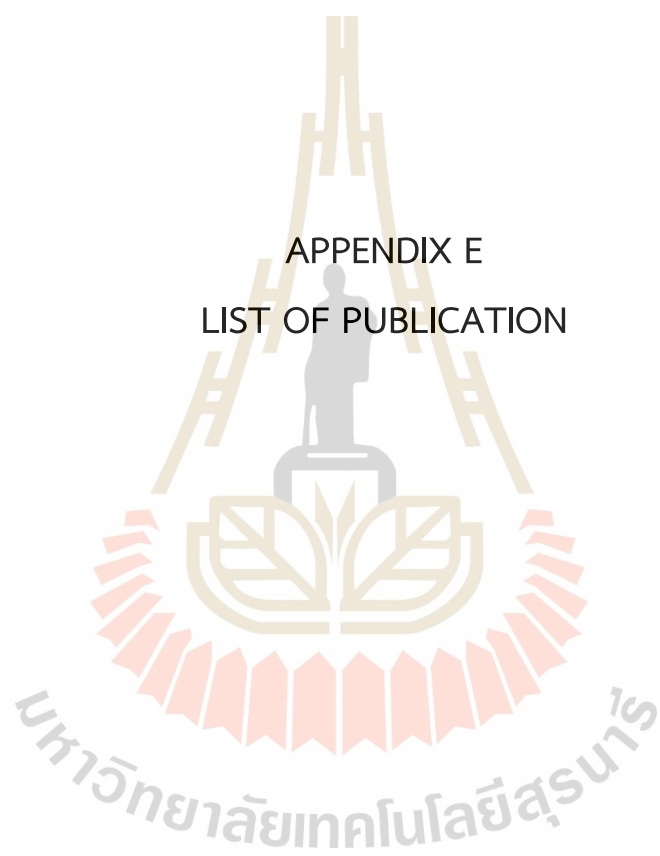
# EASR

## Engineering and Applied Science Research

# Effects of mechanical and mineralogical properties on CERCHAR abrasivity index and specific energy of some Thai rocks

Narawit Kathancharoen and Kittitep Fuenkajorn*

Geomechanics Research Unit, Institute of Engineering, Suranaree University of Technology, Nakhon Ratchasima 30000, Thailand

## Abstract

The objective of this study is to determine the correlations between CERCHAR abrasivity index (*CAI*) and mechanical and mineralogical properties of twenty rock types encountered in mining and construction industry in Thailand. These rocks represent soft to medium strong rocks on which their *CAI* properties have rarely been investigated elsewhere. Results indicate that fair correlation is obtained between *CAI* and rock strength. *CAI*'s increase linearly with friction angle, they however show no correlation with the cohesion. Minerals composing each rock type obtained from XRD analysis are used with their corresponding Moh's scale hardness to determine volumetric hardness (*Hv*) of the specimens. *Hv*'s can correlate with rock abrasivity better than the widely used equivalent quartz contents. Both parameters give better correlations with *CAI* when clastic and crystalline rocks are analyzed separately. Scratching groove volume reduces exponentially with increasing rock abrasiveness. CERCHAR specific energy (*CSE*) correlates well with all rock groups, providing that only hardness of soft minerals in clastic rock group is used in the regression. *CSE* also increases with *CAI*'s, suggesting that rocks with high abrasivity require higher energy to cut, and yield lower excavated volume than those with lower abrasivity. The research findings can be used to predict the wear of excavation tools in soft to medium strong rocks using the correlations between *CAI* test results and their mechanical and mineralogical properties.

**Keywords:** Abrasiveness, Rock strength, Friction angle, Rock hardness, Mohs scale

## 1. Introduction

Rock abrasiveness is a primary factor determining the equipment life and directly affects operation costs in terms of machine performance, worn-out parts and delays in mining and construction industry. One of the methods for determining rock abrasiveness is CERCHAR abrasivity index (*CAI*) test [1]. The method has become popular due to its simplicity, speed and low cost [2, 3]. It has been widely used in the French and British coal mining industry. In 2010, American Society for Testing and Materials (ASTM D7625-10) has standardized the CERCHAR testing method [4] and, later withdrawn in 2019. International Society for Rock Mechanics (ISRM) has also published test procedure, device, and calculation for *CAI* test as proposed by Alber et al. [5]. The ISRM suggested method has made corrections on the measurement and calculation procedure. In 2022 ASTM (D7625-22) [6] has published an updated version for CERCHAR abrasiveness index test method. It is similar to the previous one in 2010 accept that the multiplied factor for converting *CAI* from smooth surfaces to rough surfaces has been changed to be identical to that of ISRM for low abrasiveness rock (*CAI* < 4). CERCHAR test uses a steel stylus with a 90 degrees conical tip, which is pinned perpendicular on the rock surface under a constant force of 70 N. The length of stylus scratching on the rock surface is 10 mm. The wear flat width of stylus tip is measured to the nearest 0.1 mm. The scratching is repeated five times with five individual re-sharpened pins for each specimen to achieve an average *CAI* value. The use of stylus hardened to 55 ± 1 HRC is advised. A microscope for examining the wear flat stylus has a minimum magnification of 25 times for ISRM [5] and 30 times for ASTM [6].

Several investigators have identified factors affecting the CERCHAR test results which can be divided here into two main groups: test parameters and rock properties. Al-Ameen and Waller [7] conclude from their experimental results that 85% of the *CAI* is occurred within 2 mm of scratching length and only about 15% of the change in *CAI* occurs within the last 8 mm. This is confirmed by the results obtained by Plinninger et al. [8]. Variation of the scratching speeds (rates) from 3, 10 to 20 mm/s does not significantly affect *CAI* value [9]. Hamzaban et al. [10] however note that increasing pin speed can increase the wear of stylus tip. This is later supported by experimental results obtained by Kotsombat et al. [11] who conclude that reducing pin speed by up to 1 to 3 orders of magnitude can significantly decrease scratching force and *CAI* value, and results in a deeper groove on rock surface.

It has been found that physical and mechanical properties and mineral compositions of rock specimens significantly affect the wear of stylus tip during *CAI* testing. Plinninger et al. [8] conclude from their test results that *CAI* obtained from rough surfaces is about twice of smooth surfaces. Similar results are obtained by Aydın [12], Käsling and Thuro [13] and Yaralı and Duru [14]. *CAI* also increases as the rock porosity decreases [15-17]. *CAI* has been extensively used to correlate with uniaxial compressive strength of rocks [16, 18-20]. Positive linear relations have commonly been found with low to fair coefficients of correlation. Deliormanlı [21] states

that uniaxial compressive strength plays an important role for abrasiveness of the rock. This agrees with a conclusion drawn by Al-Ameen and Waller [7] that the abrasiveness is largely influenced by the rock strength ($s_c$).

Extensive studies have been carried out to correlate $CAI$ with mineral compositions of rocks [19, 22, 23]. Rocks containing hard and highly abrasive minerals (such as quartz) tend to induce higher wear of stylus tip, as compared to those containing softer and lower abrasive minerals. Grain size and shape of minerals also play a significant role in the $CAI$ values. High wear is usually obtained from rocks with large quartz grain sizes of more than 0.5 mm. For quartz grain size less than 0.1 mm, no significant wear of stylus tip is found [22]. Even though various aspects of research results from $CAI$ testing have been compiled, most of them are from medium to very strong rocks, as they can induce high wear on excavation tools and machines. $CAI$ testing on soft rocks has rarely been performed.

The objective of this study is to correlate $CAI$ with the mechanical and mineralogical properties of soft to medium strong rocks. The test specimens are prepared from rocks commonly found in Thailand, in particular those encountered in mining and construction projects. A new method for determining the effect of mineral compositions on $CAI$ values is present. The different responses of $CAI$ to crystalline rocks and clastic rocks are identified.

## 2. Sample preparation

Twenty rock types have been prepared for CERCHAR and compression testing. They are categorized here into six groups, as shown in Table 1. These rocks are commonly found in the north and northeast of Thailand, where they are subjected to various excavation tools in mining and construction industry. For example, rock salt is excavated by roadheaders in Chaiyaphum province. Granite and marble in Saraburi province are cut by diamond wire saw for decorating stone production. Tunnel boring machines (TBM) are the main tool for excavating railway tunnels in the north and northeast of the country. In Nakhon Sawan province drum cutters are widely used in gypsum open pit mines.

Test specimens used in this study are drilled from rock blocks to obtain nominal diameters of 54 mm. Their end surfaces are cut flat resulting in length-to-diameter (L/D) ratios of 1, 2 and 2.5 for CERCHAR, uniaxial and triaxial compression testing. Five specimens from each rock type are prepared for each test. For sedimentary and metamorphic rock specimens, the test surfaces are prepared parallel to the bedding and foliation planes. This is to isolate the effect of transverse isotropic texture of these rocks, which represents a scope of this study. Some post-test specimens are used for determining their mineral compositions by X-ray diffraction (XRD) analysis.

**Table 1** Mineral compositions of tested rocks from XRD analysis

| Rock Group | Rock Type | Code | Mineral Compositions |
|---|---|---|---|
| Clastic | Phu Phan Sandstone | Kpp | 86.13% Quartz, 6.27% Kaolinite, 1.65% Muscovite, 3.46% Albite, 0.60% Microcline, 1.90% Chlorite |
| | Sao Khua Sandstone | Ksk | 71.89% Quartz, 5.29% Kaolinite, 13.77% Muscovite, 6.06% Albite, 0.23% Anorthite, 1.66% Microcline, 1.04% Oligoclase, 0.08% Chlorite |
| | Phra Wihan Sandstone | JKpw | 83.50% Quartz, 3.94% Kaolinite, 0.66% Muscovite, 3.91% Albite, 1.03% Anorthite, 3.23% Microcline, 0.27% Calcite, 3.48% Chlorite |
| | Phu Kradueng Sandstone | Jpk | 38.35% Quartz, 2.94% Kaolinite, 11.87% Muscovite, 22.05% Albite, 2.39% Anorthite, 4.43% Microcline, 0.24% Calcite, 9.53% Oligoclase, 8.23% Chlorite |
| Plutonic | Tak Granite | Cgr | 27.71% Quartz, 7.97% Muscovite, 1.42% Chlorite, 18.76% Albite, 31.63% Orthoclase, 8.99% Anorthite, 3.54% Diopside |
| | Granodiorite | Trgr | 44.82% Quartz, 6.30% Muscovite, 3.66% Chlorite, 22.59% Albite, 15.30% Orthoclase, 3.66% Anorthite, 3.69% Diopside |
| Carbonate | Khao Khad Marble | Pkd | 93.50% Calcite, 0.46% Quartz, 4.35% Dolomite, 1.70% Chalcopyrite |
| | Khao Khad Limestone | Pkd | 92.24% Calcite, 5.05% Dolomite, 0.22% Fluorite, 1.79% Microcline, 0.71% Actinolite |
| | Khao Khad Travertine | Pkd | 93.48% Calcite, 0.05% Quartz, 6.02% Dolomite, 0.46% Chalcopyrite |
| Sulfate & chloride | Tak Fa Gypsum | Tkb | 1.53% Fluorite, 98.47% Gypsum |
| | Tak Fa Anhydrite | Tkb | 99.08% Anhydrite, 0.92% Fluorite |
| | Maha Sarakham Salt | KTms | 95.50% Halite, 1.83% Gypsum, 0.31% Sylvite, 0.28% Anhydrite, 0.16% Dickite |
| Silicate | Pyrophyllite | PTRv | 30.35% Dickite, 26.16% Kaolinite, 43.49% Quartz |
| | Dickite | PTRv | 84.18% Dickite, 15.26% Kaolinite, 0.57% Quartz |
| | Skarn | PTRv | 35.89% Dickite, 19.19% Kaolinite, 32.55% Quartz, 6.22% Nacrite, 3.30% Alunite, 2.87% Pyrite |
| Volcanic | Khao Kradong Basalt | Qbs | 0.69% Quartz, 9.46% Muscovite, 3.89% Chlorite, 19.45% Albite, 18.68% Anorthite, 31.70% Diopsite, 16.14% Microcline |
| | Khao Kradong Vesicular Basalt | Qbs | 0.13% Quartz, 18.14% Muscovite, 1.19% Chlorite, 43.53% Albite, 6.15% Orthoclase, 29.90% Anorthite, 0.99% Kaolinite |
| | Khao Yai Rhyolite | PTRv | 30.99% Quartz, 26.19% Muscovite, 18.69% Chlorite, 6.21% Albite, 6.29% Orthoclase, 5.61% Anorthite, 3.66% Diopsite, 1.70% Microcline, 2.65% Kaolinite, 1.15% Hematite |
| | Khao Yai Andesite | PTRv | 43.59% Quartz, 4.48% Muscovite, 4.28% Chlorite, 2.91% Albite, 0.80% Orthoclase, 0.46% Anorthite 43.50% Kaolinite |
| | Khao Yai Tuff | PTRv | 7.57% Quartz, 22.49% Muscovite, 34.42% Chlorite, 16.73% Albite, 1.97% Orthoclase, 2.60% Anorthite, 5.57% Hematite, 8.66% Calcite |

### 3. Test apparatus and methods

CERCHAR testing is performed on saw-cut surfaces of rock specimens under dry and unconfined conditions using a device based on West apparatus [24], as shown in Figure 1. The apparatus comprises vice holding rock specimen, a pin chuck or casing for stylus pin, a static load of 70 N, and a hand crank. The specimen is moved underneath the stylus. The pin has Rockwell hardness (HRC) of $55 \pm 1$. Test procedure follows the International Society for Rock Mechanics (ISRM) suggested method [5]. The scratching length is 10 mm. Test duration is 10 s, resulting in a constant scratching rate of 1 mm/s. This can be obtained by rotating the hand crank 10 rounds for 10 seconds, as the pitch of screw connecting between hand crank and vice holding is 1 mm. With several trials and timing practices, the desired stylus pin speed of 1 mm per second can be accurately achieved. The wear flat of stylus tip before and after scratching is measured under microscope with magnification of 50. Each stylus tip is measured around its axis in 0°, 90°, 180°, and 270° directions. The results are averaged for each pin. Five pins are used for each rock type. The CERCHAR abrasiveness index (*CAI*) values can be calculated as $CAI = d \times 10$, where $d$ is diameter of scratch flat area of stylus tip from rough surfaces testing. The diameter $d$ can be correlated with smooth surfaces testing ($d_s$) by [5]:

$$d = 1.14 \cdot d_s \tag{1}$$

It is recognized that smooth surface testing is an option for *CAI* test methods of ASTM [4, 6] and ISRM [5]. To meet the objective of determining the effects of mechanical and mineralogical properties of rocks on CAI, the effect of surface roughness is excluded here. It should be noted that surfaces roughness of rock is difficult to control, as the same rock type may yield different surface roughness values. This will add an uncontrollable variable to our test plan. Some investigators [8, 13, 25] who perform *CAI* tests on both rough and smooth rock surfaces have found that *CAI*'s obtained from rough surfaces show higher variation than those from smooth surfaces. As a result, they recommend to use smooth rock surfaces for *CAI* testing. In addition, mathematical representation of rock surface roughness requires relatively long surface profile (e.g. 10 cm for JRC [26]), while *CAI* testing uses only 10 mm. This may pose difficulty when such *CAI* is correlated with a roughness parameter, particularly when the roughness profile is not uniform along the entire length.
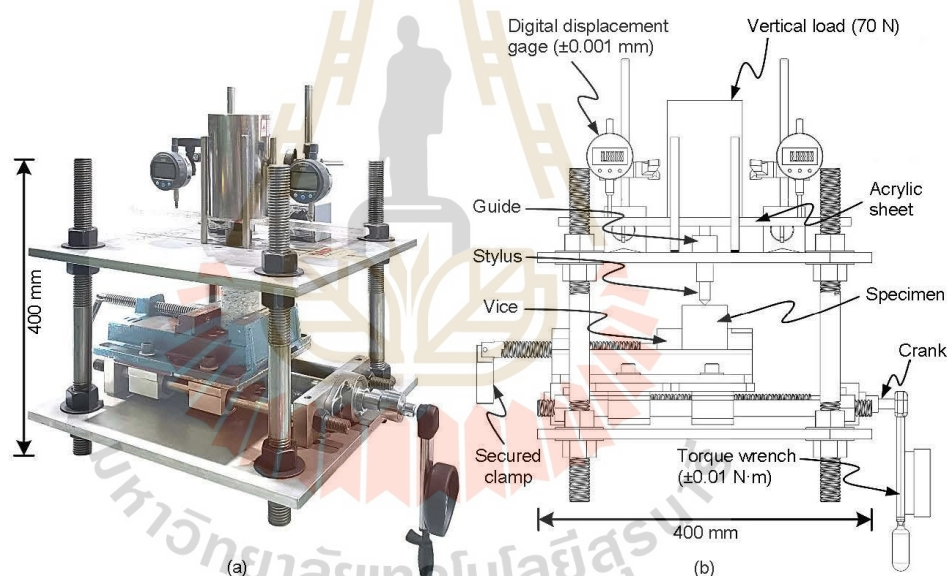


**Figure 1** Device based on West CERCHAR apparatus [24] with additional torque and vertical displacement measurement (a) and schematic drawing of CERCHAR device (b).

Additional parameters are imposed beyond those suggested by the ISRM. The vertical displacement of the stylus is measured along the scratching length by digital displacement gages with a precision of 0.001 mm to obtain groove depth produced by scratching. The lateral force applied on the stylus can be calculated from torque applied on the crank. A torque meter with a precision of 0.01 N·m is used. The lateral force can be calculated by the following equation [27]:

$$F = 2 \cdot \pi \cdot T/P \tag{2}$$

where $F$ is lateral force (N) on the stylus tip, $T$ is torque (N·m) on the crank, and $P$ is screw pitch (0.001 m).

Volume of scratching groove is obtained from laser-scanning profiles along the scratching length of 10 mm. The groove width and depth are measured to the nearest 0.001 mm.

For the mechanical characterization, uniaxial and triaxial compression tests are performed in accordance with the ASTM D7012-14e1 [28] standard. The axial stress is applied under a constant rate of 0.1 MPa/s until failure occurs. Axial and lateral displacements are measured by 0.01 mm precision dial gages. The confining pressures for the triaxial testing range between 0.69 and 12 MPa. Post-

failure characteristics are observed and recorded. The elastic modulus and Poisson's ratio are determined from the tangent of stress-strain curves at 40-50% of the failure stress.

Some post-test CERCHAR specimens are ground to obtain powder with less than 0.25 mm particle size (passing through mesh #60). About 5 to 10 grams are analyzed using X-ray diffractometer. DIFFRAC.EVA software determines the weight percentage of the mineral compositions. Table 1 shows the results from XRD analysis.

## 4. Test results

Results of CERCHAR abrasivity index and mechanical testing for all rock groups are given in Table 2. Figure 2 shows examples of scratching grooves and wear of stylus tips of some rock types. High strength rocks (e.g., sandstone, granite, and pyrophyllite) tend to show higher $CAI$ values than the lower strength rocks do. The Coulomb criterion can best describe the triaxial compressive strengths for all rock types. Their results are presented in terms of cohesion ($c$) and friction angle ($f$) in the table. Good correlation between Coulomb criterion and the test data are obtained ($R^2 > 0.9$).

### 4.1. Correlation between CAI and rock mechanical properties

$CAI$'s are plotted as a function of uniaxial compressive strength in Figure 3(a). Similar to the approaches used elsewhere [15, 18, 29], a linear equation is used to describe their relationship:

$$CAI = 0.043 \cdot s_c \tag{3}$$

Fair correlation is obtained ($R^2 = 0.475$). Figure 3(b) compares the linear equation obtained here with those presented by other investigators, as quoted in the figure. They also obtain fair correlations ($R^2 = 0.3 - 0.5$) between the two parameters.

No correlation is found between $CAI$ and cohesions of rocks (Figure 4(a)). $CAI$, however, tends to increase with friction angle, as shown in Figure 4(b), where they can be correlated by:

$$CAI = 0.076 \cdot f - 1.268 \tag{4}$$

The linear relation above shows $R^2 = 0.418$.

**Table 2** CERCHAR abrasivity indexes, rock strengths, cohesions, friction angles, equivalent quartz contents, and volumetric hardness for all rocks in this study.

| Rock Group | Rock Type | $CAI$ | $s_c$ (MPa) | $c$ (MPa) | $f$ (Degrees) | $EQC$ (%) | $H_V$ |
|---|---|---|---|---|---|---|---|
| Clastic | Phu Phan Sandstone | 3.02 | 81.4 | 8.6 | 59 | 88.31 | 6.52 |
| | Sao Khua Sandstone | 1.85 | 53.1 | 9.7 | 47 | 76.10 | 6.03 |
| | Phra Wihan Sandstone | 3.95 | 70.4 | 3.6 | 57 | 87.77 | 6.56 |
| | Phu Kradung Sandstone | 1.72 | 80.1 | 14.0 | 51 | 53.50 | 5.30 |
| Plutonic | Tak Granite | 4.88 | 84.5 | 15.7 | 56 | 56.16 | 6.04 |
| | Granodiorite | 4.58 | 72.5 | 8.6 | 59 | 66.00 | 6.19 |
| Carbonate | Khao Khad Marble | 1.98 | 36.4 | 3.2 | 65 | 2.90 | 3.06 |
| | Khao Khad Limestone | 1.43 | 54.6 | 10.2 | 55 | 3.47 | 3.12 |
| | Khao Khad Travertine | 2.09 | 59.6 | 6.0 | 59 | 2.52 | 3.05 |
| Sulfate & chloride | Tak Fa Gypsum | 0.35 | 5.6 | 1.6 | 34 | 0.97 | 2.02 |
| | Tak Fa Anhydrite | 1.09 | 32.2 | 7.8 | 26 | 2.96 | 3.26 |
| | Maha Sarakham Salt | 0.89 | 22.6 | 10.6 | 29 | 1.38 | 2.49 |
| Silicate | Pyrophyllite | 3.35 | 80.8 | 15.1 | 50 | 44.13 | 4.30 |
| | Dickite | 1.58 | 32.3 | 5.6 | 45 | 1.70 | 2.28 |
| | Skarn | 2.49 | 70.4 | 10.5 | 50 | 34.86 | 3.55 |
| Volcanic | Khao Kradong Basalt | 3.50 | 79.2 | 12.8 | 55 | 41.34 | 5.68 |
| | Khao Kradong Vesicular Basalt | 3.55 | 63.9 | 9.4 | 54 | 40.39 | 5.50 |
| | Khao Yai Rhyolite | 3.22 | 38.5 | 9.8 | 50 | 42.79 | 4.73 |
| | Khao Yai Andesite | 3.49 | 110.1 | 13.3 | 64 | 46.24 | 4.50 |
| | Khao Yai Tuff | 2.83 | 41.1 | 4.3 | 57 | 20.54 | 3.79 |

### 4.2. Correlation between CAI and mineral compositions

To consider effect of rock mineral compositions on the wear of stylus pin, Thuro [30] proposes a parameter, called equivalent quartz content ($EQC$), to represent equivalent rock hardness which can be calculated by:

$$EQC = \sum_{i=1}^{n} (W_i \cdot R_i) \tag{5}$$

$$R_i = \exp \cdot [(H_i - 2.12) / 1.05] \tag{6}$$

where $EQC$ ranges from $0 - 100\%$, $W_i$ is mineral weight percent, n is number of minerals, $R_i$ is Rosiwal abrasiveness (%), $H_i$ is hardness of each mineral based on Mohs scale [31], and the constants 2.12 and 1.05 are recommended by Thuro [30]. This approach presumes that tool wear is predominantly a result of the mineral content harder than steel ($H_i = 5.5$), especially quartz ($H_i = 7$). Calculation of $EQC$ for Phu Phan sandstone tested here is used as an example below, where their mineral compositions are taken from Table 1.
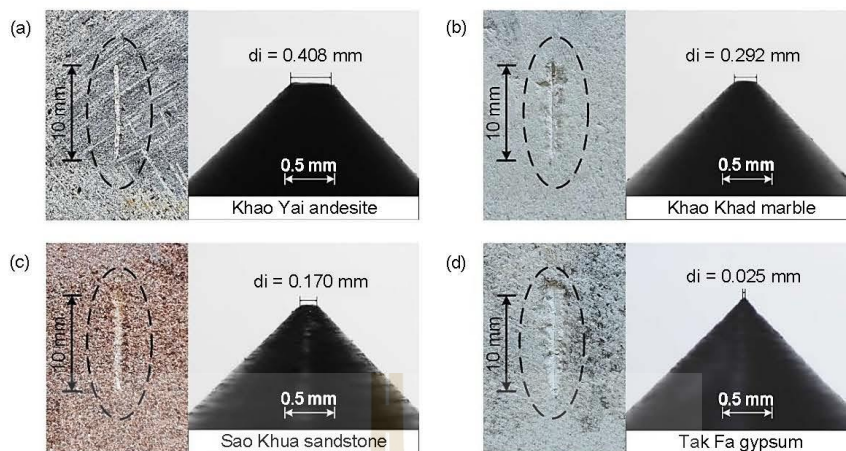
**Figure 2** Examples of scratching grooves and wear of stylus tips for some rock types: Khao Yai andesite (a), Khao Khad marble (b), Sao Khua sandstone (c) and Tak Fa gypsum (d).
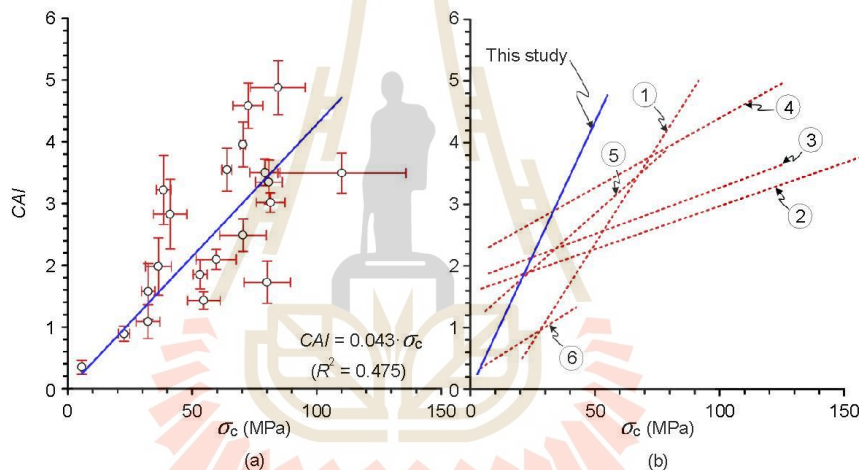


**Figure 3** *CAI* as a function of uniaxial compressive strength (a). comparison of the linear correlation of this study with those obtained elsewhere (b). ① Altindag et al. [32], ② He et al. [33] ③-④ Ko et al. [3] ⑤ Hamzaban et al. [34] ⑥ Kotsombat et al. [11].
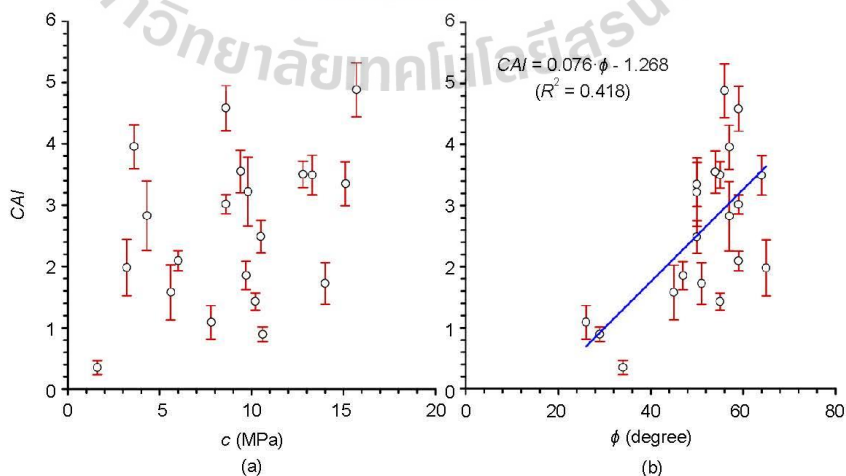


**Figure 4** CERCHAR abrasivity index (*CAI*) as a function of cohesion (a), and friction angles (b).

(Quartz)     (Kaolinite) (Muscovite)   (Albite)     (Microcline)   (Chlorite)
$$EQC = [(86.13×100)+(6.27×1.13)+(1.65×1.44)+(3.46×51.08)+(0.60×51.08)+(1.90×1.13)] /100 \tag{7}$$
$$EQC = \quad 88.31 \%$$

Similar calculations have been performed for all rocks (Table 3). $CAI$'s are plotted as a function of $EQC$ in Figure 5(a). Fair correlation ($R^2 = 0.451$) is obtained between the two parameters when a linear equation is applied. The correlations are improved when clastic and crystalline rocks are analyzed separately. $CAI$-$EQC$ relation for the clastic rock group can be represented by:

$$CAI = 0.051\ EQC - 1.264 \qquad (R^2 = 0.623) \tag{8}$$

For crystalline rock groups:

$$CAI = 0.053\ EQC + 1.227 \qquad (R^2 = 0.870) \tag{9}$$

A new method is proposed here to correlate $CAI$ with mineral compositions of rocks. While $EQC$ method uses weight percent of minerals composing each rock type, the proposed method considers volumetric percent of the minerals. This would be more sensible and direct approach to represent hardness of the rock surface subjected to stylus pin scratching. This method also uses Mohs scale as a multiplier directly for each mineral without considering the Rosiwal values. The volumetric hardness ($H$v) can be calculated by:

$$H_v = [\textstyle\sum_{i=1}^{n} (V_i \cdot H_i)] / \Sigma V_i \tag{10}$$

$$V_i = W_i / SG_i \tag{11}$$

**Table 3** Empirical constants $a$ and $b$ for $F$-$d_s$ relation, groove volume, and CERCHAR specific energy.

| Rock Group | Rock Type | $F=a\ [1-\exp(-b \cdot d_S)]$ | | $W = \int_{d_s=0}^{10} F \cdot d_s$ | $V$ | $CSE$ |
|---|---|---|---|---|---|---|
| | | $a$ | $b$ | (Joules) | (mm³) | (J/mm³) |
| Clastic | Phu Phan Sandstone | 4.603 | 0.368 | 33.87 | 2.71 | 13.22 |
| | Sao Khua Sandstone | 4.265 | 0.377 | 31.59 | 3.99 | 8.20 |
| | Phra Wihan Sandstone | 4.668 | 0.329 | 31.77 | 3.56 | 9.38 |
| | Phu Kradung Sandstone | 3.938 | 0.375 | 29.14 | 2.59 | 11.64 |
| Plutonic | Tak Granite | 3.284 | 0.440 | 25.48 | 1.20 | 21.97 |
| | Granodiorite | 3.155 | 0.430 | 24.33 | 1.24 | 19.72 |
| Carbonate | Khao Khad Marble | 3.534 | 0.395 | 26.57 | 4.55 | 6.36 |
| | Khao Khad Limestone | 3.511 | 0.425 | 29.89 | 2.48 | 12.91 |
| | Khao Khad Travertine | 3.992 | 0.390 | 26.97 | 1.72 | 16.38 |
| Sulfate & chloride | Tak Fa Gypsum | 2.908 | 0.556 | 23.88 | 10.79 | 2.71 |
| | Tak Fa Anhydrite | 4.203 | 0.306 | 28.92 | 4.81 | 6.53 |
| | Maha Sarakham Salt | 2.421 | 0.257 | 15.97 | 3.07 | 6.28 |
| Silicate | Pyrophyllite | 3.276 | 0.477 | 25.96 | 1.98 | 13.27 |
| | Dickite | 2.996 | 0.524 | 24.28 | 3.07 | 8.69 |
| | Skarn | 3.492 | 0.393 | 26.22 | 2.99 | 9.43 |
| Volcanic | Khao Kradong Basalt | 3.588 | 0.310 | 24.84 | 1.70 | 14.86 |
| | Khao Kradong Vesicular Basalt | 5.922 | 0.223 | 35.49 | 1.82 | 19.63 |
| | Khao Yai Rhyolite | 3.772 | 0.329 | 26.71 | 1.85 | 15.05 |
| | Khao Yai Andesite | 3.119 | 0.447 | 24.30 | 1.83 | 14.09 |
| | Khao Yai Tuff | 3.524 | 0.406 | 26.72 | 5.37 | 5.05 |
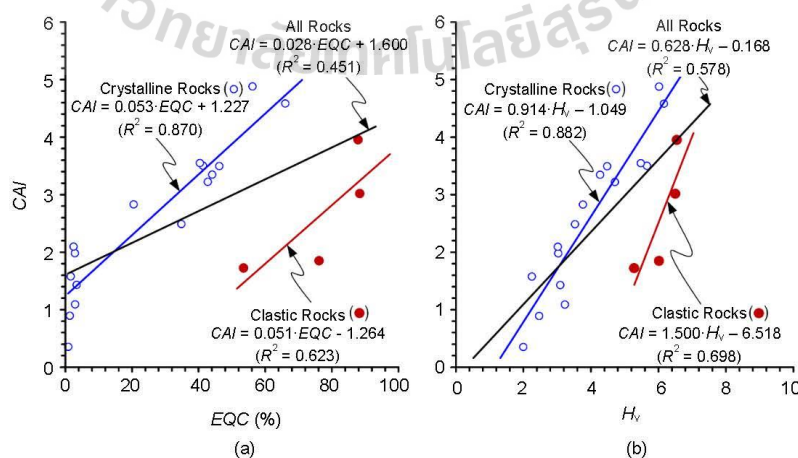


**Figure 5** CERCHAR abrasivity index ($CAI$) as a function of equivalent quartz content ($EQC$) (a), and volumetric hardness ($H$v) (b).

where $V_i$ is volumetric percent of each mineral (%), $W_i$ is mineral weight percent (%), and $SG_i$ is mineral specific gravity which can be obtained from several mineralogy textbooks [31, 35-37]. Based on the proposed equation above, $H_V$ will range from 1 to 10. Example of $H_V$ calculation for the Phu Phan sandstone is given below. The summation of volumetric percent ($\Sigma V_i$) of mineral contents is first calculated:

$$
\begin{array}{ll}
& \text{(Quartz)} \quad \text{(Kaolinite)} \ \text{(Muscovite)} \quad \text{(Albite)} \quad \text{(Microcline)} \ \text{(Chlorite)} \\
\Sigma V_i & = (86.13/2.66) + (6.27/2.63) + (1.65/2.83) + (3.46/2.63) + (0.60/2.56) + (1.90/2.95) \\
\Sigma V_i & = 32.38 + 2.38 + 0.58 + 1.32 + 0.23 + 0.64 = 37.53\%
\end{array}
\tag{12}
$$

From Equation (10) $H_V$ can then be obtained as:

$$
\begin{array}{ll}
& \text{(Quartz)} \ \text{(Kaolinite)} \ \text{(Muscovite)} \quad \text{(Albite)} \quad \text{(Microcline)} \ \text{(Chlorite)} \\
H_V = & [(32.38 \times 7) + (2.38 \times 2.25) + (0.58 \times 2.5) + (1.32 \times 6.25) + (0.23 \times 6.25) + (0.64 \times 2.25)] \ /37.53 \\
H_V = & 6.52
\end{array}
\tag{13}
$$

$H_V$ results from all tested rocks are plotted in Figure 5(b) where they are correlated with $CAI$ using a linear equation. A fair correlation is obtained ($R^2 = 0.578$). Table 2 gives numerical values of the fitting equation. Similar to $CAI$-$EQC$ relation, the correlation between $CAI$ and $H_V$ significantly improves when the clastic and crystalline rocks are analyzed separately. For clastic rocks $CAI$ can be correlated with $H_V$ by:

$$
CAI = 1.500 \ H_V - 6.518 \qquad (R^2 = 0.698) \tag{14}
$$

For crystalline rock groups:

$$
CAI = 0.914 \ H_V - 1.049 \qquad (R^2 = 0.882) \tag{15}
$$

The improvement of individual correlations for crystalline and clastic rocks suggests that the two rock groups respond differently to the wear of stylus tip (i.e. $CAI$) when hardness of rocks is considered. The diagrams in Figure 5 shows that clastic rocks tend to show higher $EQC$ and $H_V$ values than the crystalline rocks do, even though $CAI$ values for the two rock groups are within the same range. This results in a low correlation coefficient when only one equation is applied to describe their relation. The high $EQC$ and $H_V$ values are due to that grains of the tested sandstones are mainly quartz, albite and anorthite with a combined weight percent between 65% and 90% (see Table 1). Even though these minerals are highly abrasive and abundant in clastic rocks, they tend to have small impact on the wear of stylus tip. This is because the tested surface also contains much softer and lower abrasive minerals (e.g., kaolinite, muscovite, calcite and chloride). The stylus tip ploughs through the softer materials and induces dislodging of the harder grains with a small interaction between the grains and stylus tip. As a result, these highly abrasive grains have small impact on the stylus tip wear. For crystalline rocks, however, the stylus tip likely scratches through all crystals that are more densely packed (regardless of high or low abrasivity). All minerals on the tested surface are, therefore, responsible to the wear of stylus tip.

## 5. CERCHAR specific energy

Zhang et al. [38] propose a new parameter to correlate with $CAI$ and rock strength. It is called CERCHAR specific energy ($CSE$), which can be determined from $CAI$ testing but not considering the wear of stylus tip. Such approach has been recently used by several investigators [34, 38]. $CSE$ is represented by work done ($W$) applied on stylus pin during scratching to produce groove volume ($V$) on the rock surface. It can be calculated by [38]:

$$
CSE = W/V \tag{16}
$$

The work done can be calculated by [34]:

$$
W = F \cdot d_S \tag{17}
$$

where $F$ is lateral force applied on stylus pin and $d_S$ is its travelling distance (10 mm). Here the force can be calculated from torque applied on the crank of CERCHAR apparatus, using Equation (2). Figure 6 gives examples of the measured lateral forces as a function of travelling distance for Khao Kradong basalt (strong rock) and Tak Fa gypsum (soft rock). Dash lines represent force for each scratching and solid lines are their average. Since the force is not constant during scratching. They increase rapidly within the first 3-4 mm. Their increasing rates gradually reduce toward a constant magnitude. A mathematical representation is first developed to describe the evolution of $F$ as a function of $d_S$. After several trials, an exponential equation is proposed:

$$
F = a \cdot [1 - exp \cdot (-b \cdot d_S)] \tag{18}
$$

where $a$ and $b$ are empirical constants, depending on rock types. Table 3 gives their numerical values. Very good correlations are obtained for all rocks ($R^2 > 0.9$).

The work done on stylus pin can, therefore, be calculated as:

$$
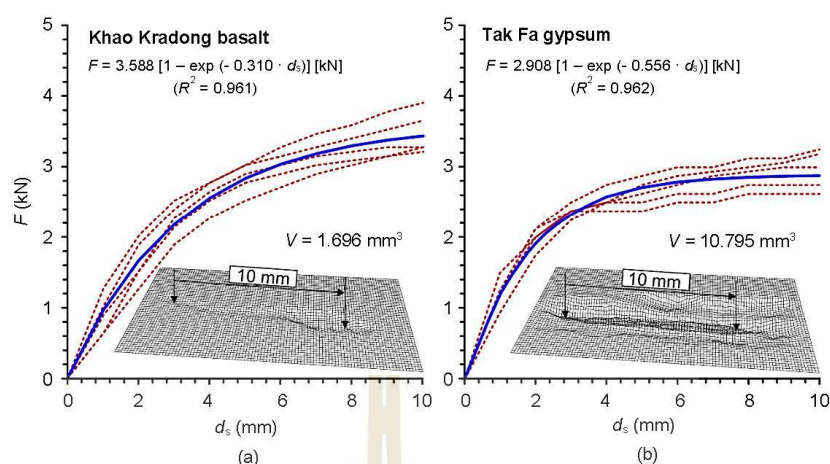W = \int_{d_S=0}^{10} F \cdot d_S \tag{19}
$$

**Figure 6** Examples of scratching forces ($F$) as a function of stylus displacement ($d_s$) and their laser-scanned groove images for Khao Kradong basalt (a) and Tak Fa gypsum (b). Dash line represents each groove. Solid lines are their average.

The calculation results are given in Table 3. The scratching groove volume ($V$) can be accurately determined by incorporating its laser scanning profile into SURFER 16.6 software (Golden Software, 2019). Substituting $W$ and $V$ into Equation (16), CERCHAR specific energy can then be obtained. Table 3 gives the average scratch volume and CERCHAR specific energy applied for each rock type. The results suggest that higher energy is required to scratch stronger and higher abrasivity rocks (e.g., granite and granodiorite) as compared to the softer and lower abrasivity rocks (e.g., salt and dickite). The wear of stylus tip as represented here by $CAI$ also shows some correlation with the scratched groove volume. High abrasiveness rocks yield smaller groove volume than the lower ones (Figure 7). $CAI$ decreases exponentially with increasing groove volume, which can be represented by a potential equation (Figure 7):

$$CAI = k \cdot V^x \tag{20}$$

where $k$ and $x$ are empirical constants. Regression analysis gives $k = 5.198$ and $x = -0.960$, where a fair correlation is obtained ($R^2 = 0.462$).

Due to the fact that $CAI$ can not correlate well with $s_c$ (as evidenced by results obtained here and elsewhere in Figure 3, some investigators [38] have attempted to correlate $CSE$ with $s_c$. This is because $CSE$ is derived from the applied stylus force and groove volume, where both parameters are governed by mineral compositions of the rock. In addition, $CSE$ does not involve the wear of stylus pin tip (i.e. $CAI$). The compressive strength is also depended on mineral compositions and physical characteristics of the rocks. Such approach is adopted for Thai rocks selected in this study. Figure 8 plots $CSE$ as a function of $s_c$ and $CAI$. Only fair correlation ($R^2 = 0.436$) is again shown between $CSE$ - $s_c$ relation based on a linear equation (Figure 8(a)):

$$CSE = 0.136 \cdot s_c + 3.817 \qquad \text{(J/mm}^3) \tag{21}$$

Slightly better correlation is obtained between $CSE$ and $CAI$. A linear equation can describe their positive correlation, showing $R^2 = 0.569$ (Figure 8(b)):

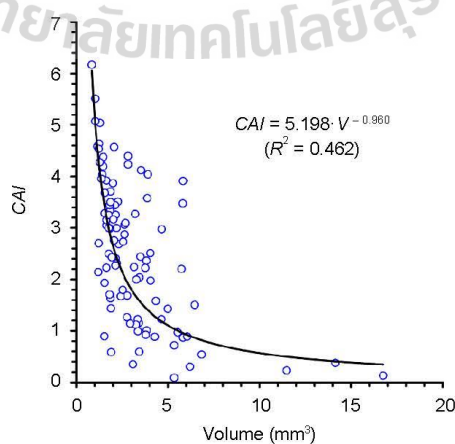$$CSE = 3.204 \cdot CAI + 3.413 \qquad \text{(J/mm}^3) \tag{22}$$



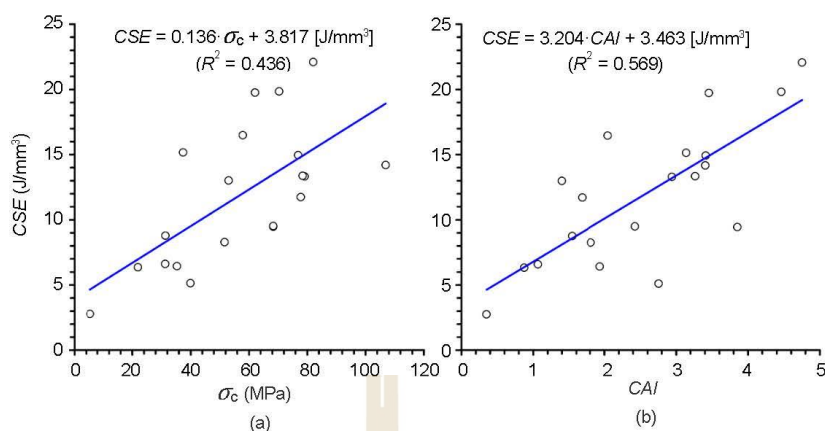**Figure 7** $CAI$ as a function of groove volume for all rock types.

**Figure 8** CERCHAR specific energy (*CSE*) as a function of uniaxial compressive strength (a), and of CERCHAR abrasivity index (b).

## 6. CERCHAR specific energy and volumetric hardness

An attempt is further made to correlate CERCHAR specific energy with an alternative parameter obtained from *CAI* testing. Suggesting by the good correlation between *CAI* and volumetric hardness ($H_V$) given in section 4 (Figure 5), particularly when crystalline and clastic rock groups are correlated separately, *CSE* is presented as a function of $H_V$ in Figure 9(a). Even though a positive linear relation is clearly shown between the two parameters, their correlation is relatively poor ($R^2 = 0.332$):

$$CSE = 2.020 \cdot H_V + 2.884 \qquad (\text{J/mm}^3) \qquad\qquad (23)$$

It is postulated that the volumetric hardness of crystalline and clastic rocks may respond differently to the scratching energy. As discussed earlier that for clastic rocks the soft minerals are the main factors affecting the wear of stylus tip. To further investigate this issue, a modified volumetric hardness ($H_V^*$) is proposed to incorporate into the CERCHAR specific energy and volumetric hardness relation. The calculation of the modified hardness ($H_V^*$) is similar to those of Equations (12) and (13) for Phu Phan sandstone, except that only soft minerals are taken into consideration (i.e., Kaolinite, microcline and chlorite). Figure 9(b) shows *CSE - $H_V$* relation with $H_V^*$ for clastic rocks, and the original $H_V$ for crystalline rocks. *CSE* increases linearly with volumetric hardness with $R^2 = 0.605$.

$$CSE = 3.181 \cdot H_V^* - 0.176 \qquad (\text{J/mm}^3) \qquad\qquad (24)$$

Based on the modification above, the *CSE-$H_V$* correlation coefficients have increased from 0.332 (Figure 9(a)) to 0.605 (Figure 9(b)) supporting that the soft and low abrasive minerals in clastic rocks are the main factor dictating how much energy is required to scratch the rocks, and how much the stylus tip is worn.
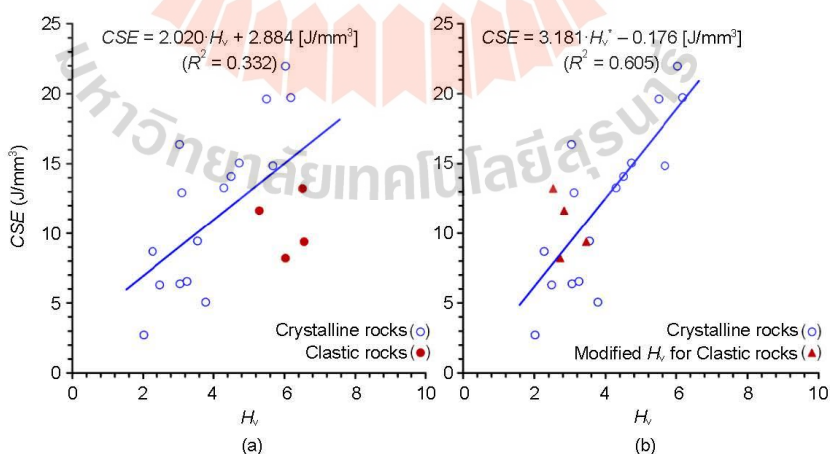


**Figure 9** CERCHAR specific energy (*CSE*) as a function of volumetric hardness ($H_V$) for both crystalline and clastic rocks (a), and for both rock groups with modified $H_V$ for clastic rocks (b).

The modified volumetric hardness ($H_V^*$) can not be applied to the *CAI-$H_V$* relation (Figure 5) because quartz contents do affect the wear of stylus tip (*CAI*) even for clastic rocks. As a result, they should not be taken out when the volumetric hardness of rock is calculated to correlate with *CAI*.

## 7. Discussions

Several investigators (as quoted in Figure 3) have recognized that only fair correlations can be obtained between uniaxial compressive strength and CERCHAR abrasivity index. Such correlation, however, has been widely performed. This is primarily because the rock strengths are readily available for most geological and mining engineering projects. Some investigators [18, 20, 21] can obtain their correlation coefficients of greater than 0.8. They however compare only few rock types with similar characteristics (e.g., sandstone, siltstone). In general rock strengths and *CAI* cannot be correlated well because the two parameters are derived from different mechanisms of failure or breakage. The failure of uniaxial test specimen is induced by the initiation and propagation of microcracks, fissures, intercrystalline boundaries, pore spaces and cleavage. When the applied stress reaches an ultimate value, these defects are connected, and compressive shear failure is induced [39]. The wear of stylus tip (*CAI*) is produced by shearing process controlling by abrasiveness and hardness of the minerals composing rock which may not have a direct relation with their strength. The mechanisms induce the wear of stylus tip are complex. The stress distribution in rock at and around the stylus tip also shows very high gradient under macroscopic scale, as demonstrated by numerical simulations by Balani, et al. [9].

Correlation between *CAI* and mineral compositions of rocks (Figure 5) gives a more promising approach to predict the wear of stylus tip, as compared to the *CAI*-$s_c$ relations. For *CAI*-*EQC* and *CAI*-$H_V$ relations, the improvement of their correlation coefficients by analyzing clastic and crystalline rocks individually suggests that *CAI* is governed not only by hardness of minerals composing rocks, but also by rock characteristics. No attempt has been made here to correlate *CAI* with $s_c$, $c$ and $f$ under different rock classifications (i.e., crystalline and clastic). This is primarily because these mechanical properties do not have direct relation with rock textures and mineral compositions.

The volumetric hardness ($H_V$) proposed in this study has a clear advantage over the *EQC* method when they are correlated with *CAI*. For soft rocks *EQC* can not distinguish the different responses of mineral compositions to *CAI* for soft rocks. As demonstrated in Figure 5(a), these soft rocks include those containing low hardness minerals, for example, travertine, dickite, salt and gypsum. This is because *EQC* uses multipliers given by Rosiwal abrasiveness ($R_i$) which places a main emphasis on hard minerals, as $R_i = 100$ (%) for quartz. $R_i$ values are decreased rapidly toward soft minerals with hardness low than 7. The volumetric hardness proposed here, however, simply uses Mohs scale hardness as multipliers to the minerals. The Mohs scale has been designed with, more or less, equal intervals for mineral hardness variation. Hence, $H_V$ can distinguish the equivalent rock hardness gradually and continuously from low to high ranges of *CAI* better than *EQC*. This is, particularly, useful for soft to medium strong rocks that are commonly found in mining and construction projects in Thailand.

It is recognized here that *CAI* is also affected by grain (crystal) size and shape, as experimentally shown by Er and Tuğrul [19] and Yaralı et al. [23]. These factors can not be analyzed in this study due to the narrow range of rock characteristics and limited number of rock types.

The concept of CERCHAR specific energy (*CSE*) is relatively new. It excludes the wear of stylus tip while deriving the relation between the applied mechanical energy of stylus pin and the mechanical properties and characteristics of rock. Only fair correlation has been obtained here for *CSE*-$s_c$ relation (Figure 8). This may be due to the different mechanisms that induce failure and breakage between the two tests, as discussed above for *CAI*-$s_c$ relation. *CSE* can correlate well with $H_V$, only if the volumetric hardness for clastic rocks is modified by considering only hardness of soft minerals (Figure 9(b)). This supports the previous postulation that clastic and crystalline rocks should be analyzed separately, not only for *CAI* - $H_V$ relation, but also for *CSE*-$H_V$ relation.

*CAI* and *CSE* have been derived from different parameters of testing. Both are useful for the rock excavation operation. *CAI* relates to the wear of excavation tools. *CSE* relates to the energy (force and distance) required to excavate a unit volume of rocks. This is why both parameters remain important and deserve further experimental investigation.

To correlate *CAI* with machine and tool wear during construction and excavation, practitioners and operators need to keep record and documentation on the rock characteristics and operating parameters during excavation process. These include, for example, rock type, mineral compositions, rotational speeds, weight on bits, penetration rates, and temperatures. The more accurate and detailed records, the better correlation between the tool wear and the *CAI* obtained from laboratory can be achieved.

## 8. Conclusions

In an attempt to determine the wear of excavation tools as affected by rock characteristics, CERCHAR abrasivity index (CAI) tests have been performed to correlate the results with various aspects of mechanical and mineral properties of twenty rock types commonly encountered in mining and construction projects in Thailand. Conclusions drawn from this study can be summarized as follows.

Only fair correlation ($R^2 = 0.473$) is obtained between *CAI* and uniaxial compressive strengths of Thai rocks selected in this study, primarily due to the differences of mechanisms governing the results obtained from the two tests, which agrees with research results obtained elsewhere. In addition, due to the differences of failure mechanisms only fair linear correlation is also shown between *CAI* and rock friction angle, while no correlation between *CAI* and rock cohesion has been found.

A new parameter called "volumetric hardness - $H_V$" is developed from this study to correlate *CAI* with mineral compositions of rocks. Their correlation is notably better than those obtained from the widely used equivalent quartz content - *CAI* relation, as it can clearly distinguish the differences of hardness of minerals composing soft to medium strong rocks (Figure 5). This is because *EQC* places main emphasis on the minerals harder than quartz, while the proposed $H_V$ considers volume of all minerals composing rocks. This study reveals also that *CAI*-*EQC* and *CAI*-$H_V$ relations can be further improved when clastic and crystalline rocks are analyzed separately in the regression. This is presumably because the grain (quartz and felspar) contents in clastic rocks tested here have small impact on the stylus tip which mean that the stylus can easily plough through much softer cementing materials.

*CAI*-$H_V$ relation has a clear advantage over *CAI*-*EQC* relation for soft to medium strong rocks. Both relations nevertheless perform equally well for very strong rocks, as suggested by the diagrams shown in Figure 5. It should be noted that *EQC* and $H_V$ require accurate determination of weight percents of minerals composing rocks, such as those obtained here from X-ray diffraction analysis. Visual observation of hand specimens or conventional petrographic study may not provide adequate results. The diagrams shown in Figures 3 through 5 suggest also that the wear of stylus tip (*CAI*) relates more to the mineral compositions of rocks than to the rock mechanical properties.

This study determines scratching volume by laser-scanning technique supported by 3-D graphic software (SURFER 16.6). This gives very accurate results (to the nearest $0.01 \text{ mm}^3$) which become useful for the CERCHAR specific energy calculation. Such

technique has never been employed elsewhere. The accurate scratch volume ($V$) also leads to a new finding of *CAI-V* relation as shown by negative exponential equation in Figure 7. Such relation has never been found or mathematically determined by other investigators.

As discussed above *CSE* has been derived from the test parameters different from those of *CAI*. It involves the energy required to remove a unit volume of rocks which mainly relates more to the volume of soft minerals rather than to those of the harder ones. Such differences represent the main characteristics of the clastic rocks tested here. The modified volumetric hardness ($Hv^*$), therefore, gives a better correlation with *CSE*, as shown in Figure 9. Care should be taken to apply $Hv^*$ to other clastic rocks. It is valid only if the cementing minerals are much softer than the grain minerals. If they have comparable hardness, application of original $Hv$ is more appropriate.

*CSE* linearly increases with *CAI* (Figure 8(b)), suggesting that rocks with high abrasivity require higher energy to cut, and yield lower excavated volume than those with lower abrasivity.

The findings obtained from this study are applicable to other soft to medium strong rocks. In particular, the approach of analyzing clastic and crystalline rocks separately is highly desirable when the effect of mineral compositions on *CAI* and *CSE* is investigated.

**9. Acknowledgement**

**10. References**

[1] Thuro K, Käsling H. Classification of the abrasiveness of soil and rock. Geomech Tunn. 2009;2(2):179-88.

[2] Prieto LA. The CERCHAR abrasivity index's applicability to dredging rock. Proceedings of Western Dredging Association (WEDA XXXII) Technical Conference and Texas A&M University (TAMU 43) Dredging Seminar; 2012 Jun 10-13; San Antonio, Texas. p. 212-9.

[3] Ko TY, Kim TK, Son Y, Jeon S. Effect of geomechanical properties on Cerchar Abrasivity Index (CAI) and its application to TBM tunnelling. Tunn Undergr Space Technol. 2016;57:99-111.

[4] ASTM. ASTM D7625-10: Standard test method for laboratory determination of abrasiveness of rock using the CERCHAR method. Philadelphia: American Society for Testing and Materials; 2010.

[5] Alber M, Yaralı O, Dahl F, Bruland A, Käsling H, Michalakopoulos TN, et al. ISRM Suggested method for determining the abrasivity of rock by the CERCHAR abrasivity test. Rock Mech Rock Eng. 2014;47(1):261-6.

[6] ASTM. ASTM D7625-22: Standard test method for laboratory determination of abrasiveness of rock using the CERCHAR abrasiveness index method. Philadelphia: American Society for Testing and Materials; 2010.

[7] Al-Ameen SI, Waller MD. The influence of rock strength and abrasive mineral content on the Cerchar Abrasive Index. Eng Geol. 1994;36(3-4):293-301.

[8] Plinninger R, Käsling H, Thuro K, Spaun G. Testing conditions and geomechanical properties influencing the CERCHAR abrasiveness index (CAI) value. Int J Rock Mech Min Sci. 2003;40(2):259-63.

[9] Balani A, Chakeri H, Barzegari G, Ozcelik Y. Investigation of various parameters effect on CERCHAR abrasivity index with PFC3D modeling. Geotech Geol Eng. 2017;35(6):2747-62.

[10] Hamzaban MT, Karami B, Rostami J. Effect of pin speed on Cerchar abrasion test results. J Test Eval. 2019;47(1):121-39.

[11] Kotsombat T, Thongprapha T, Fuenkajorn K. Scratching rate effects on CERCHAR abrasiveness index of sandstones. Proceedings of Academicsera International Conference; 2020 Sep 22-23; Chiang Mai, Thailand.

[12] Aydın H. Investigating the effects of various testing parameters on Cerchar abrasivity index and its repeatability. Wear. 2019;418-419:61-74.

[13] Käsling H, Thuro K. Determining rock abrasivity in the laboratory. ISRM International Symposium – EUROCK; 2010 Jun 15-18; Lausanne, Switzerland. Lausanne: International Society for Rock Mechanics and Rock Engineering; 2010. p. 1-4.

[14] Yaralı O, Duru H. Investigation into effect of scratch length and surface condition on Cerchar abrasivity index. Tunn Undergr Space Technol. 2016;60:111-20.

[15] Ozdogan MV, Deliormanli AH, Yenice H. The correlations between the CERCHAR abrasivity index and the geomechanical properties of building stones. Arab J Geosci. 2018;11(20):604.

[16] Sirdesai NN, Aravind A, Panchal S. Impact of rock abrasivity on TBM cutter-discs during tunnelling in various rock formations. In: Kalamkar V, Monkova K, editors. Advances in Mechanical Engineering. Singapore: Springer; 2021. p. 527-34.

[17] Yasar S, Yilmaz AO. Tool wear prediction with different models for medium strength rocks. Proceedings of the 13th International Conference Underground Construction Prague 2016; 2016 May 23-25; Prague, Czech. p. 1-10.

[18] Capik M, Yilmaz AO. Correlation between CERCHAR abrasivity index, rock properties, and drill bit lifetime. Arab J Geosci. 2017;10:1-12.

[19] Er S, Tuğrul A. Correlation of physico-mechanical properties of granitic rocks with CERCHAR abrasivity index in Turkey. Measurement. 2016;91:114-23.

[20] Teymen A. The usability of Cerchar abrasivity index for the estimation of mechanical rock properties. Int J Rock Mech Min Sci. 2020;128:104258.

[21] Deliormanlı AH. CERCHAR abrasivity index (CAI) and its relation to strength and abrasion test methods for marble stones. Constr Build Mater. 2012;30:16-21.

[22] Suana M, Peters T. The CERCHAR abrasivity index and its relation to rock mineralogy and petrography. Rock Mechanics. 1982;15:1-8.

[23] Yaralı O, Yaşar E, Bacak G, Ranjith PG. A study of rock abrasivity and tool wear in coal measures rocks. Int J Coal Geol. 2008;74(1):53-66.

[24] West G. Rock abrasiveness testing for tunnelling. Int J Rock Mech Min Sci Geomech Abstr. 1989;26(2):151-60.

[25] Aydın H, Yaralı O, Duru H. The effects of specimen surface conditions and type of test apparatus on Cerchar Abrasivity Index. Karaelmas Sci Eng J. 2016;6(2):293-4.

[26] Barton N, Choubey V. The shear strength of rock joints in theory and practice. Rock mechanics. 1977;10:1-54.

[27] Budynas RG, Nisbett JK, Shigley JE. Shigley's Mechanical Engineering Design. 9th ed. New York: McGraw-Hill; 2011.

[28] ASTM. ASTM D7012-14e1: Standard test methods for compressive strength and elastic moduli of intact rock core specimens under varying states of stress and temperatures. West Conshohocken: American Society for Testing and Materials; 2014.
[29] Rostami K, Hamidi JK, Nejati HR. Use of rock microscale properties for introducing a cuttability index in rock cutting with a chisel pick. Arab J Geosci. 2020;13:1-12.
[30] Thuro K. Drillability prediction: geological influences in hard rock drill and blast tunnelling. Geol Rundsch. 1997;86:426-38.
[31] Klein C. Manual of Mineral Science. 22$^{nd}$ ed. Hoboken: John Wiley & Sons; 2002.
[32] Altindag R, Sengun N, Sarac S, Mutluturk M, Guney A. Evaluating the relations between brittleness and Cerchar abrasion index of rocks. Proceedings of the ISRM Regional Symposium - EUROCK 2009; 2009 Oct 29-31; Cavtat, Croatia. p. 195-200.
[33] He J, Li S, Li X, Wang X, Guo J. Study on the correlations between abrasiveness and mechanical properties of rocks combining with the microstructure characteristic. Rock Mech Rock Eng. 2016;49:2945-51.
[34] Hamzaban MT, Memarian H, Rostami J. Determination of scratching energy index for CERCHAR abrasion test. J Min Environ. 2018;9(1):73-89.
[35] Haldar SK, Tišljar J. Introduction to mineralogy and petrology. Amsterdam: Elsevier; 2014.
[36] Nesse WD. Introduction to mineralogy. New York: Oxford University Press; 2000.
[37] Perkins D. Mineralogy. 3$^{rd}$ ed. Harlow: Pearson Education Limited; 2013.
[38] Zhang G, Konietzky H, Frühwirt T. Investigation of scratching specific energy in the Cerchar abrasivity test and its application for evaluating rock-tool interaction and efficiency of rock cutting. Wear. 2020;448-449:203218.
[39] Jaeger JC, Cook NGW, Zimmerman R. Fundamentals of rock mechanics. 4$^{th}$ ed. Oxford: Blackwell; 2007.

# BIOGRAPHY

Mr. Narawit Kathancharoen was born on March 30, 1996 in Bangkok, Thailand. He received his Bachelor's Degree in Engineering (Geological Engineering) from Suranaree University of Technology in 2018. For his post-graduate, he continued to study with a Doctor of Philosophy Program in the Geological Engineering Program, Institute of Engineering, Suranaree university of Technology. During graduation, 2018-2023, he was a part time worker in position of research associate at the Geomechanics Research Unit, Institute of Engineering, Suranaree University of Technology.